Department of Mathematics and Statistics

Modelling of Human Behaviour and Response to the Spread of Infectious Diseases

Piau Phang

This thesis is presented for the Degree of
Doctor of Philosophy
of
Curtin University

December 2016

Declaration

To the best of my knowledge and belief this thesis contains no material previously published by any other person except where due acknowledgment has been made.

This thesis contains no material which has been accepted for the award of any other degree or diploma in any university.

_____

Piau Phang

1 December, 2016

Acknowledgments

First and foremost, I would like to express my deep gratitude to Professor Yong-Hong Wu, my main supervisor and Associate Professor Benchawan Wiwatanapataphee, my co-supervisor, for their patient guidance, helpful suggestions, enthusiastic encouragement and mentorship in all the time of research and writing of this thesis. Advice given by them has been a great help in the completion of this thesis.

I am particularly grateful to Malaysia Government for the financial support during the period of my study. I would also like to extend my thanks to Ministry of Higher Education Malaysia and Universiti Malaysia Sarawak for giving me the opportunity to study in Perth, Australia.

Research facilities provided by the Department of Mathematics and Statistics, Curtin University was greatly appreciated. My special thanks are extended to all the staff and students of Curtin University for their assistance and friendships throughout my study at Curtin University. Last but not the least, I would like to thank my family: my mother, my wife and daughter for supporting me spiritually throughout my postgraduate study period.

Abstract

Behavioural factors play an important and crucial role in determining the intensity of the self-initiated pre-cautionary health protective actions and the success of a voluntary vaccination programme for infectious diseases. The individual-level of decision making on whether or not to adopt altered behaviour in reducing the risk of infection as well as to opt for vaccination in getting the vaccine-induced immunity is usually based on simple cost-benefit considerations, which could be incorporated into epidemic models through game-theoretical approaches. In this thesis, three different models addressing these two types of behavioural changes are constructed through the replicator dynamical equations, the vaccination population games framework and the asymmetric smoothed best response function, respectively.

By using a multi-population replicator dynamical equation framework, the first model focuses on the altered and normal behaviours of strategy interactions between two subpopulations with different preferences and relative strengths. Without imitations, the strategy switching is only minimal in natural selection process. With imitations, the strategy distributions depend on the existing preference, the relative strength of subpopulations, the cost of altering behaviour, the social group pressure and the extra benefit to individuals adopting the preferred behaviour in their respective subpopulation. The social group pressure could be a "double-edged sword" in influencing the altered behavioural changes and hence the resulting epidemic dynamics.

The vaccination behaviour is explored with two approaches. First, in

the vaccination population game framework, the second model in this thesis deals with the impact of three characteristics of imperfect vaccine in a two-class vaccine-induced immunity epidemic model on individual-scale vaccination strategy choosing based on the population-scale vaccination rate. When vaccine is not effective in reducing the susceptibility of the vaccinated individuals, the greater reduction of infectivity to vaccinated infected individuals would be beneficial in circumventing the persistence of disease despite instant vaccination is achieved in the population. If vaccine is able to provide longer duration of high immunity to vaccinated individuals and/or faster recovery in breakthrough infection, the cost thresholds for no vaccination would increase. Due to the imperfect vaccine, there exist multiple Nash equilibria vaccination rates which complicate the disease control efforts.

Second, by quantifying the probability of choosing vaccination strategy with a Gompertz-type of asymmetric function, the third model in this thesis looks into the smoothed best response of prevalence-based cost-benefit considerations for voluntary vaccination within a mean-field framework. The asymmetric smoothed best response produces the same vaccination coverage and epidemic dynamics as those given by the symmetrically smoothed best response except when the cost of vaccination is perceived to be very high. This suggests that the Gompertz function is suitable in modelling the behavioural changes for individuals who are usually risk-averse in nature.

List of Publications Related to this Thesis

1. Piau Phang, Benchawan Wiwatanapataphee, Yong-Hong Wu, Social and economic influences on human behavioural response in an emerging epidemic. *Proceedings of 2016 Asian Mathematical Conference*, (in press).

Contents

List of Tables

List of Figures

Chapter 1

Introduction

1.1 Background

The early twentieth century witnessed one major disease outbreak, namely the 1918-1920 influenza pandemic that infected 500 million people across the world and killed 50 to 100 million people, which amount to three to five percent of the world's population at that time [98]. Despite significant medical advances in the twenty-first century, health-related events occur in excess of normal expectancy and public news about infectious disease outbreaks become more common nowadays. During the period from November 2002 to July 2003, severe acute respiratory syndrome (SARS) spread from southern China and Hong Kong to infect individuals in 37 countries [94] and caused an eventual 8096 cases and 774 deaths, with 9.6% fatality rate [112]. Also, the confirmed death cases in the 2009 flu pandemics reached 14,285 worldwide [29].

Considering these historical and recent statistics as well as scientific advancement in health and medicine, it should not be denied that controlling and responding to future pandemics will be more challenging due to a number of emerging global trends including increased and denser urbanization, increased local and global travel, as well as a generally older and immune-compromised population [61]. The emergence of high-profile respiratory infectious diseases such as SARS epidemic, Middle East Respiratory Syndrome (MERS), Zika

and variant influenza A (H1N1) virus infection, persistent prevalence of childhood communicable diseases such as measles-mumps-rubella (MMR) and pertussis, as well as non-vaccine-preventable sexually-transmitted diseases such as human immune-deficiency virus infection / acquired immune-deficiency syndrome (HIV/AIDS) have not only threaten millions of people throughout the world, but also brought substantial economic and social impacts. Therefore, it becomes an acute need for governments and public health systems to evaluate the control measures designed to prevent infectious disease spreading.

Epidemiology is the science of study focusing on the cause-and-effect of health and disease conditions in the population, targeted on improving control measures and policy-making decisions. Borrowing terminologies from the theory of complexity, disease spreading is a complex (i.e. not fully knowable, but reasonably predictable) dynamic problem, or sometimes, can even be regarded as chaotic (i.e. neither knowable nor predicable) problem, such as the cases of SARS which spread on the Asian continent in 2003. The unpredictability in the occurrence of disease outbreaks is the consequence of an uncountable number of interactions among numerous components ranging from epidemiological characteristics (e.g. mode of transmission, contact pattern, genetic susceptible or resistance, latent or infectious period, recovery rate, type and amount of disease control etc.) to socio-demographic factors (e.g. age, gender, as well as social, cultural and economic activities etc.), geographic factors (e.g. spatial location, travelling and visitation, neighbourhood and community structure etc.) and also environmental factors (e.g. climate, seasons, landscape, land use etc.).

Moreover, human behaviour plays a central role in the spread of infectious diseases, and understanding the influence of individuals behavioural changes and responses on the spread of diseases can be the key to improving disease control efforts [39]. For instance, sexual behavioural changes (i.e. the use of condom, sexual abstinence until marriage etc.) have been identified as the key

to success in the control of HIV in Uganda [43]. However, for mild infections such as a minor cold, people rarely fundamentally change their behaviour, but with lethal or novel infectious diseases, they will change their behaviour considerably to try to reduce their risk of infection. For instance, the dramatic reduction in travel and social contact were observed in Hong Kong and Singapore during the 2003 SARS epidemic [32].

In the context of epidemiology, human behavioural change is referred to as individuals change of their behaviour in a way that is relevant for the spread of disease, that is how people act or response to a disease outbreak. For instance, behaviours such as facemask wearing, increased hand-washing, and avoidance of crowded places were observed during the Hong Kong SARS epidemic [54] and H1N1 influenza pandemic [71]. Indeed, focusing on individual behaviours as a key determinant of the dynamics of infectious diseases in mathematical epidemiology could be categorized into a specific discipline known as behavioural epidemiology [1], and the mathematical models constructed are called disease-behaviour models. Without incorporating behavioural changes and/or responses, the disease spreading models will predict the "worst" possible scenario [22].

Behavioural changes in relation to the infectious disease spreading can be categorized into two broad classes based on the motivation to start taking a particular preventive action, namely changes imposed by public health authorities and individual self-initiated behavioural changes [73]. The changes imposed by public-health authorities refer to actions taken by people in the population as a result of public control measures, including the closure of schools and workplaces, bans on public gatherings such as social and sports events, as well as travel restrictions to high-risk regions. These will change the mobility or contact patterns of individuals in the population. As for the self-initiated behavioural changes, individuals adopt their activities voluntarily due to the concerns induced by the disease, such as avoiding crowded

places, social distancing (i.e. staying at home), wearing protective face masks, practicing better hygiene, reducing travels (which could be categorized into non-pharmaceutical interventions), or using preventive medicines and taking vaccination voluntarily (which indeed are the pharmaceutical interventions). From the mathematical modelling perspective, the pharmaceutical interventions change the disease state of the individuals. For instance, by taking voluntary vaccination, individuals shift from susceptible class to vaccinated/recovered class. Meanwhile, it is assumed that certain epidemiological parameters, such as the disease transmission rate in the epidemic models, may be modified as the results of adopting non-pharmaceutical interventions.

In reality, individual's responses often shift as an epidemic progresses. Human behaviour in the context of epidemiology is based on attitudes, belief systems, opinions and awareness of a disease, and all these factors can change over time, both in individual and population levels [39]. Nevertheless, it is generally believed that risk perception (i.e. the awareness or belief about the potential hazard) shapes individual behaviour [57], and moreover the risk perception may in turn be shaped by the consequences of individual behaviour [102]. For instance, individuals often refuse or avoid vaccinations they perceived to be risky. On the other hand, a successful immunization program (i.e. a high proportion of people opt for vaccination) will strongly bring the disease prevalence down and therefore reduce the perceived infection risk, resulting in a decline in vaccine demand [1]. In addition, the perceived benefits (resp. costs) may be conceivably constructed as the beliefs about the positive (resp. negative) outcomes associated with a behaviour in response to a real or perceived disease prevalence. Therefore, it can thus be suggested that the difference between the benefits and costs of adopting certain health preventive actions will stimulate (resp. discourage) individuals in altering their behaviours voluntarily.

In general, every rational individual has certain level of crisis awareness. If

an (non risk-seeking) individual realizes that there are infected people around him/her, he/she will spontaneously take some preventive actions to protect himself/herself [83]. It is likely that awareness and knowledge are closely related. Awareness of individuals often comes from two different sources of information, namely the globally and locally available information [39, 73]. Newspapers, television stations, websites and other media channels that disseminated information published by public health authorities are some typical examples of the globally available information. For instance, health-related newscasts would change individuals' perceptions on vaccine safety and efficacy [8]. Meanwhile, the locally available information includes the spread of information by word of mouth among acquaintances in local community or social neighbourhood. As nowadays information could be quickly spread in social media, it is not surprising that even with just the word of mouth of aware individuals advising their social acquaintances to take flu shot, the dynamics of seasonal-like influenza epidemic may be shifted dramatically [42]. Thus, social influence (i.e. the behavioural change of individuals affected by others in a social network [96]) becomes a widely accepted phenomenon in studying the change of individual- and population-scale health-protective behaviour in the course of epidemic outbreaks.

In the context of health beliefs, according to [69], in order for behaviour to change, people must feel personally vulnerable to a health threat, view the possible consequences as severe, and see that taking action is likely to either prevent or reduce the risk at an acceptable cost with few barriers. In other words, the cost-benefit consideration is of utmost relevance in making decision whether or not to alter the behaviour. Not only that, they also pointed out that some internal or external stimulus is required to ensure that actual behaviour change occurs. In [111], some key internal (e.g. beliefs, perceptions, etc.) and external (e.g. healthcare practitioners' advice, vaccine availability, cost etc.) stimuli which influence the individual behavioural changes during a disease outbreak are listed. Since the self-initiated behavioural change is not

mandatory, individuals will decide to adopt it, or not, by making some cost-benefit considerations as well as under the influence of various factors such as social factors and the information received. We focus on this individual-level decision making, by taking the game-theoretical approaches, for both pharmaceutical (specifically, voluntary vaccination) and non-pharmaceutical interventions (specifically, pre-cautionary health protective actions) of the self-induced behavioural changes in this thesis.

1.2 Game-theoretical approaches in the disease-behaviour models

In the context of game theory, a game is an abstract formulation of an interactive decision situation with possibly conflicting interests [97]. A game consists of players (which are the decision-makers), strategies (or actions, behaviours), payoffs (or fitness, in the field of biology) and strategy switching rules. Hence, game theory could be considered as a mathematical approach for studying the conflict and/or cooperation between decision-makers (e.g. human, animals, companies, countries etc). The classical game theory assumes that the players are fully rational and have complete information about the game (i.e. his/her own and opponent (or interaction partner) strategy profiles (i.e. the set of all possible strategies) as well as the payoffs received by them for each possible combination of strategies), whereas the evolutionary game theory relaxes the full rationality assumption in which players may have incomplete information in the strategy interactions. A rational player will always choose the best strategy that maximizes his/her payoff, in response to the strategy chosen by others, which is a concept known as the best response correspondence.

In modelling the human behaviour on the disease spread, at microscopic level, the players or the decision-makers are usually referred to as the susceptible individuals who decide whether or not to adopt some pharmaceutical and/or non-pharmaceutical interventions. Hence, the term "vaccination

behaviour" in disease-behaviour models reflects that upon receiving information on the diseases, individuals who are given the chance for updating their strategies (i.e. play the game) will choose in between two strategies, i.e. vaccination and non-vaccination, in a voluntary vaccination program. By choosing the vaccination strategy, it is assumed that individuals go to vaccinate and the vaccine-induced immunity takes effect in protecting them from infection risks immediately, which can be termed as the positive payoff (i.e. the benefit) for the vaccination strategy. While, if the non-vaccination strategy is chosen, the individual is subjected to the infection risk, which is indeed the negative payoff (i.e. the cost). Therefore, individuals are said to make use of cost-benefit analysis (considerations) in choosing what is best for them.

For two-person games in the classical game theory, the strategy profile and its payoff may be given in the form of a static payoff matrix. The outcome of the strategy interactions (or simply, the solution of the games) is, either a pure or mixed strategy, Nash equilibrium if no player could increase his/her payoff by unilaterally switching to other strategy. However, in a population consisting of infinitely many players (and hence infinitely repeated games played), the strategy choice for a focal player depends on the payoff difference between his/her own payoff and the strategy interaction partner's payoff, in which the strategy update rule is indeed the pairwise payoff comparison, where one of the players may switch to the strategy of the other. This microscopic level of strategy switching (or mutation, in biology) could be either explicitly implemented as a rule-based model in agent-based simulation frameworks or implicitly modelled in population (or mean-field) games.

In population games, all players (or agents) have identical payoff matrix and it is assumed that players are randomly matched for strategy interactions (i.e. play the game) with some probability at each time step, which indeed governs the speed of game dynamics. Therefore, for any player, he/she would be regarded as playing the game against a single representative individual

who plays the population's average strategy as a mixed strategy [97]. Hence, it is the evolution of strategy frequencies at macroscopic level that is of most concern in the population games. Also, the expected payoff of players playing a certain strategy is now expressed as a function of the strategy frequencies, rather than a static scalar value in classical game theory. Therefore, this framework leads to the evolutionary game theory which focuses on the dynamics of strategy adaptation. Examples of population games in game theory literature include the replicator dynamics [100], the best response dynamics and the logit dynamics (also known as the smoothed best response [36]).

In replicator dynamics, the per capita growth rate of a given strategy is proportional to the payoff difference between the strategy and the average payoff of the population. Hence, the evolution of strategy frequencies could be described in the form of the replicator dynamical equation, which is a first-order ordinary differential equation. Also, the stationary states of the replicator equation give the evolutionary stable strategies (corresponding to the Nash equilibria in classical game theory). In biology, strategies are mostly inherited. However, the underlying mechanism of strategy switching in epidemiology involves social learning and hence the replicator dynamics is also known as imitation dynamics in disease-behaviour models. Hence, the terminologies "game dynamics", "replicator dynamics" and "imitation dynamics" are used interchangeably throughout this thesis.

As individuals are heterogeneous or may belong to certain groups with specific preferences, they may perceive the risk of infection in different way and make decisions under the influence of intra- or inter-group pressure. Individuals also tend to imitate other behaviour (or strategy) in their mutual interactions. As a result, individual behavioural changes in epidemic outbreak could be studied through coupling the replicator dynamical equation and an epidemic compartmental model, which was pioneered by Bauch [2] who investigated the vaccination behaviour in childhood diseases. Bauch's

framework was modified to investigate the susceptible spontaneous behaviour change (specifically whether or not to alter their behaviour in order to reduce their infection risks) in [74]. In this thesis, we extend the one-population model of [74] to a two-subpopulation model by using the multi-population game dynamical modelling framework proposed in [47, 48] so as to take into account the heterogeneity between groups in decision making.

Behaviour change spreads due to not only the information of disease incidence, but also the observations of individuals about their own behaviour status as compared to the population-level of average behaviour status. This leads to the development of modelling the implications of the population-scale epidemic dynamics on individual-scale decision choices by making use of the Markov decision process theory [77, 79] in disease-behaviour models. As vaccine efficacy plays an important role in shaping individual perceived benefits and costs of vaccination, we extend the one-class imperfect immunity model in [79] within their vaccination population games framework by incorporating three additional characteristics of imperfect vaccine, as those proposed in [30] to the two-class vaccine-induced immunity "vaccination population games".

In game theory, the best response refers to the strategy that gives the most favourable outcome to an individual, which may be expressed mathematically in a step-wise function. As far as the voluntary vaccination behaviour is concerned, the epidemic models incorporating the best response dynamics of cost-benefit analysis in strategy switching are mostly implemented in mean-field models. However, the continuous version of the smoothed best response which is expressed in Fermi's strategy updating rule (it is indeed a symmetrical sigmoid function), is mostly implemented in agent-based simulation models. We follow the framework of [116] in which a logistic function is used to model the continuous (or adult) voluntary vaccination decision making based on a simple cost-benefit analysis, but extend the smoothed best response from symmetric property to asymmetric one by using another type

of sigmoid functions known as Gompertz functions.

1.3 Objectives

The primary aim of this work is to study the individual-level decision making on adopting the self-initiated pre-cautionary health preventive actions or taking the voluntary vaccination in the course of epidemic outbreak with three game-theoretical modelling frameworks. Specifically, this project has the following objectives:

(i) Formulate a two-subpopulation game-dynamical model to study the interplays between the individual self-initiated pre-cautionary health protective behaviour, imitation and epidemic dynamics under the influence of cost-benefit consideration and social group pressure.

(ii) Investigate the impact of imperfect vaccines and two-class vaccine-induced immunity on vaccine coverage and epidemic dynamics based on the vaccination population games framework.

(iii) Develop an epidemic model with individual vaccination strategy adoption governed by asymmetric smoothed best response function.

Our goal in this thesis is not to study a disease in particular, but to carry out a deeper investigation with regard to the impact of incorporating human behaviours in epidemic modelling. Rather than constructing complicated model structures to investigate various aspects of human behaviours and responses in the spread of infectious diseases, we build three simple mean-field disease-behaviour models with minimal equations and simplest epidemic dynamics to capture the fundamental concepts in two aspects of human behaviour, namely vaccination behaviour and self-initiated pre-cautionary health protective behaviour. Besides that, the parameter values used in the

numerical simulations are not intended to be highly realistic, but rather to illustrate particular scenarios or principles and explain the dynamical behaviour which the models can exhibit by incorporating certain aspect of game theory in the modelling. Also, no model validations with real data were carried out. The focuses of this work are given to the mathematical formulations and numerical simulations, rather than the theoretical analysis and the methods of solution to the models.

1.4 Main contributions of this thesis

The contributions of this thesis include the following aspects.

(i) Construction of a new two-subpopulation imitation dynamical model whereby susceptibles in different subpopulations have different preferences in adopting health protective behaviour.

(ii) Construction of vaccination population games with three additional characteristics of imperfect vaccine in a two-class vaccine-induced immunity epidemic model.

(iii) Development of a new asymmetric smoothed best response function for determining the individual voluntary vaccination strategy adoption in an epidemic model with vaccination.

1.5 Outline of the thesis

This thesis consists of six chapters. Chapter One gives the background and the objectives of the research as well as the structure of the thesis. Chapter Two presents the literature review in a wider scope on two types of human behavioural changes on the disease spread. The basics in epidemic models

with partially vaccine-induced immunity, without game theory elements, are also given to serve as the fundamental concepts for further investigations on corresponding models but with game-theoretical elements. It is followed by three separate models in the subsequent three chapters with their own specific backgrounds and literatures. Chapter Three concerns the self-initiated pre-cautionary health protective behavioural changes whereas Chapter Four and Five deal with vaccination behaviours.

In Chapter Three, the one-population natural selection and imitation dynamics model for behavioural changes involving self-initiated pre-cautionary health protective actions in an emerging disease is extended to two subpopulations model with different preferences. The derivations of the two-subpopulation replicator dynamical equations for the natural selection as well as imitation process involving the cost-benefit analysis and social group pressure are given. We explore the impact of the subpopulation with existing preference and relative strength, the cost of altering behaviour, the social group pressure and the extra benefit to individuals adopting the subpopulation's preferred strategy on the strategy distributions. We show that the numerical simulation results are in good agreement with the local stability analysis.

Chapter Four investigates the impact of imperfect vaccine on the individual-scale voluntary vaccination decision-making based on the population-scale epidemiological status within the framework of vaccination population games. The analysis of the associated reproduction number for the epidemic model with two classes of infected and/or vaccinated individuals is given and the existence of the phenomenon of backward bifurcation is shown by using the center manifold theorem. Then, we give the procedure involved in finding the utility function and the cost threshold for vaccination population game analysis in a step-by-step approach. The simulation results highlight the possible vaccination coverage for three additional characteristics of imperfect vaccines and the existence of multiple Nash equilibria vaccination rates.

The first part of Chapter Five is devoted to the literature review on two types of function (or correspondence, namely the best response and the smoothed best response) used in describing the probability of choosing the vaccination strategy in both the mean-field well-mixed and the agent-based network epidemic models. As we propose to use the smoothed best response function in the epidemic mean-field model with partially vaccine-induced immunity, we present the mathematical formulations of the Gompertz function in governing the individuals smoothed best response on the cost and benefit considerations of getting vaccination. The dynamical behaviour of the resulting system is studied through a combination of the Jacobian matrix, the graphical approach and again the center manifold theorem. We then explore the difference between the (asymmetric) Gompertz function and the (symmetric) logistic function on the vaccine uptake level in this chapter.

A brief summary of the research is given in the first part of Chapter Six. Several possible future studies on the current topic are then given in the second part of Chapter six.

Chapter 2

Literature Review

In this chapter, we present the literature reviews for game-theoretical mathematical modelling of vaccination behaviour and pre-cautionary health protective behaviour. Besides that, we give the fundamental concepts dealing with epidemic models with partially vaccine-induced immunity.

2.1 Mathematical modelling of voluntary vaccination behaviour using game-theoretical approach

Game-theoretical approach, specifically the replicator dynamical equation, was initially used in [2] to investigate the interplays between individual voluntary vaccination behaviour, vaccine coverage and vaccine-preventable childhood disease dynamics in a well-mixed population. In this context, the players of the game are parents who decide between two strategies, that is whether to vaccinate their children or not based on the payoff maximization (or equivalently, loss-minimization) behaviour. This strategy decision-making can be largely determined through the cost-benefit analysis on the expected payoffs of the strategies. Vaccination incurs certain fixed costs (e.g. time and money spent, the vaccine adverse effects, etc.) but is sufficient to confer lifelong immunity (assuming the vaccine is perfect), while non-vaccinators are exposed to the prevalence-dependent risk of infection and the subsequent monetary loss (e.g. absence from school / workplace, treatment expenses etc.). There

is a temptation to free-ride on the herd immunity of others by opting not to vaccinate but may still be free from infection. The individuals' fully rationality and self-interest behaviour lead to oscillations in vaccine coverage over time [2, 78] and hence voluntary vaccination is unlikely to achieve society-optimal level [5] for a complete disease eradication [3]. However, the presence of altruistic individuals who are willing to increase payoff of others regardless beneficial to oneself or not can significantly shift the vaccine coverage towards the society optimum [91].

Unlike vaccine-preventable childhood diseases, the vaccine for recurrent infectious diseases such as influenza are usually effective only for one season owing to mutation of pathogens and waning immunity [104]. Hence, the evolutionary game theory is employed to capture the strategy interactions between vaccinators and non-vaccinators during a voluntary vaccination program, before the next seasonal epidemic begins (see e.g., [35, 104]). An individual's payoff is assigned according to their vaccination status and disease status during the last epidemic season. Individuals adjust their vaccination strategy through observations on their randomly selected role model's (or neighbour's) payoff outcomes and imitate the more successful one with the probability governed by Fermi strategy updating rule (see e.g. [35, 11, 13]). This pairwise payoff comparison takes into account the bounded rationality of human behaviour in which there is a possibility that the worst performing strategy is being imitated. Since individuals make repeated vaccination decisions based on their expectations about future events, this individual-level adaptive decisions collectively determine the vaccine coverage and therefore influence the disease dynamics, and conversely, the disease dynamics influence the likelihood that individuals will choose to vaccinate. Due to their inherent complexity, this scenario is usually modelled through a bottom-up approach, specifically, within an agent-based modelling simulation framework.

Individuals interpret the information that they obtain through observa-

tions in the social contact and conjecture about the vaccination strategies of others. Hence, social contact structure has a significant impact on voluntary vaccination behaviour and its corresponding disease dynamics. Unlike well-mixed population in which diseases are not eradicated due to the free-riding effect, social contact structures enable disease eradication when vaccine risk is not too high and disease risk is not too low [72], particularly effective in scale-free network than regular networks (since hub nodes of scale-free networks are more inclined to take vaccination) [119], as well as in adaptive networks than static networks [90]. The clustering of non-vaccinator individuals in structural population, either caused by imitation [62] or opinion formation process [12, 86], has a strong unfavourable effect on disease eradication especially when vaccination coverage is approximately achieving herd immunity. However, with the presence of committed vaccinators to stimulate other imitators to take vaccination, the effect of clustering of susceptible non-vaccinator can be significantly reduced [58]. Besides that, individuals' high conformity to social influence will strengthen the negative correlation between cost of vaccination and vaccine coverage [114].

From a cost-benefit analysis perspective, individual vaccination decision-making is strongly governed by their perceptions on the severity of the disease outbreak and the perceived risk of vaccination. These risk perceptions are closely related to individuals' prior knowledge and awareness. As stated in the review paper [39], all epidemic models incorporating human behaviour make assumptions on the source and type of information that individuals' decision is based on. The interplay between voluntary vaccination behaviour, publicly available information and childhood disease dynamics was initially modelled analytically without incorporating the concept of imitation game dynamics. Even so, similar to models with imitation dynamics, information dependent vaccination also demonstrates clearly the oscillatory behaviour of vaccine coverage when parents use not only the current but also the past information [26], the delayed information [9] about the disease and informa-

tion on the disease's mortality [27] to make their vaccination decisions. As compared to how people arrive at their choices based on locally available "private" information, public information communicated by public health authorities [25] and newscasts providing individuals with more epidemiological information [8] are able to stabilize the imitation-induced oscillations, to allow disease elimination. Moreover, the possibility for the individuals to go for vaccination increases with the amount of information and the degree of sensitivity towards the information obtained by individuals [83] as well as the reporting rate of severe disease infections, but decreases with the reporting rate of vaccine-related adverse effect [114]. Individuals' own characteristics (such as their experience and memory) also have an impact on the adoption of vaccination. The vaccination and disease dynamics become less variable when individuals integrate more of their prior epidemic seasons experience in their decision-making [18, 110].

2.2 Mathematical modelling of self-initiated pre-cautionary health protective behaviour using game-theoretical approach

One of the underlying assumptions in modelling the self-initiated pre-cautionary health protective behaviour in the spread of infectious diseases is that upon receiving any information on diseases, individuals may activate their behavioural responses by voluntarily taking some non-pharmaceutical intervention measures to reduce their infection risks. For instance, by social distancing practices (either staying at home from workplaces or schools, or avoiding crowded places and social events etc.), the contact rates between susceptible and infected individuals can be significantly reduced and hence the disease transmission rate, say β, may be modified. This implies that individuals are not risk-seeking. Also, the pre-cautionary health protective behaviour is assumed to be effective in reducing the disease transmission but not able to totally eliminate the infectious diseases. Therefore, a modification parameter

(or a susceptibility reduction factor), say $\alpha \in (0, 1)$, is being multiplied with β in well-mixed epidemic models [73, 74, 75] or agent-based network epidemic models [17, 33] incorporating pre-cautionary health protective behavioural changes.

Similar to the vaccination behaviour, individuals may make use of simple cost-benefit considerations or imitate other's behaviour in choosing whether or not to alter their behaviour to reduce their infection risks. In literatures involving well-mixed epidemic models with game-theoretical approaches, the population average reduction of force of infection due to pre-cautionary health preventive actions could be expressed in two ways. First, by using the replicator dynamical equation [74, 75], the authors assumed that susceptibles who alter their behaviours may have to pay some fixed extra inconvenient costs (e.g. absence from schools or works, cancelling travels) than doing nothing (termed as "normal" behaviour in [74]). Hence, the population average reduction of force of infection is determined by the proportion of susceptible adopting altered behaviour at any time in the course of epidemic outbreak. Second, in social distancing games [76, 77], in which the Markov decision process theory was employed, the population average reduction of force of infection is expressed as a monotone decreasing function of the intensity of investments of susceptibles social distancing practice. This means that the larger the investments (which could be analogous to the cost of altered behaviour in [74]), the lower the population average force of infection will be.

2.3 Epidemic models with continuous vaccination and partially vaccine-induced immunity

Although there is a rapidly growing literature on investigating voluntary vaccination behaviour using the game-theoretical approach, most of the frameworks assume that vaccine confers lifelong immunity. There has been relatively little research on accessing the impact of vaccine efficacy on vaccination

behaviour. As Chapter Four and Five in this thesis are devoted to address the issue of imperfect vaccine on vaccination behaviour, we briefly discuss the basics of the imperfect vaccine to the epidemic dynamics, without the components of game theory in this section.

The Susceptible-Infectious-Recovered-Vaccinated (SIRV) epidemic compartmental model with imperfect vaccine for the continuous vaccination is given below.

$$\frac{dS}{dt} = \Lambda - \beta\frac{I}{N}S - \bar{\pi}S - \mu S, \tag{2.1a}$$
$$\frac{dI}{dt} = \beta\frac{I}{N}S + \sigma\beta\frac{I}{N}V - \gamma I - \mu I, \tag{2.1b}$$
$$\frac{dR}{dt} = \gamma I - \mu R, \tag{2.1c}$$
$$\frac{dV}{dt} = \bar{\pi}S - \sigma\beta\frac{I}{N}V - \mu V, \tag{2.1d}$$

where the total population size is $N = S + I + R + V$. Λ is the (constant) recruitment rate of susceptible corresponding to births and immigrations, μ is the constant natural death rate of the population, β is the disease transmission rate, γ is the recovery rate, $\sigma \in [0, 1)$ is the probability of vaccine failure while $1 - \sigma$ gives the vaccine efficacy and $\bar{\pi}$ is the population average vaccination rate, which could be constant or time-varying depending on the modelling assumptions.

We further define σ as the probability of vaccine failure in degree [50, 59, 63] simply to reflect the scenario of partial immunity (i.e. the vaccine-induced immunity may not be fully protective [41]). This is particularly relevant as the strain of infectious diseases such as influenza often mutates rapidly enough [7] that being vaccinated does not guarantee individuals are fully protected from the risk of infection. Thus, the expression $1 - \sigma$ predefines the degree of the reduction of susceptibility for the vaccinated individuals. $\sigma = 0$ means that the vaccine is fully effective in reducing the susceptibility and system

(2.1) could be reduced to the SIR model whereby both the vaccine-acquired and infection-acquired immunity would remove the individuals from the susceptible pool. On the other hand, $\sigma = 1$ implies that the vaccine is totally useless and from the perspective of controlling the infectious diseases, it is not worth to introduce such a vaccine to the host population. Hence, we will not consider the case of $\sigma = 1$ in this thesis. In other words, we assume that the vaccine is at least offering some degree of protection to the vaccinated individuals.

For the epidemic compartmental model in system (2.1), which does not involve a vector (i.e. a carrier of disease-causing agent) and different host types, the concept of the basic reproduction number ($\mathcal{R}_0$) is sufficient to quantify the driving force of the spread of infection [82]. The $\mathcal{R}_0$ is defined as the average (or expected) number of individuals (secondary infection) infected by one typical infective (primary infection), over his/her entire duration of infection, in a whole susceptible population. For an epidemic compartmental model with n disease compartments (i.e. the individuals in the compartments are infected), the basic reproduction number can be computed using the method of the next generation matrix [23] by the steps given below.

Step 1: Find $\mathcal{F}_i(\mathbf{x}_0)$ and $\mathcal{V}_i(\mathbf{x}_0)$, $i = 1, 2, \ldots, n$, where $\mathcal{F}_i \geq 0$ represents new infections in compartment i, $\mathcal{V}_i \leq 0$ represents a net outflow from compartment i (such as the recovery rate, death rate etc.), and $\mathbf{x}_0$ is the disease free equilibrium (DFE).

Step 2: Find the $n \times n$ next generation matrix $K = \mathsf{F}\mathsf{V}^{-1}$ at DFE, where F and V are the $m \times m$ matrices defined by $\mathsf{F} = \frac{\partial \mathcal{F}_i(\mathbf{x}_0)}{\partial x_j}$ and $\mathsf{V} = \frac{\partial \mathcal{V}_i(\mathbf{x}_0)}{\partial x_j}$, with $1 \leq j \leq m$.

Step 3: Find the spectral radius (the dominant eigenvalue) of the matrix K, which gives the basic reproduction number $\mathcal{R}_0$.

At $t \to \infty$, we have $N \to \frac{\Lambda}{\mu}$. For the case where the vaccine offers complete protection ($\sigma = 0$), by assuming $\Lambda = \mu$ (and without loss of generality, we have $N = 1$), system (2.1) has DFE, $E_0 = (S_0, I_0, R_0, V_0) = (\frac{\mu}{\bar{\pi}+\mu}, 0, 0, \frac{\bar{\pi}}{\bar{\pi}+\mu})$. The spectral radius of the next generation matrix is given by $\mathcal{R}_{\mathrm{C}} = \frac{\beta}{\gamma+\mu}\frac{\mu}{\bar{\pi}+\mu}$. The notation $\mathcal{R}_{\mathrm{C}}$ reflects the reproduction number with vaccination as a control measure and is usually known as the control reproduction number. It is defined as the average number of secondary infections produced by a primary infected person in a population consisting of susceptible and vaccinated individuals. If $\bar{\pi} = 0$, then the $\mathcal{R}_{\mathrm{C}}$ is reduced to $\mathcal{R}_0 = \frac{\beta}{\gamma+\mu}$. When $\bar{\pi} > 0$, if $\mathcal{R}_{\mathrm{C}} > 1$ (and hence $\mathcal{R}_0 > 1$), then the disease grows. If $\mathcal{R}_{\mathrm{C}} < 1$ (resp. $\mathcal{R}_0 < 1$), then the disease dies out with the presence (resp. absence) of vaccination program. It can be seen that $\mathcal{R}_{\mathrm{C}} < 1$ if and only if $\bar{\pi} > \bar{\pi}_{\mathrm{critical}} = \mu(\mathcal{R}_0 - 1)$, where $\bar{\pi}_{\mathrm{critical}}$ is the critical vaccination coverage level.

Similarly, for vaccine with partial immunity ($0 < \sigma < 1$), we have the same DFE E_0 but the effective reproduction number is given by $\mathcal{R}_{\mathrm{eff}} = \frac{\beta}{\gamma+\mu}\frac{\sigma\bar{\pi}+\mu}{\bar{\pi}+\mu}$ with the critical vaccination coverage level becomes $\bar{\pi}_{\mathrm{c}} = \frac{\mu(\mathcal{R}_0-1)}{1-\sigma\mathcal{R}_0}$. The most important consequence of relaxing the assumption of fully-protective vaccine is that although $\bar{\pi} > \bar{\pi}_{\mathrm{c}}$ leads to $\mathcal{R}_{\mathrm{eff}} < 1$, it no longer guarantees disease eradication.

2.3.1 The existence of multiple endemic equilibria

When $0 < \sigma < 1$, the endemic equilibrium point(s) of system (2.1) is given by $E^* = (S^*, I^*, R^*, V^*)$ where $R^* = \frac{\gamma}{\mu}I^*$, $S^* = \frac{(\gamma+\mu)N^*}{\beta} - \sigma V^*$ and $V^* = \frac{\bar{\pi}(\gamma+\mu)N^*}{\beta[\sigma\bar{\pi}+\sigma\lambda^*+\mu]}$ with $\lambda^* = \beta\frac{I^*}{N^*}$. Since $S^* + I^* + R^* + V^* = N^*$, we obtain

$$I^* = N^*\left(1 - \frac{\gamma+\mu}{\beta} - (1-\sigma)\frac{\bar{\pi}(\gamma+\mu)}{\beta[\sigma\bar{\pi}+\sigma\lambda^*+\mu]}\right)\frac{\mu}{\gamma+\mu} \tag{2.2}$$

By substituting expression (2.2) into $\lambda^* = \beta\frac{I^*}{N^*}$, after some algebraic manip-

ulations, we obtain

$$Q(\lambda^*) = A(\lambda^*)^2 + B\lambda^* + C,$$

where

$$\begin{aligned} A &= \sigma(\gamma+\mu) > 0, \\ B &= (\gamma+\mu)\left[\sigma\bar{\pi} + \mu + \sigma\mu(1-\mathcal{R}_0)\right], \\ C &= \mu(\gamma+\mu)(\bar{\pi}+\mu)\left[1-\mathcal{R}_{\text{eff}}\right]. \end{aligned} \tag{2.3}$$

The endemic equilibrium point(s) (or endemic state(s)), $I^* = \lambda^* \frac{N^*}{\beta}$, arises as the solution(s) of quadratic equation (2.3) in which λ^* could be obtained by quadratic formula $\lambda^* = \frac{-B \pm \sqrt{B^2-4AC}}{2A}$. Hence, it is obvious that there is a possibility of the existence of multiple endemic equilibria when the vaccine only offers partial immunity ($0 < \sigma < 1$), as compared to the assumption that the vaccine offers full protection to vaccinated individuals ($\sigma = 0$).

As the type and number of solutions to the quadratic equation will be determined by the sign of the expression $B^2 - 4AC$, solving $B^2 - 4AC = 0$ for $\mathcal{R}_{\text{eff}}$ gives

$$\mathcal{R}_{\text{eff}} = 1 - \frac{B^2}{4\sigma\mu(\gamma+\mu)^2(\bar{\pi}+\mu)} \equiv \mathcal{R}^c_{\text{eff}} \tag{2.4}$$

where the sub-threshold $\mathcal{R}^c_{\text{eff}} < 1$. Also, it is easy to see that $B > 0$ implies that $\mathcal{R}_0 < 1 + \frac{\sigma\bar{\pi}+\mu}{\sigma\mu} \equiv \mathcal{R}^c_0$. The solutions to quadratic equation (2.3) and the corresponding property of the SIRV model could be deduced as the following cases.

(i) If $\mathcal{R}_{\text{eff}} > 1$ ($\Leftrightarrow C < 0$), then $B^2 - 4AC > 0$ regardless the sign of B. The quadratic $Q(\lambda^*)$ has two real roots with opposite sign. Since only the positive root is biological feasible, the partial immunity model has a unique positive endemic equilibrium.

(ii) If $\mathcal{R}_{\text{eff}} = 1$ ($\Leftrightarrow C = 0$), then $Q(\lambda^*) = \lambda^*(A\lambda^* + B) = 0$. We have $\lambda^* = 0$ (i.e. DFE, $I^* = 0$) or $\lambda^* = -\frac{B}{A}$. The model has a unique endemic equilibrium if $B < 0$ (i.e. $\mathcal{R}_0 > \mathcal{R}_0^c$).

(iii) For the case of $\mathcal{R}_{\text{eff}} < 1$ ($\Leftrightarrow C > 0$), we analyse the following subcases: (a) If $B \geq 0$ (i.e. $\mathcal{R}_0 \leq \mathcal{R}_0^c$) or $B^2 - 4AC < 0$, then $Q(\lambda^*)$ has no positive (or real) roots. (b) If $B < 0$ (i.e. $\mathcal{R}_0 > \mathcal{R}_0^c$), then the $Q(\lambda^*)$ has two positive real roots if $B^2 - 4AC > 0$ (i.e. $\mathcal{R}_{\text{eff}} > \mathcal{R}_{\text{eff}}^c$). Besides that, $Q(\lambda^*)$ has a positive real root of multiplicity 2 if $B^2 - 4AC = 0$. This positive real root of multiplicity of 2 is simply given by $\lambda^* = -\frac{B}{2A} > 0$.

Therefore, we conclude that there exist multiple endemic equilibria for system (2.1), with $0 < \sigma < 1$ whenever $\mathcal{R}_{\text{eff}}^c < \mathcal{R}_{\text{eff}} < 1$. This existence of multiple endemic states is the main characteristics of a phenomenon known as backward bifurcation, which has been observed in numerous epidemic models with vaccine that only offers partial immunity.

2.3.2 Backward bifurcation

In dynamical systems, bifurcation phenomenon is pertinent to the occurrence of the qualitative change in the structural behaviours (e.g. the equilibria and its stability) of the system when a parameter value of the system is varied. Generally, mathematical models with multiple steady states give rise to bifurcation phenomena. In epidemic control, the basic reproduction number $\mathcal{R}_0$ and/or other associated reproduction numbers, for instance, $\mathcal{R}_{\text{C}}$ and $\mathcal{R}_{\text{eff}}$, are indeed the disease threshold condition, i.e. the condition necessary for disease invasion (the existence of endemic state) in the population. As $\mathcal{R}_0$ increases and approaches unity, the DFE (which is characterized by the absence of infectious individuals) changes its stability from stable to unstable, in which this phenomenon involves a transcritical bifurcation.

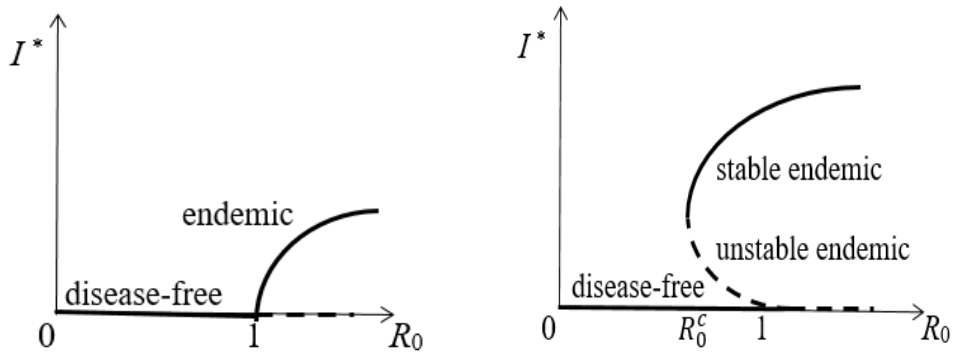

(a) Forward bifurcation (b) Backward bifurcation

Figure 2.1: The schematic diagram of forward and backward bifurcation.

In this context, there are two types of transcritical bifurcation, namely forward (supercritical) bifurcation and backward (subcritical) bifurcation, which give the "direction" of the endemic state (i.e. I^*) close to the disease threshold, $\mathcal{R}_0 = 1$ (Figure 2.1, the solid lines denote stability and the dashed lines denote instability). If the endemic state exists only for $\mathcal{R}_0 > 1$ but not for $\mathcal{R}_0 < 1$, a forward bifurcation occurs (Figure 2.1(a)) and the endemic level increases slightly and continuously as $\mathcal{R}_0$ increases through unity. However, if the backward bifurcation occurs, as $\mathcal{R}_0$ increases and once it goes across unity, I^* suddenly jumps from DFE to a high endemic level. Even though the $\mathcal{R}_0$ is reduced back below one, there exist two endemic states, a low level of unstable endemicity and a higher level of stable endemicity (see Figure 2.1(b)). Depending on the initial number of infected individuals, the system may end up with the lower endemic level or the higher one. Further reducing the epidemic threshold $\mathcal{R}_0$ to a subthreshold $\mathcal{R}_0^c$, the saddle-node bifurcation occurs in which the two endemic states collide and annihilate each other. In short, backward bifurcation is a phenomenon typically characterized by the co-existence of multiple stable equilibria when the associated reproduction number of the epidemic model is less than one [68].

As far as the immunity in the host is concerned, the phenomenon of backward bifurcation has often been observed in epidemic models with imperfect vaccine [30, 52, 65], exogeneous reinfection [49, 89], resistance mechanism [80] and structured acquired immunity [81]. From the epidemiological point of view, the phenomenon of backward bifurcation has a negative impact on disease control because reducing $\mathcal{R}_0$ (or its associated reproduction number) below the unity does not guarantee disease eradication. The disease control becomes highly dependent on the initial proportion of infectious individuals in the population. The reproduction number must be further reduced to below the subthreshold $\mathcal{R}_0^c$ for disease elimination.

2.3.3 The center manifold theorem

The qualitative analysis on the quadratic equation presented in Subsection 2.3.1 for showing the existence of multiple endemic equilibria and consequently the backward bifurcation could be carried out in a more systematic way by using the center manifold theorem, proven in [14], as given below.

Theorem 2.1. Consider the following system of ordinary differential equations with a parameter ϕ:

$$\frac{dx}{dt} = f(x, \phi), \quad f: \mathbb{R}^n \times \mathbb{R} \to \mathbb{R} \quad \text{and} \quad f \in \mathbb{C}^2(\mathbb{R}^n \times \mathbb{R}), \tag{2.5}$$

where 0 is an equilibrium of the system that $f(0, \phi) = 0$ for all ϕ and assume

(A1) $J = D_x f(0,0) = \frac{\partial f_i(0,0)}{\partial x_j}$ is the linearization of system (2.5) around the equilibrium 0 with ϕ evaluated at 0. Zero is a simple eigenvalue of J and all other eigenvalues of J have negative real parts.

(A2) Matrix J has a right eigenvector $\mathbf{w}$ and a left eigenvector $\mathbf{v}$ corresponding to the zero eigenvalue.

Let f_i be the ith component of f and

$$a = \sum_{i,j,k=1}^{n} v_i w_j w_k \frac{\partial^2 f_i}{\partial x_j \partial x_k}(0,0), \tag{2.6a}$$

$$b = \sum_{i,j=1}^{n} v_i w_j \frac{\partial^2 f_i}{\partial x_j \partial \phi}(0,0). \tag{2.6b}$$

The local dynamics of system (2.5) around 0 are totally determined by the signs of a and b.

(i) $a > 0$, $b > 0$. When $\phi < 0$ with $|\phi| \ll 1$, the equilibrium point $x = 0$ is locally asymptotically stable, and there exists a positive unstable equilibrium; when $0 < \phi \ll 1$, 0 is unstable and there exists a negative and locally asymptotically stable equilibrium.

(ii) $a < 0$, $b < 0$. When $\phi < 0$ with $|\phi| \ll 1$, the equilibrium point $x = 0$ is unstable; when $0 < \phi \ll 1$, 0 is locally asymptotically stable equilibrium and there exists a positive unstable equilibrium.

(iii) $a > 0$, $b < 0$. When $\phi < 0$ with $|\phi| \ll 1$, the equilibrium point $x = 0$ is unstable, and there exists a locally asymptotically stable negative equilibrium; when $0 < \phi \ll 1$, 0 is stable and there exists a positive unstable equilibrium.

(iv) $a < 0$, $b > 0$. When ϕ changes from negative to positive, the equilibrium point $x = 0$ changes its stability from stable to unstable. Correspondingly, a negative unstable equilibrium becomes positive and locally asymptotically stable.

2.4 Concluding remarks

The literature review on modelling of vaccination behaviour and pre-cautionary health protective behaviour in epidemic models with game-theoretical approaches has been briefly covered in the first part of this chapter. Then, the basics of the epidemic models with partially vaccine-induced immunity, namely the existence of the multiple endemic equilibria, the phenomenon of backward bifurcation and the center manifold theorem used to examine the types of transcritical bifurcation are presented in the second part of this chapter, which serves as the fundamental concepts for more complicated systems in Chapter Four and Five.

Chapter 3

Human Behavioural Responses in an Emerging Epidemic with Two-subpopulation Game-dynamical Model

3.1 Introduction

The role of human behaviour in the spread and control of infectious diseases has received significant attention [39] and has been recognized as a specific discipline in epidemiology, known as behavioural epidemiology [1]. Various behavioural changes, including vaccination, the self-initiated pre-cautionary health protective actions such as social distancing, wearing mask, reducing risky sexual behaviour, reducing travels, practicing better hygiene and avoidence of congregated places, have been incorporated into mathematical and computational epidemic models. Without including behavioural changes, the disease spreading model will predict the "worst" possible scenario [22]. The disease-behaviour models capture the interplay between infectious disease dynamics and individual behaviours under the influence of various factors such as economic [51], social [4] and information [21]. In the course of epidemic outbreak, individuals are not passive; they weigh up the costs associated with certain self-initiated pre-cautionary health protective actions with the benefit of reducing the infection risk, and then choose the best option or strategy that maximizes their own benefit. The individual-level preferences

and strategic decision-making process can be concisely described in the language of game theory.

Unlike the game theory in the field of biology in which strategies are inherited, the underlying mechanism for the evolution of strategy adoption in epidemiology is the imitation process. Individual strategic decision-making can be conveniently fixed into a simple one-population susceptible-infective-recovered (SIR) compartmental model in a well-mixed population setting through the game-dynamical equation. For instance, a replicator equation is used to model imitation dynamics and is coupled into a SIR epidemic model in [2] to investigate the interplay between individual voluntary vaccination behaviour, vaccine coverage and vaccine-preventable childhood disease dynamics, in which parents make the cost-benefit analysis to decide whether or not to vaccinate their children. This model has been extended in [70] by introducing social norm into it. Along similar lines, Poletti and co-authors [74] modelled the spontaneous behavioural changes driven by cost-benefit considerations on the perceived risk of infection whereby their game-dynamical equation involves both the natural selection process and the imitation process. Even with these simple well-mixed one-population models that couple epidemic and imitation dynamics, rich epidemic dynamics, including oscillations and simulation results fitted with real disease incidence data, can be achieved.

In one-population mean-field models, every individual has the same kind of disease-causing contacts and strategy interactions in the homogeneous population. However, individuals are heterogeneous. The minimal level of details required to model the differences in individual behaviour has been identified as one of the nine challenges in incorporating the dynamics of human behaviour in infectious disease models [38]. This challenge is essentially the heterogeneity between groups. That is, people that belong to certain group may be more inclined to certain behaviour or perceive the risk of disease prevalence in a

specific way. These give rise to the development of multi-group epidemic and game-dynamical models.

Compared to one-population models, very few multi-group setting of compartmental models have been used in epidemic modelling incorporating human behaviour. Furthermore, among them, most of the studies are related to vaccination behaviour, with specific investigations on different age groups [6, 93], different countries [67], and different risk perceptions, for instance pro-vaccinator (i.e. vaccine believer) versus anti-vaccinator (i.e. vaccine skeptics) [60, 92]. On the other domain of human behaviour in epidemiology, the multi-population model was used in [75, 76] to study self-initiated precautionary health protective behaviour during epidemic. However, all these studies assume that individuals only make cost-benefit considerations without considering other social factors in their decision making. Hence, we focus on the self-initiated pre-cautionary health protective actions adopted by susceptibles in an emerging epidemic in two-subpopulation setting. The imitation dynamics in our proposed model is constructed by taking account of a combination of cost-benefit and social points of view.

Our proposed model differs from the epidemiology game between two subpopulations constructed by Reluga [76] in the aspects of epidemic dynamics and individual-level decision making. Reluga's epidemic model is in metapopulation setting whereas our proposed epidemic model is still in one single well-mixed population. We make use of the metapopulation concepts in our game dynamical model. This allows us to focus on the heterogeneity of individuals in their decision making whereby susceptibles have competitive strategy interactions in different subpopulations or groups, apart from keeping the full model simpler. In other words, we assume that the physical contacts that cause disease spread is homogeneous, but the behavioural contagion among susceptibles are heterogeneous. By doing so, we are able to study the behavioural response in different groups with different preferences, and conse-

quently how it affects the epidemic dynamics.

The early theoretical extension of game dynamics from one population to two populations can be found in the seminal papers [99, 88]. In two-subpopulation games, in principle, a player could be randomly paired with one other player either from the same or different subpopulation. This leads to two types of strategy interactions, namely intra- (i.e. within) and inter- (i.e. between) subpopulation interactions. If one particular subpopulation consists of only one kind of players, bi-matrix games are suitable for the situation whereby there are only inter-subpopulation but no intra-subpopulation interactions [19, 97]. This specification rules out own subpopulation effects [34]. However, since we are living in a modern society with people from different backgrounds, religious beliefs, cultures, and professions, both intra- and inter-subpopulation strategy interactions are important in shaping our decision making. Therefore, we choose the multi-population game-dynamical modelling framework proposed in [47, 48] in constructing our game-dynamical model. The framework allows strategies within and between groups (subpopulations) with different preferences or beliefs. This is essential in investigating the heterogeneity between groups of individuals in their decision making.

Our proposed model consists of two different dynamics, namely SIR epidemic dynamics and imitation dynamics. To distinguish the homogeneity of our epidemic system and the heterogeneity of our game dynamical system, in this chapter, we use the term 'population' when describing epidemic dynamics and 'subpopulation' when describing imitation dynamics, i.e. epidemic spread in one 'population' with individuals divided into two 'subpopulations' with different preferences in their strategy switching.

In Section 3.2, we construct a two-subpopulation game dynamical model for natural selection and imitation process by taking accounts of the cost-benefit analysis and group pressure. We then carry out the local stability

analysis for the model at disease free equilibrium (DFE) in Section 3.3. Results and discussion are given in Section 3.4 followed by some concluding remarks in Section 3.5.

3.2 Mathematical formulations

In the course of epidemic outbreak, upon receiving information on disease prevalence, rational individuals would react by deciding whether or not to alter their behaviour and adopt some pre-cautionary health protective actions to lower their risk of infection. By adopting altered behaviour, an individual's risk of infection is reduced by a factor of $\alpha \in (0, 1)$ but he/she has to pay some inconvenient cost. Thus, to study this kind of individual decision making using game theory, we assume that individuals have two strategies, namely normal behaviour (or strategy) and altered behaviour whereby the strategy switching is performed by imitating one of the other individuals in the population with the aim to maximize their own payoff. Hence, in this section, we formulate this imitation dynamics by using the so-called "normal against altered behaviour game", leading to a replicator dynamical equation coupled with the SIR epidemic dynamics.

3.2.1 SIR epidemic and a two-subpopulation natural selection model

Following the procedures and definitions in [74], we first extend the system of one-population "natural" selection model into two-subpopulation model. The natural selection is referred to as a form of strategy switching without cost-benefit considerations. We assume that only susceptible involves in "normal against altered behaviour game". Also, each subpopulation has different preferences. We assume that subpopulation 1 prefers normal behaviour and subpopulation 2 prefers altered behaviour. It is worth mentioning that although each subpopulation is designated with their respective preference,

individuals belong to each subpopulation are still given the freedom to adopt either strategies based on the cost-benefit analysis in imitation process. The preference of each subpopulation will later be modelled by adding an extra profit to susceptibles adoting the preferred behaviour in their respective subpopulation.

As a start, in the two-subpopulation setting, at any time step t, the proportion of susceptibles in the population can be subdivided in the following three equivalent forms:

$$\begin{aligned} S(t) &\equiv S_n(t) + S_a(t) \\ &\equiv \left[S_n^1(t) + S_n^2(t)\right] + \left[S_a^1(t) + S_a^2(t)\right] \\ &\equiv \left[p(t)S^1(t) + (1-q(t))S^2(t)\right] + \left[(1-p(t))S^1(t) + q(t)S^2(t)\right]. \end{aligned} \tag{3.1}$$

where the variables S with superscript 1 (or 2) are referred to as the susceptibles that belong to subpopulation 1 (or 2), whereas the variables S with a letter n (or a) in the subscript represent the proportion of susceptibles adopting normal (or altered) behaviour. We assume that the subpopulation of susceptibles does not change throughout the course of epidemic outbreak, i.e. no migrations between subpopulations. Since we focus on the evolution of strategy (or behaviour) frequency distributions under the mechanism of natural selection (and imitation dynamics, as discussed in the next subsection), we denote the proportion of susceptibles adopting the preferred behaviour in subpopulations 1 and 2 with p and q respectively. Hence, it follows that $p(t) \equiv \frac{S_n^1(t)}{S_n^1(t)+S_a^1(t)} \equiv \frac{S_n^1(t)}{S^1(t)}$ and $q(t) \equiv \frac{S_a^2(t)}{S_n^2(t)+S_a^2(t)} \equiv \frac{S_a^2(t)}{S^2(t)}$.

Using all the forms in equation (3.1), we derive the rate equation of susceptibles as follows:

$$
\begin{aligned}
\frac{dS(t)}{dt} &= \frac{dS_n(t)}{dt} + \frac{dS_a(t)}{dt} \\
&= -\beta S_n(t) I(t) - \alpha\beta S_a(t) I(t) \\
&= -\beta \left[S_n^1(t) + S_n^2(t)\right] I(t) - \alpha\beta \left[S_a^1(t) + S_a^2(t)\right] I(t) \\
&= -\beta \left[p(t) S^1(t) + (1 - q(t)) S^2(t)\right] I(t) \\
&\qquad - \alpha\beta \left[(1 - p(t)) S^1(t) + q(t) S^2(t)\right] I(t) \\
&= -\beta \left[p(t) + \alpha(1 - p(t))\right] S^1(t) I(t) - \beta \left[(1 - q(t)) + \alpha q(t)\right] S^2(t) I(t).
\end{aligned} \tag{3.2}
$$

Let $f = f_1$ represent the (relative) power of subpopulation 1 and $(1 - f) = f_2$ the power of subpopulation 2, in which the relative power not only represents the relative size of the subpopulation, but also reflects how much influence a subpopulation has on the strategy choice of individuals [47], and essentially the sizes of both subpopulations evolve in a constant ratio [19]. At any time step t, we assume that the total number of susceptible individuals is subdivided into subpopulation 1 and subpopulation 2 according to its relative power. Thus, $S^1(t) = f\, S(t)$ and $S^2(t) = (1-f)S(t)$. Equation (3.2) becomes

$$
\begin{aligned}
\frac{dS(t)}{dt} &= -\beta \left[p(t) + \alpha(1 - p(t))\right] f S(t) I(t) - \beta \left[(1 - q(t)) + \alpha q(t)\right] (1 - f) S(t) I(t) \\
&= -\beta \left[f p(t) + \alpha f (1 - p(t)) + (1 - f)(1 - q(t)) + \alpha(1 - f) q(t)\right] S(t) I(t).
\end{aligned} \tag{3.3}
$$

From differential calculus, the evolution of the frequency of preferred strategy in subpopulation 1 is given by

$$
\begin{aligned}
\frac{dp(t)}{dt} &= \frac{d}{dt}\Big(\frac{S_n^1(t)}{S^1(t)}\Big) \\
&= \frac{1}{S^1(t)} \frac{d}{dt} S_n^1(t) - \frac{S_n^1(t)}{S^1(t)} \frac{1}{S^1(t)} \frac{d}{dt} S^1(t) \\
&= \frac{1}{fS(t)} \left[-\beta p(t) f S(t) I(t)\right] - p(t) \frac{1}{fS(t)} f \frac{dS(t)}{dt}.
\end{aligned} \tag{3.4}
$$

Substituting (3.3) into (3.4) and simplifying, we obtain

$$\frac{dp(t)}{dt} = \beta p(t)\left[fp(t) + \alpha f(1-p(t)) + (1-f)(1-q(t)) + \alpha(1-f)q(t) - 1\right] I(t). \tag{3.5a}$$

Similarly, the evolution of the frequency of preferred strategy in subpopulation 2 is given by

$$\frac{dq(t)}{dt} = \beta q(t)\left[fp(t) + \alpha f(1-p(t)) + (1-f)(1-q(t)) + \alpha(1-f)q(t) - \alpha\right] I(t). \tag{3.5b}$$

Both equations in (3.5) do not depend explicitly on the densities of susceptible individuals but only on their strategy frequencies. This is aligned with the idea of replicator dynamics even with the restriction in the two-population evolutionary dynamics developed in [20]. However, the density of infectious individuals has an equal effect on all strategies frequency in a given subpopulation.

Combining equations (3.3) and (3.5) into the SIR epidemic model, the "natural" selection process for behavioural distributions in two subpopulations with different preferences (normal against altered behaviour) embedded in the disease transmission dynamics can be rewritten as follows:

$$\frac{dS(t)}{dt} = -\beta X(t)S(t)I(t), \tag{3.6a}$$
$$\frac{dI(t)}{dt} = \beta X(t)S(t)I(t) - \gamma I(t), \tag{3.6b}$$
$$\frac{dR(t)}{dt} = \gamma I(t), \tag{3.6c}$$
$$\frac{dp(t)}{dt} = \beta p(t)\left[X(t) - 1\right] I(t), \tag{3.6d}$$
$$\frac{dq(t)}{dt} = \beta q(t)\left[X(t) - \alpha\right] I(t), \tag{3.6e}$$

where

$$X(t) = fp(t) + \alpha f(1-p(t)) + (1-f)(1-q(t)) + \alpha(1-f)q(t). \tag{3.6f}$$

in which X reflects the population average reduction of force of infection which is determined by the strategy frequency and the relative power in both subpopulations as well as the pre-determined α value. Hereinafter, the independent variable t is dropped for simplicity of notation. We assume that individual behavioural response on disease outbreak (i.e. whether to adopt normal or altered behaviour) is spontaneous and hence the demographic parameters (birth and death rate) are not included in the model. Also, individuals in the system (3.6) do not use cost-benefit analysis in changing their strategy in natural selection model.

By setting $f = 1$ (resp. $f = 0$), the two-subpopulation natural selection model (3.6) reduces to the one-subpopulation model. In the case in which only subpopulation 1 (resp. 2) exists, only equation (3.6d) (resp. equation (3.6e)) is relevant. After some simplifications, we obtain $\frac{dp}{dt} = p(1-p)(\alpha\beta I - \beta I)$ (resp. $\frac{dq}{dt} = q(1-q)(\beta I - \alpha\beta I)$). Since $\alpha\beta I - \beta I < 0$ (resp. $\beta I - \alpha\beta I > 0$), the fraction of S_n^1 (resp. S_a^2) is always decreasing (resp. increasing) in the natural selection process.

3.2.2 The two-subpopulation game-dynamical replicator equations with strategy change through cost-benefit considerations and social group pressure

Apart from driven by natural selection, we assume that individuals also change their strategy in "normal against altered behaviour game" through imitations. To take into account the heterogeneity of individuals' strategy adoptions in different subpopulations (or groups), our imitation dynamics is modelled based on the modelling frameworks in [47, 48]. The payoff matrices and game-dynamical replicator equations appeared in [47, 48] are given in details in Appendix A.

We model our imitation dynamics by taking a combination of cost-benefit

Table 3.1: The 2×2 payoff matrices for the two-subpopulation "normal against altered behaviour game"

The payoff matrices for individuals belonging to subpopulation 1.

(i) A_{ij}^{11}, within-subpopulation interactions

		Interaction partner's behaviour	
Focal		normal (preferred)	altered
agent's behaviour	normal (preferred)	$-c_{1,n}+\Omega_n^1+\delta_1 p$	$-c_{1,n}+\Omega_n^1$
	altered	$-c_{1,a}$	$-c_{1,a}+\delta_1(1-p)$

(ii) A_{ij}^{12}, between-subpopulation interactions

		Interaction partner's behaviour	
Focal		normal	altered (preferred)
agent's behaviour	normal (preferred)	$-C_{1,n}+\Omega_n^1+\delta_{12}p(1-q)$	$-C_{1,n}+\Omega_n^1$
	altered	$-C_{1,a}$	$-C_{1,a}+\delta_{12}(1-p)q$

The payoff matrices for individuals belonging to subpopulation 2.

(i) A_{ij}^{22}, within-subpopulation interactions

		Interaction partner's behaviour	
Focal		normal	altered (preferred)
agent's behaviour	normal	$-c_{2,n}+\delta_2(1-q)$	$-c_{2,n}$
	altered (preferred)	$-c_{2,a}+\Omega_a^2$	$-c_{2,a}+\Omega_a^2+\delta_2 q$

(ii) A_{ij}^{21}, between-subpopulation interactions

		Interaction partner's behaviour	
Focal		normal (preferred)	altered
agent's behaviour	normal	$-C_{2,n}+\delta_{21}(1-q)p$	$-C_{2,n}$
	altered (preferred)	$-C_{2,a}+\Omega_a^2$	$-C_{2,a}+\Omega_a^2+\delta_{21}q(1-p)$

analysis and social point of view. We construct the 2×2 payoff matrices for the two-subpopulation "normal against altered behaviour game", as given in Table 3.1.

Imitation driven by cost-benefit considerations

In normal and altered strategy game, the cost incurred to a player (individual, or agent) adopting a certain strategy will only depend on the type of strategies chosen, but not on the interaction partner's strategy. Hence, we use the notations similar to those employed by [92] in representing costs in different behavioural groups. Specifically, in Table 3.1, we use the lowercase letter $c_{u,v}$ to represent the relevant costs incurred for within-subpopulation

strategy interactions and the uppercase letter $C_{u,v}$ for between-subpopulation interactions, in which the first subscript $u \in \{1, 2\}$ denotes the subpopulation where the focal agent belongs to, and the second subscript $v \in \{n, a\}$ denotes their adopted strategies, i.e. the normal or altered behaviour. We admit that the cost for normal behaviour may sound not realistic, and use it here simply to ensure the elements of payoff matrices have non-zero payoff.

This allow us to assume different costs for normal and/or altered behaviour in different subpopulations and types of strategy interaction. For instance, for within-subpopulation strategy interactions, we could assume that the perceived costs of normal behaviour are likely to be lower in subpopulation 1 than in subpopulation 2, i.e. $c_{1,n} < c_{2,n}$ since normal behaviour is preferred (or favourable) in subpopulation 1. Similarly, we could also assume that the perceived costs of any strategies for between-subpopulation interactions are likely to be greater than their corresponding within-subpopulation interactions, i.e. $C_{u,v} > c_{u,v}$.

To reflect the incompatible preferences, we assume that one of the two strategies in a particular subpopulation is more attractive than the other strategy. For each individual, if one strategy is more attractive, he/she will be better paid if that strategy is chosen [24]. Hence, unlike [47, 48], the incompatible preferences in our proposed model are reflected by adding an extra profit Ω for individuals choosing the preferred strategy in their respective subpopulation, as in [24]. We further denote that the extra profit for individuals adopting preferred normal (resp. altered) behaviour in subpopulation 1 (resp. 2) as Ω_n^1 (resp. Ω_a^2). Since altered behaviour is beneficial in reducing the force of infection, we assume that $\Omega_a^2 \geq \Omega_n^1$.

Imitation under social group pressure

In strategy interactions, it can be phenomenologically assumed that individuals apply group pressure to support conformity and discourage dis-coordinated behaviour. In the one-population game, this could be modelled by subtracting a non-negative value δ from the off-diagonal payoffs or by adding δ to the diagonal elements in the payoff matrix [47, 48]. In the two-subpopulation game, it is possible to assign different magnitudes of group pressure for intra- (i.e. δ_1, δ_2) and inter-subpopulation (i.e. δ_{12}, δ_{21}) strategy interactions, as given in Table 3.1.

By taking the approach similar to [70], the group pressure in our proposed model is included in such a way that individuals playing a strategy receive an additional payoff in proportion to how many others in the subpopulation are also playing that strategy. Note that the average group pressures imposing on the coordinated behaviour (i.e. the agent and his / her interaction partner are from different subpopulation, but both display the same behaviour) in inter-subpopulation interactions are assumed to be equal, i.e. $\delta_{12} = \delta_{21}$, and we have $\delta_{12}p(1-q) = \delta_{21}(1-q)p$ and $\delta_{12}(1-p)q = \delta_{21}q(1-p)$.

Since there are no good epidemiological reasons to claim that the conformity rewards will surplus the cost of altered and/or normal behaviour, δ has to be chosen carefully, small enough to keep the payoffs in negative value. If the group pressure is too large, the outcomes of a game can be transformed [47].

The integration of cost-benefit considerations and social group pressure in deriving the imitation dynamics of two-subpopulation model

To derive the imitation dynamics for our two-subpopulation model, the same approach and simplifications presented in Appendix A are used, together with two further simplifications. Firstly, we set $c_{1,a} = C_{1,a} = c_{2,a} = C_{2,a} \equiv C_a$ and

$c_{1,n} = C_{1,n} = c_{2,n} = C_{2,n} \equiv C_n$ to assume that the cost of altered (resp. normal) behaviour neither depends on the subpopulation an individual belongs to, nor the intra- and inter-subpopulation interactions. Secondly, we set $\delta_1 = \delta_2 = \delta_{12} = \delta_{21} \equiv \delta_0$ for the similar assumptions. These assumptions could be easily relaxed, however, by doing so, there would be nine more parameters to deal with. Understanding the imitation dynamics with all these parameters being varied is not really feasible.

With the above two simplifications and after some algebraic manipulations, we obtain the following imitation dynamical equations:

$$\begin{aligned}\frac{dp}{dt} &= p(1-p)\kappa\big(f\left[C_a - C_n + \Omega_n^1 + \delta_0(2p-1)\right] \\ &\qquad + (1-f)\left[C_a - C_n + \Omega_n^1 + \delta_0(p(1-q)^2 - (1-p)q^2)\right]\big), \qquad (3.7a)\\ \frac{dq}{dt} &= q(1-q)\kappa\big((1-f)\left[C_n - C_a + \Omega_a^2 + \delta_0(2q-1)\right] \\ &\qquad + f\left[C_n - C_a + \Omega_a^2 + \delta_0(q(1-p)^2 - (1-q)p^2)\right]\big). \qquad (3.7b)\end{aligned}$$

where κ is a proportionality constant denoting how willing individuals are to switch to new strategy based on the payoff difference. In a nutshell, the system (3.7) implies that the susceptibles decide whether to adopt normal or altered behaviour by weighting the inconvenient cost of health protective actions against their associated risk of infection under the influence of both intra- and inter-group (or subpopulation) pressure. Similar to the one-population model of [70], $\delta_0(2p-1)$ and $\delta_0(2q-1)$ are the intra-group pressure imposed on subpopulation 1 and 2, respectively.

We take a closer look on the quadratic terms appeared in the expressions of the inter-group pressure in (3.7). The inter-group pressure can be expanded in the following way:

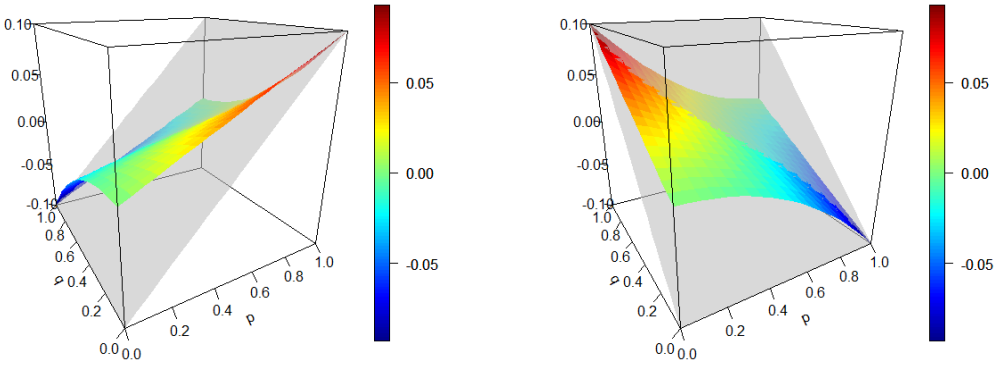

(a) Subpopulation 1

(b) Subpopulation 2

Figure 3.1: The comparison of the magnitude of intra- and inter-group pressure.

$$p(1-q)^2 - (1-p)q^2 = p(1-q) \times (1-q) - (1-p)q \times q$$
$$\equiv \Pr(S_n^1 \text{ meet } S_n^2) \times S_n^2 - \Pr(S_a^1 \text{ meet } S_a^2) \times S_a^2, \quad (3.8a)$$
$$q(1-p)^2 - (1-q)p^2 = q(1-p) \times (1-p) - (1-q)p \times p$$
$$\equiv \Pr(S_a^2 \text{ meet } S_a^1) \times S_a^1 - \Pr(S_n^2 \text{ meet } S_n^1) \times S_n^1. \quad (3.8b)$$

The first (resp. second) probability (Pr) in equation (3.8a) can be interpreted as the inter-group pressure of the coordinated normal (resp. altered) behaviour imposed by susceptibles with normal (resp. altered) behaviour in subpopulation 2 on susceptibles with normal (resp. altered) behaviour in subpopulation 1. By only considering equation (3.8a), if the inter-group pressure of the coordinated normal behaviour is greater (resp. smaller) than the inter-group pressure of the coordinated altered behaviour in inter-subpopulation strategy interactions, the normal behaviour spreads (resp. does not spread) in subpopulation 1. Equation (3.8b) could also be interpreted in the similar way.

However, in the two-subpopulation setting, the players of the game are al-

lowed to have both intra- and inter-subpopulation strategy interactions. The combined effects of both intra- and inter-group pressure on a particular subpopulation could be rather complex. Hence, we plot the magnitudes of the intra- and inter-group pressure acting on subpopulations 1 and 2, respectively, for $0 \leq p, q \leq 1$, with $\delta_0 = 0.1$ in Figure 3.1. The colour surfaces are the variations in the inter-group pressure over all possible values of p and q, whereas the grey planes are the intra-group pressure. Since we set $\delta_0 = 0.1$, the range of either intra- or inter-group pressure is in the interval $[-0.1, 0.1]$. We observe that when both p and q are small (i.e. $p, q < 0.5$), the inter-group (resp. intra-group) pressure has positive (resp. negative) effect on the conformity of the preferred strategy in each subpopulation. On the other hand, when both p and q are large (i.e. $p, q > 0.5$), the inter-group pressure discourages conformity of the preferred strategy in each subpopulation whereas the intra-group pressure stimulates it. In other words, when p and q are either both small or both large, the effect of social group pressure acting on both subpopulations are identical.

However, when p is large (i.e. S_n^1 is majority in subpopulation 1) and q is small (i.e. S_a^2 is minority in subpopulation 2), the inter-group pressure imposed by subpopulation 2 on subpopulation 1 reaches its peak (Figure 3.1(a)). This is because of $\Pr(S_n^1 \text{ meet } S_n^2) \times S_n^2 \gg \Pr(S_a^1 \text{ meet } S_a^2) \times S_a^2$. Then, we have $p(1-q)^2 - (1-p)q^2 > 0$, and the magnitude of this inter-group pressure is even higher than its corresponding intra-group pressure. For this situation to occur in subpopulation 2, p needs to be small and q needs to be large (Figure 3.1(b)). This proportion of strategy frequency corresponds to a scenario whereby the preferred strategy has become the social norm in the population. And, both intra- and inter-group pressures stimulate more individuals following social norm.

The perceived risk of disease prevalence and the speed of two different dynamics

Let the payoffs (Π) associated with adopting normal and altered behaviour are

$$\Pi_n(\tau) = -m_n M(\tau) \equiv -C_n, \tag{3.9a}$$

$$\Pi_a(\tau) = -k_0 - m_a M(\tau) \equiv -C_a, \tag{3.9b}$$

as defined in [74], where $m_n > m_a$. The parameters m_n and m_a are related to the risk of developing disease symptoms induced by individuals with normal and altered behaviours, respectively, while k_0 represents the additional cost of any self-initiated pre-cautionary measure (e.g. social distancing, less traveling, avoidence of congregated places etc.). $M(\tau)$ is the perceived risk of disease prevalence. τ is the time unit for imitation process which has different time scales from the disease transmission, $t = \epsilon\tau$. Since payoff maximization is also cost minimization, we also denote two time-dependent payoffs as the cost of normal behaviour, C_n and the cost of altered behaviour, C_a, respectively, in equations (3.9).

Assume that the susceptibles have full information on disease prevalence, i.e. $M(\tau) = I(\tau)$, which is certainly not realistic. We made this assumption in order to use minimal number of equations in our proposed model. Thus, the expression $C_a - C_n$ in equation (3.7a) can be expressed as

$$\begin{aligned} C_a - C_n &= k_0 + m_a I(\tau) - m_n I(\tau) \\ &= \frac{\epsilon k_0}{\epsilon} - (m_n - m_a) I\left(\frac{t}{\epsilon}\right) && \text{let} \quad \epsilon k_0 = k \\ &= \frac{k}{\epsilon}\left[1 - \left(\frac{m_n - m_a}{k}\right) I(t)\right] && \text{let} \quad m = \frac{m_n - m_a}{k} \\ &= \frac{k}{\epsilon}\left[1 - m I(t)\right]. \end{aligned} \tag{3.10a}$$

Similarly,

$$C_n - C_a = -\frac{k}{\epsilon}\left[1 - mI(t)\right]. \tag{3.10b}$$

The complete model of SIR epidemics coupled with two-subpopulation natural selection process and imitation dynamics

Substituting equations (3.10) into equations (3.7), let $\delta = \epsilon\delta_0$, $\Omega_n = \epsilon\Omega_n^1$, $\Omega_a = \epsilon\Omega_a^2$ and $\rho = \frac{\kappa}{\epsilon}$, the full system of our model becomes

$$\frac{dS}{dt} = -\beta XSI, \tag{3.11a}$$

$$\frac{dI}{dt} = \beta XSI - \gamma I, \tag{3.11b}$$

$$\frac{dR}{dt} = \gamma I, \tag{3.11c}$$

$$\begin{aligned}\frac{dp}{dt} = {} & \beta p(X-1)I + p(1-p)\rho \times \Big(f\left[k(1-mI) + \Omega_n + \delta(2p-1)\right] \\ & + (1-f)\left[k(1-mI) + \Omega_n + \delta(p(1-q)^2 - (1-p)q^2)\right] \Big),\end{aligned} \tag{3.11d}$$

$$\begin{aligned}\frac{dq}{dt} = {} & \beta q(X-\alpha)I + q(1-q)\rho \times \Big((1-f)\left[-k(1-mI) + \Omega_a + \delta(2q-1)\right] \\ & + f\left[-k(1-mI) + \Omega_a + \delta(q(1-p)^2 - (1-q)p^2)\right] \Big),\end{aligned} \tag{3.11e}$$

where $X = fp + \alpha f(1-p) + (1-f)(1-q) + \alpha(1-f)q$. The parameter ρ gives the speed of the imitation process with respect to the disease transmission process as well as a measure of how willing the players are to switch to new strategy based on the payoff difference. If $\rho = 0$, individuals in system (3.11) do not include the cost-benefit analysis in changing their strategies, and system (3.11) reduces to the natural selection model.

As the direct consequences of following the multi-population game dynamical modelling framework in [47, 48], the two subpopulations in our proposed model face a conflict of interest by having different preferences in adopting normal or altered strategy. Therefore, the $\pm$ sign in $+k(1-mI)$ and

$-k(1-mI)$ reflects that the evolution of strategy frequency under the cost-benefit considerations in one subpopulation is the opposite of the outcome on another subpopulation. In a way, this model the common belief that an increase (resp. a decrease) of the cost of adopting altered behaviour will drive more susceptibles in subpopulation 1 (resp. 2) adopting normal (resp. altered) behaviour.

3.3 Local stability analysis

In this section, we present the local stability analysis for the model with no extra benefit, i.e. $\Omega_n = \Omega_a = 0$. At the disease free equilibrium (DFE), $I = 0$, the two-subpopulation replicator dynamical equations (3.11d) and (3.11e) become

$$\frac{dp}{dt} = p(1-p)\rho\, U(p,q) \qquad \equiv u(p,q), \tag{3.12a}$$

$$\frac{dq}{dt} = q(1-q)\rho\, V(p,q) \qquad \equiv v(p,q), \tag{3.12b}$$

where

$$U(p,q) = f\left[k + \delta(2p-1)\right] + (1-f)\left[k + \delta(p(1-q)^2 - (1-p)q^2)\right], \tag{3.12c}$$

$$V(p,q) = (1-f)\left[-k + \delta(2q-1)\right] + f\left[-k + \delta(q(1-p)^2 - (1-q)p^2)\right]. \tag{3.12d}$$

We first find all the possible fixed (or stationary) points of the system (3.12) by equating equations (3.12a) and (3.12b) to 0, respectively.

$$\text{Let} \quad \frac{dp}{dt} = 0 \quad \Leftrightarrow \quad p = 0, 1 \quad \text{or} \quad U(p,q) = 0,$$

$$\text{Let} \quad \frac{dq}{dt} = 0 \quad \Leftrightarrow \quad q = 0, 1 \quad \text{or} \quad V(p,q) = 0.$$

From $p = 0, 1$ and $q = 0, 1$, we obtain the first four fixed points which are located at four respective corners of the pq-plane. Also, another four fixed points on the boundary of the pq-plane can be obtained by setting $q = 0$ or 1

(resp. $p = 0$ or 1) and solving $U(p, q) = 0$ (resp. $V(p, q) = 0$) for the p (resp. q) value. Apart from that, if there exist $0 < p, q < 1$ values that satisfy the two equations $U(p, q) = 0$ and $V(p, q) = 0$ simultaneously, then the system of equations (3.12) does have fixed point on the inner part of the pq-plane. That is, the system (3.12) could possibly have four to nine fixed points in total.

To determine the stability of the system around the fixed points (p_l, q_l), following [48], we first calculate the Jacobian matrix of the system (3.12).

$$J = \begin{bmatrix} \frac{\partial u}{\partial p} & \frac{\partial u}{\partial q} \\ \frac{\partial v}{\partial p} & \frac{\partial v}{\partial q} \end{bmatrix} = \begin{bmatrix} J_{11} & J_{12} \\ J_{21} & J_{22} \end{bmatrix}, \tag{3.13}$$

where

$$\begin{aligned} J_{11} &= (1 - 2p_l)\rho\, U(p_l, q_l) + p_l(1 - p_l)\rho \left[2\delta f + (1 - f)\delta \left((1 - q_l)^2 + q_l^2\right)\right], \\ J_{12} &= p_l(1 - p_l)\rho \left[2(1 - f)\, \delta \left(2p_l q_l - p_l - q_l\right)\right], \\ J_{21} &= q_l(1 - q_l)\rho \left[2f\delta \left(2p_l q_l - p_l - q_l\right)\right], \\ J_{22} &= (1 - 2q_l)\rho V(p_l, q_l) + q_l(1 - q_l)\rho \left[2\delta(1 - f) + f\delta \left((1 - p_l)^2 + p_l^2\right)\right]. \end{aligned} \tag{3.14}$$

At the fixed point (p_l, q_l), the eigenvalues (i.e. η_l and ν_l) of the Jacobian matrix are given by the determinant below:

$$\begin{vmatrix} J_{11} - \eta_l & J_{12} \\ J_{21} & J_{22} - \nu_l \end{vmatrix} = 0, \tag{3.15a}$$

which gives the characteristic equation,

$$(J_{11} - \eta_l)(J_{22} - \nu_l) - J_{12}J_{21} = 0. \tag{3.15b}$$

From equations (3.14) and (3.15), we obtain the solution of the eigenvalues at all possible points, as listed in the Table 3.2.

From the results given in Table 3.2, we can determine the nature (the

Table 3.2: The fixed points and their associated eigenvalues when $\Omega_n, \Omega_a = 0$

l	Fixed point (p_l, q_l)	Associated eigenvalues, η_l and ν_l
1	$(0,0)$	$\eta_1 : -\rho(f\delta - k)$ $\nu_1 : -\rho(k + (1-f)\delta)$
2	$(1,0)$	$\eta_2 : -\rho(k + \delta)$ $\nu_2 : -\rho(k + \delta)$
3	$(0,1)$	$\eta_3 : \rho(k - \delta)$ $\nu_3 : \rho(k - \delta)$
4	$(1,1)$	$\eta_4 : -\rho(f\delta + k)$ $\nu_4 : -\rho(-k + (1-f)\delta)$
5	$(p_5 = \frac{f\delta - k}{\delta f + \delta}, 0)$	$\eta_5 : p_5(1-p_5)\rho(f\delta + \delta)$ $\nu_5 : \rho((1-f)(-k-\delta) + f(-k - \delta p_5^2))$
6	$(p_6 = \frac{\delta - k}{\delta f + \delta}, 1)$	$\eta_6 : p_6(1-p_6)\rho(f\delta + \delta)$ $\nu_6 : -\rho((1-f)(-k+\delta) + f(-k + \delta(1-p_6)^2))$
7	$(1, q_7 = \frac{k+\delta}{2\delta - \delta f})$	$\eta_7 : -\rho(f(k+\delta) + (1-f)(k + \delta(1-q_7)^2))$ $\nu_7 : q_7(1-q_7)\rho(2(1-f)\delta + \delta f)$
8	$(0, q_8 = \frac{k + \delta(1-f)}{2\delta - \delta f})$	$\eta_8 : \rho(f(k-\delta) + (1-f)(k - \delta q_8^2))$ $\nu_8 : q_8(1-q_8)\rho(2(1-f)\delta + \delta f)$

stability state) of each of the fixed points based on the solution of the two eigenvalues at the point. If both eigenvalues are negative, the fixed point is a stable node, for example, at the point $(p_2, q_2) = (1, 0)$, η_2 and ν_2 are always negative and hence the point is always a stable node. If the eigenvalues are both positive at a fixed point, then the point is an unstable point; and if the eigenvalues have opposite sign then the point is a saddle point. For example, at the point $(p_3, q_3) = (0, 1)$, $\eta_3 < 0$ and $\nu_3 < 0$ if $k < \delta$ and $\eta_3 > 0$ and $\nu_3 > 0$ if $k > \delta$. So, the point is stable if $k < \delta$ or otherwise unstable. At the point $(1, 1)$, $\eta_4 < 0$ and $\nu_4 > 0$ if $k > (1-f)\delta$ and so this point is a saddle point if $k > (1-f)\delta$. It can be seen that when $\delta \to 0$, the fixed points (p_l, q_l) with $l = 5, 6, 7, 8$ do not exist.

Similarly, for the two subpopulation models with extra profit given to susceptibles adopting the preferred behaviour, i.e. $\Omega_n, \Omega_a \neq 0$, by carrying out a similar local stability analysis, we obtain the fixed points and its associated eigenvalues as listed in Table 3.3, where $p_5 = \frac{f\delta - \Omega_n - k}{\delta f + \delta}$, $p_6 = \frac{\delta - \Omega_n - k}{\delta f + \delta}$, $q_7 = \frac{k - \Omega_a + \delta}{2\delta - \delta f}$, and $q_8 = \frac{k - \Omega_a + \delta(1-f)}{2\delta - \delta f}$. It is interesting to note that by adding

Table 3.3: The fixed points and their associated eigenvalues when $\Omega_n, \Omega_a \neq 0$

l	Fixed point (p_l, q_l)	Associated eigenvalues, η_l and ν_l
1	$(0,0)$	$\eta_1 : -\rho(f\delta - k - \Omega_n)$ $\nu_1 : -\rho(k - \Omega_a + (1-f)\delta)$
2	$(1,0)$	$\eta_2 : -\rho(k + \Omega_n + \delta)$ $\nu_2 : -\rho(k - \Omega_a + \delta)$
3	$(0,1)$	$\eta_3 : \rho(k + \Omega_n - \delta)$ $\nu_3 : \rho(k - \Omega_a - \delta)$
4	$(1,1)$	$\eta_4 : -\rho(f\delta + \Omega_n + k)$ $\nu_4 : -\rho(-k + \Omega_a + (1-f)\delta)$
5	$(p_5, 0)$	$\eta_5 : p_5(1-p_5)\rho(f\delta + \delta)$ $\nu_5 : \rho((1-f)(-k + \Omega_a - \delta) + f(-k + \Omega_a - \delta p_5^2))$
6	$(p_6, 1)$	$\eta_6 : p_6(1-p_6)\rho(f\delta + \delta)$ $\nu_6 : -\rho((1-f)(-k + \Omega_a + \delta) + f(-k + \Omega_a + \delta(1-p_6)^2))$
7	$(1, q_7)$	$\eta_7 : -\rho(f(k + \Omega_n + \delta) + (1-f)(k + \Omega_n + \delta(1-q_7)^2))$ $\nu_7 : q_7(1-q_7)\rho(2(1-f)\delta + \delta f)$
8	$(0, q_8)$	$\eta_8 : \rho(f(k + \Omega_n - \delta) + (1-f)(k + \Omega_a - \delta q_8^2))$ $\nu_8 : q_8(1-q_8)\rho(2(1-f)\delta + \delta f)$

the extra profit into the model, it affects the stability of the fixed points substantially. For instance, if Ω_a is sufficiently large, i.e. $\Omega_a > k + \delta$, then $\nu_2 > 0$. Thus, it is possible to have the fixed point $(1, 0)$ as a saddle point, rather than a stable node as in the case with no extra profit.

3.4 Results and discussion

3.4.1 The two-subpopulation model with no extra profit for adopting the preferred behaviour (i.e. $\Omega_n = \Omega_a = 0$)

The key parameter which characterizes the speed of the imitation process with respect to the "natural" selection process is ρ. By setting $\rho = 0$ (Figure 3.2(a)), the imitation dynamic model is reduced to the "natural" selection model. Without the influence of imitation, the altered behaviour in subpopulation 2 grows in a modest scale, whereas the normal behaviour in subpopulation 1 declines slightly in a single epidemic outbreak for all

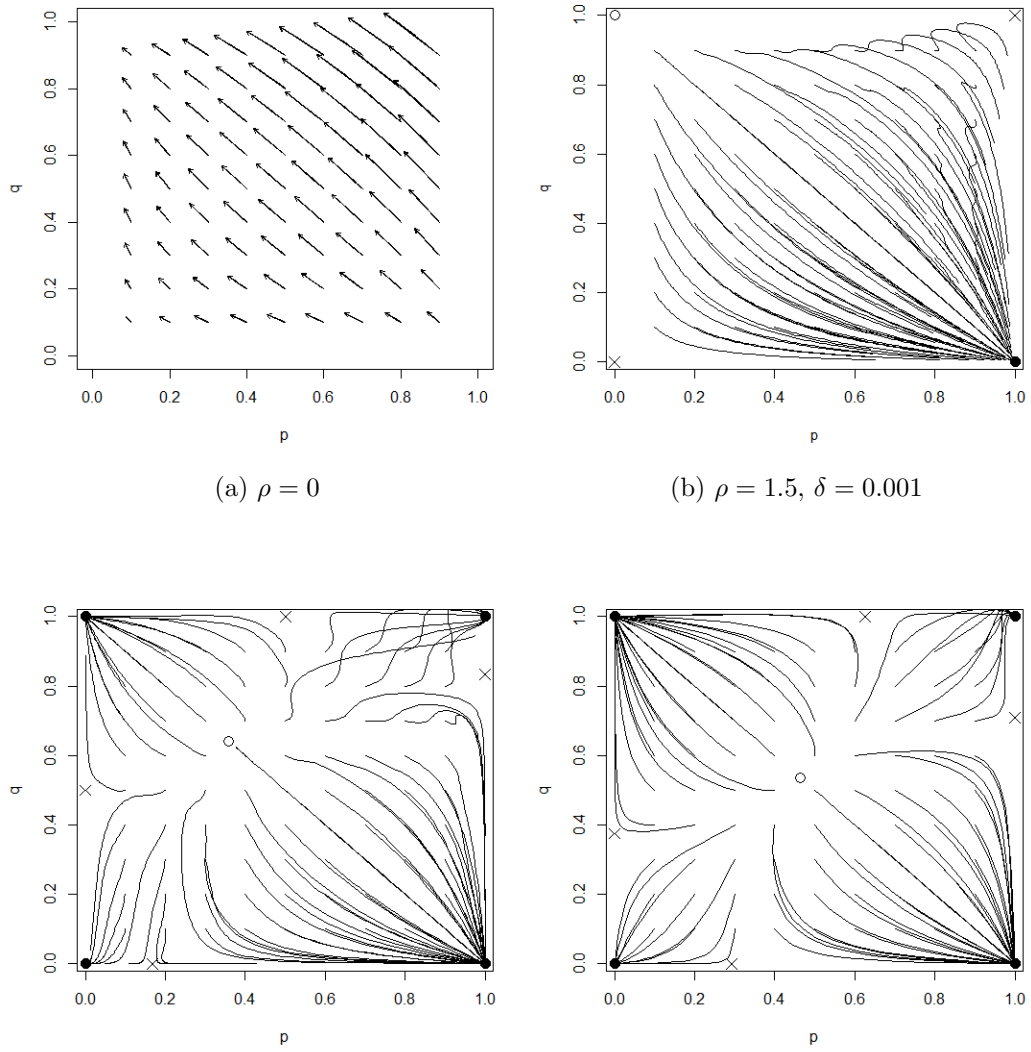

(a) $\rho = 0$

(b) $\rho = 1.5$, $\delta = 0.001$

(c) $\rho = 1.5$, $\delta = 0.1$

(d) $\rho = 1.5$, $\delta = 0.4$

Figure 3.2: The $(p(t), q(t))$ trajectories for the natural selection model and the imitation dynamic model with different magnitudes of group pressure δ.

initial conditions $(p(0), q(0))$. The initial conditions $(p(0), q(0))$ can be regarded as the previous history of proportion of susceptibles adopting normal and altered strategies in both subpopulations, which is indeed the existing preferences of particular subpopulation. We simulate all results by using $0.1 \leq p(0), q(0) \leq 0.9$ in order to make sure that all pure strategies of the imitation game are present in the initial subpopulations. In Figure 3.2, $\{\bullet, \circ, \times\}$ denotes $\{\text{stable}, \text{unstable}, \text{saddle}\}$ point, respectively. Unless oth-

erwise specified, the combination of parameter values $(\beta, \gamma, \alpha, \rho, f, m, k, \delta) = (0.625, 0.25, 0.86, 1.5, 0.5, 0.1, 0.025, 0.1)$ is used for all simulations in this chapter, together with the initial conditions $S(0) = 0.95$, $I(0) = 0.05$. This pair of β and γ values gives the basic reproduction number, $R_0 = \frac{\beta}{\gamma} = 2.5$ which is the R_0 for airborne droplet transmission, such as influenza ($R_0 = 2$ to 3) [64]. The simulations end at 80 time steps, with $\triangle t = 1$.

By incorporating social group pressure and cost-benefit analysis into the imitation dynamics of the two-subpopulation model, i.e. set $\rho > 0$, there exist four basins of attraction in the game dynamics leading to four fixed points, respectively, provided $\delta > k$, as shown in Figure 3.2(c) and (d). The stationary solution $(p, q) = (1, 0)$ (resp. $(0, 1)$) means that all individuals finally adopt the behaviour preferred in subpopulation 1 (resp. 2), meanwhile $(p, q) = (1, 1)$ (resp. $(0, 0)$) corresponds to the case where both subpopulations will (resp. will not) end up with subpopulation-specific norms (i.e. every subpopulation just does what it likes [48]). By comparing Figure 3.2(a) to other figures in Figure 3.2, we conclude that without the imitation dynamics, the "natural" selection can only drive a small portion of susceptibles to switch their strategies, i.e. the expected temporal change of behavioural pattern of susceptibles in both subpopulations is minimal. By including the imitation dynamics with the social group pressure, the behavioural pattern of susceptibles will eventually end up in one of the four specific directions.

The existence of four basins of attraction can be explained qualitatively as follows. When both $p(0)$ and $q(0)$ are small, i.e. the proportions of the preferred behaviour in their respective subpopulation are low, from the perspective of any susceptibles adopted the preferred behaviour, the impact of intra-group pressure has on strategy switching is smaller than the inter-group pressure. In other words, susceptibles with preferred behaviour in either subpopulation will have higher probability of meeting one other susceptible with the coordinated behaviour from another subpopulation than from the same

subpopulation. For any specific pairs of p and q, the effect of the intra-group pressure is always larger than the inter-group pressure, this results in a fall of the preferred behaviour in both subpopulations. Thus, non-preference behaviour survives in their respective subpopulation and everybody behaves non-coorperatively in the end. For large $p(0)$ and $q(0)$, the proportion of the preferred behaviour in their respective subpopulation is high. The intra-group pressure thus has a considerate effect on stimulating more susceptibles adopting the preferred behaviour. Hence, both subpopulations will be eventually occupied by susceptibles with their respective subpopulation preferred behaviour. For initial conditions with large (resp. small) $p(0)$ but small (resp. large) $q(0)$, the majority of susceptibles in both subpopulations are with normal (resp. altered) behaviour, and both intra- and inter-group pressure in subpopulations will drive more susceptibles to adopt the normal (resp. altered) behaviour. Therefore, trajectories $(p(t), q(t))$ evolve toward the fixed point $(1, 0)$ (resp. $(0, 1)$).

For the imitation dynamic model with the magnitude of group pressure $\delta = 0.001$ (Figure 3.2(b)), almost all $(p(t), q(t))$ flow lines move towards the fixed point $(1, 0)$. All susceptibles are expected to end up with normal behaviour as the epidemic outbreak is over. However, if a large δ value is used, for instance $\delta = 0.4$ (Figure 3.2(d)), the effect of group pressure is more pronounced and the trajectories $(p(t), q(t))$ follow a more distinct path towards their respective fixed points.

Based on the fixed points and eigenvalues given in Table 3.2, we examine the nature of each fixed point in Figure 3.2(b) and 3.2(c) by evaluating its associated eigenvalues, as given in Table 3.4. The numerical simulation results as shown in Figure 3.2 are in good agreement with the results of the local stability analysis in Section 3.3. With the combination of parameter values used in Figure 3.2(b), there are no real solutions within the range $[0, 1]$ for the simultaneous equations $U(p_9, q_9) = 0$ and $V(p_9, q_9) = 0$ (i.e. equations (3.12c)

Table 3.4: The fixed points and their associated eigenvalues for Figure 3.2 (b) and 3.2(c)

l	Fixed point (p_l, q_l)	Figure 3.2(b)			Figure 3.2(c)		
		η_l	ν_l	Type of point	η_l	ν_l	Type of point
1	$(0, 0)$	0.037	-0.038	SP	-0.038	-0.113	stable
2	$(1, 0)$	-0.039	-0.039	stable	-0.188	-0.188	stable
3	$(0, 1)$	0.036	0.036	unstable	-0.113	-0.113	stable
4	$(1, 1)$	-0.038	0.037	SP	-0.113	-0.038	stable
5	$(0.167, 0)$	Note: All p_5, p_6, q_7 and q_8 values are out of range $[0, 1]$. Therefore, no fixed points on the boundary of the pq-plane.			0.031	-0.115	SP
6	$(0.5, 1)$				0.056	-0.056	SP
7	$(1, 0.833)$				-0.115	0.031	SP
8	$(0, 0.5)$				-0.056	0.056	SP
9	$(0.36, 0.64)$	No inner fixed points.			0.029	0.059	unstable

SP = saddle point

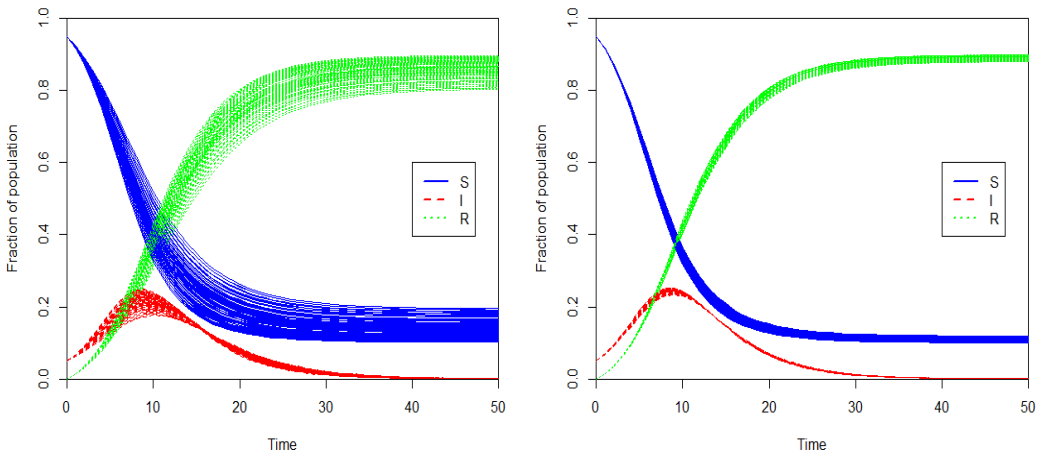

(a) $\alpha = 0.78$ (b) $\alpha = 0.94$

Figure 3.3: The time evolution of SIR dynamics with different reductions of force of infection, α.

and (3.12d)). However, for Figure 3.2(c), there exists one real solution which gives the inner fixed point $(p_9, q_9) = (0.36, 0.64)$.

As suggested in [74], the reduction of force of infection received by altered susceptible is in the range of $\alpha \in (0.78, 0.94)$. Hence, by taking its lowest and highest value, the time evolutions of the SIR dynamics with all possible initial conditions $(p(0), q(0))$ are plotted in Figure 3.3. A lower α

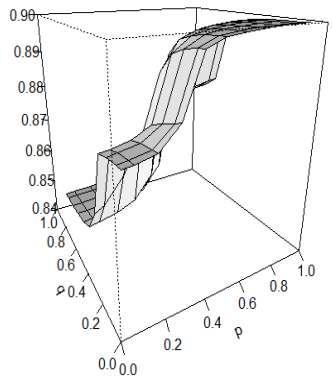

(a) $f = 0.5$

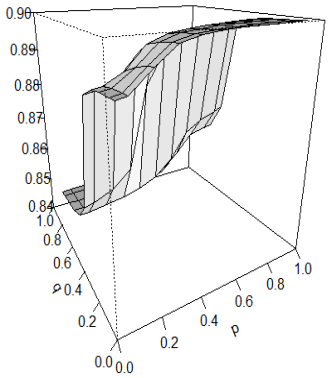

(b) $f = 0.25$

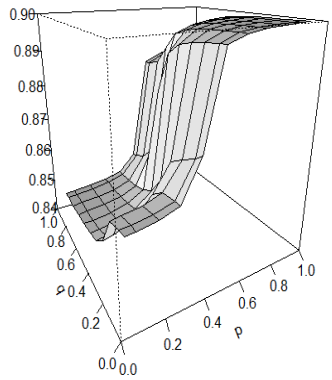

(c) $f = 0.75$

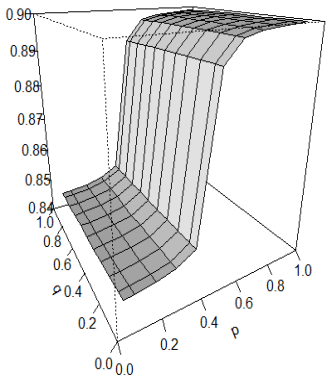

(d) $f = 0.99$

Figure 3.4: The epidemic final size with different (relative) power of subpopulation, f.

value implies greater benefits to altered susceptibles and results in considerable variance in the epidemic final sizes. On the other hand, for $\alpha = 0.94$, the altered susceptibles do not reduce much of their probability of being infected and the epidemic final sizes become more consistent with all initial conditions $(p(0), q(0))$ considered. Hence, we use the median value $\alpha = 0.86$ throughout the simulations in this chapter.

Instead of the typical SIR time evolution presented in Figure 3.3, we illustrate the correlation between the previous history of proportion of strategies in both subpopulations and the epidemic final size, with $\alpha = 0.86$ and $\delta = 0.4$ in Figure 3.4. When the two subpopulations are equally strong (i.e. $f = 0.5$), the severity of the epidemic outbreak is low (resp. high) if the initial proportion of susceptible with preferred altered behaviour is high (resp. low) (Figure 3.4(a)). However, if we incorporate the heterogeneity between subpopulations, the epidemic final sizes may be significantly changed. For the scenario whereby the subpopulation 2 is stronger than subpopulation 1, if the initial proportion of susceptibles with preferred altered behaviour is minority in its subpopulation, the epidemic final sizes almost reach its peak regardless of the initial proportion of susceptibles with preferred normal behaviour in another subpopulation (Figure 3.4(b)).

In contrast, the epidemic final sizes are relatively high when the initial proportion of susceptibles with normal behaviour in subpopulation 1 is dominant, regardless the initial proportion of susceptibles with altered behaviour in subpopulation 2, when subpopulation 1 is more powerful than subpopulation 2 (Figure 3.4(c)). It can thus be suggested that not only the heterogeneity among individuals but also the heterogeneity of subpopulations has an important impact on the epidemic dynamics. If the more powerful subpopulation prefers normal (resp. altered) behaviour and the initial proportion of the preferred strategy is majority (resp. minority), the epidemic final size is high regardless the initial proportion of the other subpopulation. Figure 3.4(d) highlights the scenario of population with single preference whereby we purposely impose an extreme high relative strength on subpopulation 1 by setting $f = 0.99$. By doing so, the whole population can be regarded as comprising of only one single group with normal behaviour as their preference. Without heterogeneity between groups in a population, the epidemic final sizes evolve smoothly as compared to the model of two subpopulations with different relative strengths.

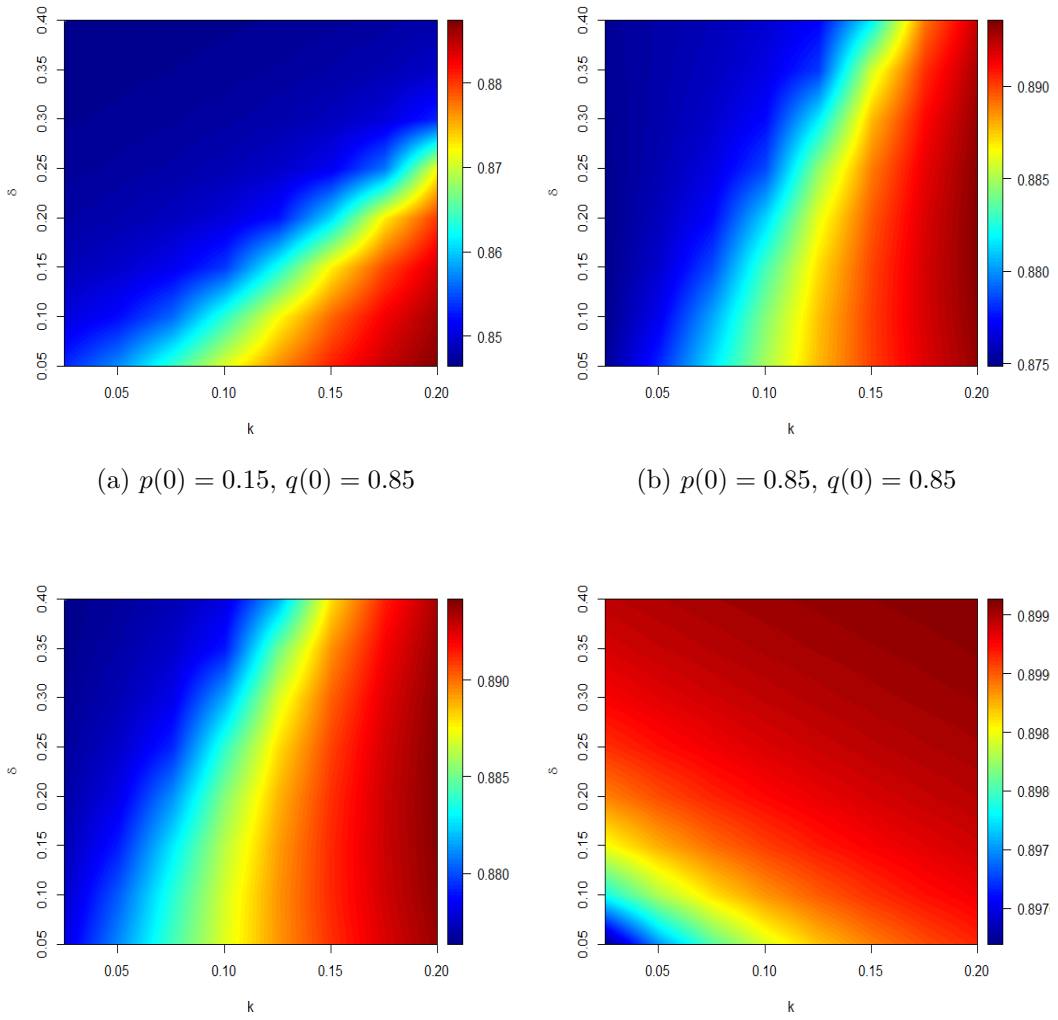

(a) $p(0) = 0.15$, $q(0) = 0.85$

(b) $p(0) = 0.85$, $q(0) = 0.85$

(c) $p(0) = 0.15$, $q(0) = 0.15$

(d) $p(0) = 0.85$, $q(0) = 0.15$

Figure 3.5: The contour plots of the epidemic final size in parameter space (δ, k).

As our two-subpopulation model incorporates both cost-benefit considerations and social group pressure, each of these factors should be weighed according to its relative impact on the epidemic final size. Hence, we explore the parameter space (δ, k) for $\delta \in [0.05, 0.4]$ and $k \in [0.025, 0.2]$ for four different initial proportions of strategies in two subpopulations in Figure 3.5. In particular, Figure 3.5(a) (resp. 3.5(d)) corresponds to the case with high initial proportion of altered (resp. normal) susceptible in both sub-

populations. The lowest epidemic final size in Figure 3.5(a) and the highest in Figure 3.5(d), among four panels in Figure 3.5, again suggests that the previous history of strategies adopted by susceptible in both subpopulations has a significant effect on epidemic dynamics. Figure 3.5(b) and 3.5(c) show similar results simply because both subpopulations are equally strong and the proportions of susceptibles with altered and normal behaviour in the initial population are quite compatible.

All panels in Figure 3.5 show that the increase of additional costs to those adopting altered behaviour during epidemic outbreak would discourage people to take up pre-cautionary health protective actions and hence results in higher epidemic final size. For a specific cost of altered behaviour, the severity of epidemic outbreak could be reduced if the intensity of the social group pressure increases (Figure 3.5(a) to 3.5(c)). However, interestingly, the social group pressure could be a "double edged sword" if the initial proportions of the normal behaviour susceptibles are already the majority in both subpopulations. The increases of social group pressure acting on normal susceptibles will give rise to higher epidemic final size (Figure 3.5(d)). This finding aligns with that of [70], who identified that social norms could either support or hinder immunization goals.

3.4.2 The two-subpopulation model with extra profit for adopting the preferred behaviour (i.e. $\Omega_n, \Omega_a \neq 0$)

For the two-subpopulation model presented in Section 3.4.1, when the effect of social group pressure is sufficiently large, the $(p(t), q(t))$ trajectories form four basins of attraction. However, this social group pressure may be balanced out by extra profit Ω given to individuals adopting the preferred strategy in their respective subpopulation. Therefore, including the extra profit Ω results in a variety of interesting game dynamics in which four basins of attraction

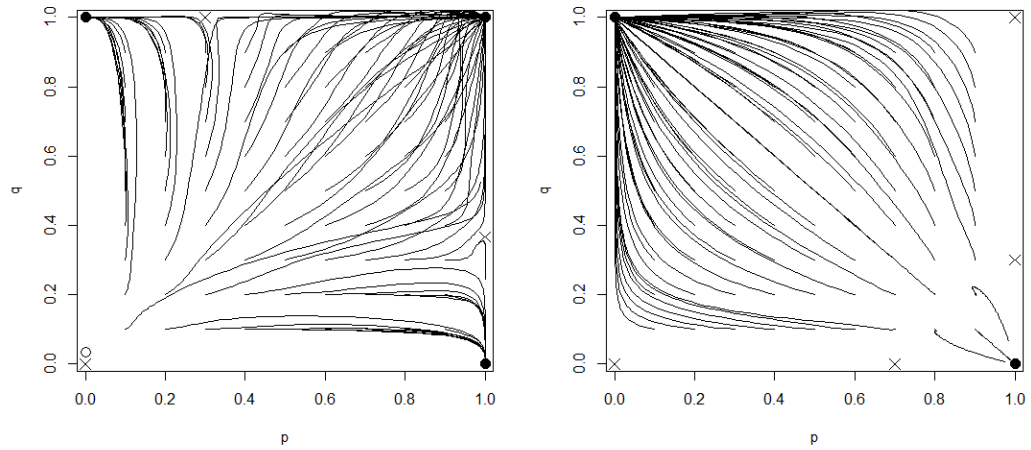

(a) $\Omega_n = 0.03$, $\Omega_a = 0.07$ (b) $\Omega_n = -0.08$, $\Omega_a = 0.08$

Figure 3.6: Comparing the $(p(t), q(t))$ trajectories between the imitation process with different extra profits.

could be reduced to only two (or three) basins of attraction. For instance, with $\Omega_n = 0.03$ and $\Omega_a = 0.07$ (Figure 3.6(a)), both subpopulations end up with subpopulation-specific norms (coexisting "subcultures", as defined in [47]) whenever the initial fractions $p(0)$ and $q(0)$ are not very different. With $\Omega_n = -0.08$ and $\Omega_a = 0.08$ in which negative value of Ω_n implies that for individuals in subpopulation 1, he/she will be punished if adopting the preferred normal strategy, we find that all individuals in both subpopulations finally adopt the preferred altered strategy in subpopulation 2 for most of the initial conditions $(p(0), q(0))$ (Figure 3.6(b)). The location and stability of the fixed points in Figure 3.6 are verified with the local stability analysis and are given in Table 3.5.

3.5 Concluding remarks

We conclude this chapter with the following remarks.

(i) Without imitation dynamics, the "natural" selection drives only a small

Table 3.5: The fixed points and their associated eigenvalues for Figure 3.6

l	(p_l, q_l)	Figure 3.6(a)			(p_l, q_l)	Figure 3.6(b)		
		η_l	ν_l	Type of point		η_l	ν_l	Type of point
1	$(0, 0)$	0.008	-0.008	SP	$(0, 0)$	-0.158	0.008	SP
2	$(1, 0)$	-0.233	-0.083	stable	$(1, 0)$	-0.068	-0.067	stable
3	$(0, 1)$	-0.068	-0.218	stable	$(0, 1)$	-0.233	-0.233	stable
4	$(1, 1)$	-0.158	-0.143	stable	$(1, 1)$	0.008	-0.158	SP
5	NA	-	-	-	$(0.7, 0)$	0.047	-0.029	SP
6	$(0.3, 1)$	0.047	-0.179	SP	NA	-	-	-
7	$(1, 0.367)$	-0.188	0.052	SP	$(1, 0.3)$	-0.029	0.047	SP
8	$(0, 0.033)$	0.007	0.007	unstable	NA	–	-	-

SP = saddle point, NA = no answer

number of susceptibles switching their strategy.

(ii) By including sufficiently large magnitude of social group pressure in imitation dynamics, there exist four basins of attraction for the behavioural pattern of susceptibles in the two-subpopulation model.

(iii) With other parameter values fixed, the outcome of the strategy switching depends on the initial proportion of susceptibles with normal and altered strategies in both subpopulations.

(iv) There exists a correlation between the previous history of proportion of strategies in both subpopulations and the epidemic final size.

(v) The increase of additional cost to the susceptibles with altered behaviour discourages people from taking up pre-cautionary health protective actions and hence results in higher epidemic final size. For a specific cost of altered behaviour, the social group pressure could be a "double edged sword", though.

Chapter 4

SIRVS Epidemic Model with Two-class Vaccine-induced Immunity and Vaccination Population Games

4.1 Introduction

Behavioural factors play an important and crucial role in determining the success of a voluntary vaccination programme for infectious diseases. Individual vaccination decisions are usually based on a complex balance of perceived costs of vaccination and disease. The perceived cost of vaccination is highly influenced by the perceived probability of vaccine complications (for instance, the vaccine side effects (VSE)) and the degree of protection conferred by vaccines, which is closely related to the vaccine efficacy and vaccine failure. Both the vaccine efficacy and vaccine failure will be termed as vaccine imperfection in this chapter.

According to [109], the vaccine efficacy is defined as the theoretical success rate whereas the vaccine efficiency is indeed the practical observed success in preventing vaccinated individuals from getting infections. In reviewing the literature, it is not uncommon that the vaccine imperfections have been taken into account for a more realistic modelling exercise in epidemiology, for instance, in [65]. Imperfect vaccines always increase the critical vaccination

threshold that may lead to disease eradication [40] simply because being vaccinated does not always confer vaccine-acquired immunity. Overall, vaccine failure could arise in three aspects. First, vaccine may fail to generate immunity in a fraction of people vaccinated, which is defined as vaccine failure in take ("all-or-nothing") [31, 59]. Second, vaccine may only offer partial protection to vaccinated individuals either in reducing an individual susceptibility to infection or subsequent transmission if the individual becomes infected, as well as speeding up recovery. Such vaccines permit vaccine failure in degree, described as "leaky" in [50, 59]. Centers for Disease Control and Prevention (CDC) [15] claims that if someone who has been vaccinated with chickenpox vaccine does get the disease, it is usually very mild and they can recover faster than those who are not vaccinated. Third, for many diseases, the vaccine-(and disease-) acquired immunity wanes over time which is described as vaccine failure in duration [46, 59]. For instance, pertussis (whooping cough) vaccines for adolescents and adults could protect about 7 out of 10 people in the first year after getting vaccinated, but only fully protecting 3 or 4 out of 10 people in four years after getting the vaccine [16].

Since individuals are not vaccinated at the same time in voluntary vaccination, it is possible, therefore, that vaccinated individuals with fully protective vaccine-acquired immunity coexist with other vaccinated individuals with partially protective vaccine-acquired immunity in the population. The epidemic dynamics of this coexistence of fully and partially protected vaccinated individuals is well-captured in a SIRVS epidemic model extended with two classes of vaccine-induced immunity [30], where vaccinated individuals first have high vaccine-acquired immunity with full protection from infection and their immunity wanes in two stages, from high to low immunity (where individuals still have some partial protection) and from low to no immunity following a gamma distribution. Apart from that, another two features in the extended model in [30] are that the vaccine may reduce transmissibility and accelerate recovery in breakthrough infections for vaccinated infected individ-

uals. These make the model suitable for investigating the epidemic dynamics with vaccine failure in degree and in duration.

It is possible to hypothesise that no one takes vaccination until the vaccine is sufficiently efficient in protecting vaccinated individuals from infection, and also, an increase in vaccine efficacy will boost vaccine uptake level. However, in a population of self-interested individuals, high vaccine efficacy leads to uptake drops due to free-riding effects [113]. When vaccine immunity wanes slowly, vaccine coverage is expected to be low but stable [110]. This is because when vaccines are able to provide long-term protection, the risk awareness among individuals may be hard to maintain and this could lead to substantial drop in vaccination coverage and is likely to result in severe infrequent epidemics [105]. The imperfections of vaccine also increase the probability of non-vaccinating and the overall cost of optimum vaccination strategy [87]. When the vaccination cost is higher than the threshold value for the vaccine imperfection, vaccination behaviours do not spread across the population and the disease could also invade in scale-free networks [13]. Another implication of the vaccination confers partial immunity on vaccination behaviours is the existence of multiple equilibria of vaccination rate in voluntary vaccination program [79].

These findings suggest that a strong interplay between vaccine imperfection, vaccination coverage and disease dynamics arises. However, the findings may be somewhat limited by the definition of vaccine efficacy in the above-mentioned literatures whereby they are merely referred to the reduction of susceptibility to infection. The impacts of several other characteristics of imperfect vaccines on individual vaccination decision-making remain unanswered at present. Hence, in this chapter, we employ the SIRVS epidemic model with two classes of vaccine-induced immunity and additional characteristics of imperfect vaccine (namely, the reduction of transmissibility and faster recovery) in [30], together with the vaccination population games framework [79], to

investigate the interplay between these characteristics of imperfect vaccines, the relative cost of vaccination to infection, the force of infection, the individual and population vaccination rates.

In Section 4.2, the full SIRVS epidemic model with two classes of vaccine-induced immunity is presented. Since models with imperfect vaccines exhibit backward bifurcation [44], we then show that the SIRVS model with two classes of vaccine-induced immunity undergoing backward bifurcation by using center manifold theory in Subsection 4.2.1. Subsection 4.2.2 concerns the analysis of the effective reproduction number. Then the details of vaccination population games for two classes of vaccine-induced immunity model are explored in Section 4.3. Results are discussed in Section 4.4 and some concluding remarks are given in Section 4.5.

4.2 Analysis of the SIRVS epidemic model with two classes of vaccine-induced immunity

The population-scale dynamics of the vaccination population games can be described by the SIRVS model with two classes of vaccine-induced immunity in the extended model in [30]:

$$\begin{aligned}
\frac{dS}{dt} &= \Lambda - \lambda S - \bar{\pi} S + \omega_R R + \omega_V V_2 - \mu S, \\
\frac{dI}{dt} &= \lambda S - \gamma_u I - \mu I, \\
\frac{dW}{dt} &= \sigma \lambda V_2 - \gamma_v W - \mu W, \\
\frac{dR}{dt} &= \gamma_u I + \gamma_v W - \omega_R R - \mu R, \\
\frac{dV_1}{dt} &= \bar{\pi} S - \gamma_1 V_1 - \mu V_1, \\
\frac{dV_2}{dt} &= \gamma_1 V_1 - \sigma \lambda V_2 - \omega_V V_2 - \mu V_2,
\end{aligned} \tag{4.1}$$

where Λ denotes the (constant) recruitment rate of susceptible corresponding to births and immigration, and μ is the natural death rate of the population.

The total population at time t, $N(t)$, is divided into six mutually exclusive subpopulations, namely susceptible (S), two compartments for respective two classes of infected individuals (I and W), recovered (R), two compartments for respective two classes of vaccinated individuals (V_1 and V_2). Specifically, those individuals in the V_1 class are the vaccinated individuals with high vaccine-induced immunity. They are fully protected from infection until their vaccine-induced protection is reduced and they then move to the V_2 class at a rate γ_1. While these vaccinated individuals reside in the V_2 class, they only gain low vaccine-induced immunity, i.e. partial protection provided by the vaccine. When the breakthrough infection of individuals in the V_2 class occurs, they move to the vaccinated infected class, W at the rate $\sigma\lambda$, where $0 \leq \sigma < 1$ is the relative risk of infection for vaccinated individuals in the V_2 class compared to unvaccinated susceptible individuals, or simply the probability of vaccine failure in degree, with the vaccine efficacy given by $1 - \sigma$. Thus, it is assumed that the vaccine is regarded as fully effective to individuals in the V_1 class and imperfect to individuals in the V_2 class. Meanwhile, the unvaccinated susceptible individuals, S, move to the unvaccinated infected class, I, at the rate λ.

The individuals in the I and W classes differ from two aspects resulted from the imperfect vaccine. First, unlike the unvaccinated infected individuals in the I class with disease transmissibility β, the vaccinated infected individuals in the W class can only transmit infection at a reduced rate $\theta\beta \leq \beta$, where $0 < \theta \leq 1$ is a modification parameter that accounts for the reduced infectiousness of vaccinated infected individuals. Therefore, the force of infection of model (4.1) is given by $\lambda = \beta\frac{I+\theta W}{N}$. Second, the vaccine may accelerate recovery in breakthrough infections. Hence, the vaccinated infected individuals will have faster recovery than the unvaccinated infected individuals, i.e. $\gamma_u < \gamma_v$.

Since $N(t) = S(t) + I(t) + W(t) + R(t) + V_1(t) + V_2(t)$, the rate of change

of the total population in model (4.1) is given by $\frac{dN}{dt} = \Lambda - \mu N$. At $t \to \infty$, we have $N \to \frac{\Lambda}{\mu}$. Hence, we assume $\Lambda = \mu$ so that the population size is constant. The model (4.1) also takes into account two vaccine failures in duration, namely vaccine- and disease-acquired immunity wanes at rate ω_V and ω_R, respectively.

The model (4.1) has a disease-free equilibrium (DFE) given by $E_0 = (S_0, I_0, W_0, R_0, V_{10}, V_{20}) = (S_0, 0, 0, 0, V_{10}, V_{20})$ where

$$\begin{aligned} S_0 &= \frac{(\omega_V + \mu)(\gamma_1 + \mu)}{\omega_V\gamma_1 + (\omega_V + \gamma_1 + \mu)(\bar{\pi} + \mu)}, \\ V_{10} &= \frac{(\omega_V + \mu)\bar{\pi}}{\omega_V\gamma_1 + (\omega_V + \gamma_1 + \mu)(\bar{\pi} + \mu)}, \\ V_{20} &= \frac{\gamma_1\bar{\pi}}{\omega_V\gamma_1 + (\omega_V + \gamma_1 + \mu)(\bar{\pi} + \mu)}. \end{aligned} \tag{4.2}$$

Since the population is not completely susceptible and the vaccine efficacy plays a crucial role in shaping the epidemic dynamics, we shall use the effective reproduction number, denoted by $\mathcal{R}_{\text{vac}}$, instead of the basic reproduction number, $\mathcal{R}_0$. In one class of infective epidemic model with vaccination, $\mathcal{R}_{\text{vac}}$ measures the average number of new infective individuals generated by a single infectious individual in a population where a certain fraction of the susceptible population are vaccinated. However, since the model (4.1) has two infective compartments (i.e. I and W) with different infectivity, we employ the method of next generation matrix in [103] to obtain the following effective reproductive number:

$$\begin{aligned} \mathcal{R}_{\text{vac}} &= \frac{\beta S_0}{\gamma_u + \mu} + \frac{\sigma\beta\theta V_{20}}{\gamma_v + \mu} \\ &= \frac{\beta}{(\gamma_u + \mu)(\gamma_v + \mu)} \left[\frac{(\gamma_v + \mu)(\omega_V + \mu)(\gamma_1 + \mu) + \sigma\theta\gamma_1\bar{\pi}(\gamma_u + \mu)}{\omega_V\gamma_1 + (\omega_V + \gamma_1 + \mu)(\bar{\pi} + \mu)} \right]. \end{aligned} \tag{4.3}$$

Following [103], $\mathcal{R}_{\text{vac}}$ represents the number of secondary infections, both unvaccinated and vaccinated, produced by an "index case", distributed in both I and W classes, with one part in I and $\frac{\sigma V_{20}}{S_0}$ parts in W (for the detail of this

interpretation, see Appendix B).

Let $E^* = (S^*, I^*, R^*, W^*, V_1^*, V_2^*)$ be any endemic equilibrium point (EEP) of the model (4.1). The non-zero equilibria of the model satisfy the following quadratic equation

$$a_2(\lambda^*)^2 + a_1\lambda^* + a_0 = 0 \tag{4.4}$$

where

$$a_2 = \sigma(\omega_R + \gamma_u + \mu)(\gamma_1 + \mu)(\gamma_v + \mu), \tag{4.5a}$$

$$\begin{aligned} a_1 = {} & \sigma(\gamma_u + \mu)\big[\gamma_1\bar{\pi}(\omega_R + \gamma_v + \mu) + (\gamma_v + \mu)(\omega_R + \mu)(\gamma_1 + \bar{\pi} + \mu)\big] \\ & + (\gamma_1 + \mu)(\gamma_v + \mu)\big[(\omega_V + \mu)(\omega_R + \gamma_u + \mu) - \beta\sigma(\omega_R + \mu)\big], \end{aligned} \tag{4.5b}$$

$$a_0 = (\omega_R + \mu)(\gamma_u + \mu)(\gamma_v + \mu)\big[\omega_V\gamma_1 + (\omega_V + \gamma_1 + \mu)(\bar{\pi} + \mu)\big](1 - \mathcal{R}_{\text{vac}}). \tag{4.5c}$$

In epidemic models with imperfect vaccines, there are two types of transcritical bifurcation at $\mathcal{R}_{\text{vac}} = 1$, namely forward and backward bifurcation [14]. From the epidemiological perspective, it is not enough to only reduce the $\mathcal{R}_{\text{vac}}$ to less than unity to eliminate a disease if backward bifurcation occurs. As imperfect vaccine is one of the causes for backward bifurcation [44], we first show that backward bifurcation occurs in the SIRVS epidemic model with two classes of vaccine-induced immunity by using the center manifold theory [14, 30], as given in Theorem 2.1.

4.2.1 Center manifold analysis near the disease-free equilibrium

We explore the backward bifurcation using the center manifold theory (see Section 2.3.3) in the following four simple steps.

Step 1: Show that one of the eigenvalues for the Jacobian matrix of the model at DFE is zero when $\beta = \beta^*$.

The Jacobian matrix of model (4.1) at the DFE is given below.

$$J = \begin{bmatrix} -\bar{\pi} - \mu & -\beta S_0 & -\beta\theta S_0 & \omega_R & 0 & \omega_V \\ 0 & \beta S_0 - \gamma_u - \mu & \beta\theta S_0 & 0 & 0 & 0 \\ 0 & \sigma\beta V_{20} & \sigma\beta\theta V_{20} - \gamma_v - \mu & 0 & 0 & 0 \\ 0 & \gamma_u & \gamma_v & -\omega_R - \mu & 0 & 0 \\ \bar{\pi} & 0 & 0 & 0 & -\gamma_1 - \mu & 0 \\ 0 & -\sigma\beta V_{20} & -\sigma\beta\theta V_{20} & 0 & \gamma_1 & -\omega_V - \mu \end{bmatrix} \tag{4.6}$$

The Jacobian matrix (4.6) has the following eigenvalues:

$$\lambda_1 = -\mu, \tag{4.7a}$$

$$\lambda_2 = -\omega_R - \mu, \tag{4.7b}$$

$$\lambda_{3,4} = -\frac{1}{2}\left(\bar{\pi} + \omega_V + \gamma_1 + 2\mu\right) \pm \frac{1}{2}\sqrt{(\bar{\pi} + \omega_V + \gamma_1)^2 - 4\left[\omega_V\gamma_1 + \bar{\pi}(\omega_V + \gamma_1)\right]}, \tag{4.7c}$$

$$\begin{aligned} \lambda_{5,6} = {} & \frac{1}{2}\left(\beta S_0 + \sigma\beta\theta V_{20} - \gamma_u - \gamma_v - 2\mu\right) \\ & \pm \frac{1}{2}\sqrt{(S_0 + \sigma\theta V_{20})^2\beta^2 - 2(\gamma_u - \gamma_v)(S_0 - \sigma\theta V_{20})\beta + (\gamma_u - \gamma_v)^2}. \end{aligned} \tag{4.7d}$$

Since all the parameter values are non-negative, λ_1 and λ_2 are always negative while $\lambda_{3,4}$ have negative real part. Let $\beta = \beta^*$ be the disease transmission rate that makes the effective reproduction number $\mathcal{R}_{\text{vac}}$ equal to 1. By substituting

$$\begin{aligned} \beta = \beta^* &= \frac{(\gamma_u + \mu)(\gamma_v + \mu)}{(\gamma_v + \mu)S_0 + \sigma\theta V_{20}(\gamma_u + \mu)} \\ &= \frac{(\gamma_u + \mu)(\gamma_v + \mu)\left[\omega_V\gamma_1 + (\bar{\pi} + \mu)(\omega_V + \gamma_1 + \mu)\right]}{(\gamma_v + \mu)(\omega_V + \mu)(\gamma_1 + \mu) + \sigma\theta\gamma_1\bar{\pi}(\gamma_u + \mu)} \end{aligned} \tag{4.8}$$

into equation (4.7d), $\lambda_{5,6}$ can be simplified as $\lambda_5 = 0$ and

$$\lambda_6 = -\frac{(\gamma_v + \mu)^2 S_0 + (\gamma_u + \mu)^2\sigma\theta V_{20}}{(\gamma_v + \mu)S_0 + (\gamma_u + \mu)\sigma\theta V_{20}} < 0,$$

since the initial conditions S_0 and V_{20} as well as the parameters γ_u, γ_v, σ, θ, μ are all non-negative. That is, at $\beta = \beta^*$, the Jacobian matrix (4.6) at DFE has a simple eigenvalue 0 and all other eigenvalues have negative real parts. Therefore, the center manifold theory can be used to analyse the dynamics of the model near $\beta = \beta^*$.

By setting $\beta = \beta^*$, the DFE is locally stable when $\beta < \beta^*$ ($\Leftrightarrow \lambda_5 < 0$) and locally unstable when $\beta > \beta^*$ ($\Leftrightarrow \lambda_5 > 0$). Therefore, the critical value $\beta = \beta^*$ is a bifurcation value.

Step 2: Obtain the left and right eigenvector associated with the zero eigenvalue.

The Jacobian matrix (4.6) at DFE and $\beta = \beta^*$ has the left eigenvector

$$\mathbf{v} = [v_1, v_2, v_3, v_4, v_5, v_6], \tag{4.9}$$

where $v_1 = v_4 = v_5 = v_6 = 0$, $v_2 = \gamma_v + \mu$ and $v_3 = \theta(\gamma_u + \mu)$. Furthermore, it has a right eigenvector

$$\mathbf{w} = [w_1, w_2, w_3, w_4, w_5, w_6]^T, \tag{4.10}$$

where

$$\begin{aligned}
w_1 &= \frac{\gamma_1 + \mu}{\bar{\pi}} w_5, \\
w_2 &= \frac{(\gamma_v + \mu)(\omega_V + \mu)(\gamma_1 + \mu)}{\sigma \bar{\pi} \gamma_1 (\gamma_u + \mu)} w_3, \\
w_3 &= w_3, \\
w_4 &= \frac{\gamma_u w_2 + \gamma_v w_3}{\omega_R + \mu}, \\
w_5 &= -\frac{(\gamma_v + \mu)\left[(\omega_V + \mu)^2 (\gamma_1 + \mu) + \omega_V \sigma \bar{\pi} \gamma_1\right] - (\omega_V + \mu) m_2}{\sigma \gamma_1 \mu \, m_1} w_3, \\
w_6 &= -\frac{(\gamma_v + \mu)(\gamma_1 + \mu)\left[\omega_V + \mu + \sigma(\bar{\pi} + \mu)\right] - m_2}{\sigma \mu \, m_1} w_3,
\end{aligned}$$

with

$$m_1 = \omega_V\gamma_1 + (\bar{\pi}+\mu)(\omega_V+\gamma_1+\mu),$$
$$m_2 = \frac{\omega_R\left[\gamma_u(\gamma_v+\mu)(\omega_V+\mu)(\gamma_1+\mu)+\gamma_v\sigma\bar{\pi}\gamma_1(\gamma_u+\mu)\right]}{(\gamma_u+\mu)(\omega_R+\mu)}.$$

Since the elements of eigenvector $\mathbf{v}$ and $\mathbf{w}$ must satisfy the equality $\mathbf{v}\cdot\mathbf{w}=1$ [10], using equations (4.9) and (4.10), we have $v_2w_2+v_3w_3=1$ which gives

$$w_3 = \frac{\sigma\bar{\pi}\gamma_1(\gamma_u+\mu)}{(\gamma_v+\mu)^2(\omega_V+\mu)(\gamma_1+\mu)+\sigma\theta\bar{\pi}\gamma_1(\gamma_u+\mu)^2}. \tag{4.11}$$

Step 3: Compute all the mixed derivatives for the bifurcation coefficients a and b.

By using the transformation $S=x_1$, $I=x_2$, $W=x_3$, $R=x_4$, $V_1=x_5$ and $V_2=x_6$, so that $N=\sum_{j=1}^{6}x_j$, the model (4.1) can be rewritten as $\frac{d\mathbf{x}}{dt}=\mathbf{f}$ where

$$\begin{aligned}
\frac{dx_1}{dt} &= f_1 = \Lambda-\lambda x_1-\bar{\pi}x_1+\omega_R x_4+\omega_V x_6-\mu x_1,\\
\frac{dx_2}{dt} &= f_2 = \lambda x_1-\gamma_u x_2-\mu x_2,\\
\frac{dx_3}{dt} &= f_3 = \sigma\lambda x_6-\gamma_v x_3-\mu x_3,\\
\frac{dx_4}{dt} &= f_4 = \gamma_u x_2+\gamma_v x_3-\omega_R x_4-\mu x_4,\\
\frac{dx_5}{dt} &= f_5 = \bar{\pi}x_1-\gamma_1 x_5-\mu x_5,\\
\frac{dx_6}{dt} &= f_6 = \gamma_1 x_5-\sigma\lambda x_6-\omega_V x_6-\mu x_6,
\end{aligned} \tag{4.12}$$

where $\lambda=\beta\frac{x_2+\theta x_3}{\sum_{j=1}^{6}x_j}$. The bifurcation coefficients in this six compartmental model at DFE $\mathbf{x}_0$ are given by

$$a = \sum_{i,j,k=1}^{6} v_i w_j w_k \frac{\partial^2 f_i}{\partial x_j \partial x_k}(\mathbf{x}_0,\beta^*), \tag{4.13a}$$

$$b = \sum_{i,j=1}^{6} v_i w_j \frac{\partial^2 f_i}{\partial x_j \partial \beta}(\mathbf{x}_0,\beta^*). \tag{4.13b}$$

Since $v_2 \neq 0$ and $v_3 \neq 0$ in (4.9), we only need to find the mixed derivatives of f_2 and f_3 in (4.12) at the DFE. For f_2, we obtain

$$\begin{aligned} \frac{\partial^2 f_2}{\partial x_1 \partial x_2} &= \frac{\partial^2 f_2}{\partial x_2 \partial x_1} = \beta, & \frac{\partial^2 f_2}{\partial x_1 \partial x_3} &= \frac{\partial^2 f_2}{\partial x_3 \partial x_1} = \beta\theta, \\ \frac{\partial^2 f_2}{\partial x_2 \partial \beta} &= S_0, & \frac{\partial^2 f_2}{\partial x_3 \partial \beta} &= \theta S_0, \end{aligned}$$

and all other mixed derivatives for f_2 are zero. For f_3, we obtain

$$\begin{aligned} \frac{\partial^2 f_3}{\partial x_2 \partial x_6} &= \frac{\partial^2 f_3}{\partial x_6 \partial x_2} = \sigma\beta, & \frac{\partial^2 f_3}{\partial x_3 \partial x_6} &= \frac{\partial^2 f_3}{\partial x_6 \partial x_3} = \sigma\beta\theta, \\ \frac{\partial^2 f_3}{\partial x_2 \partial \beta} &= \sigma V_{20}, & \frac{\partial^2 f_3}{\partial x_3 \partial \beta} &= \sigma\theta V_{20}, \end{aligned}$$

and all other mixed derivatives for f_3 are zero.

Step 4: Compute a and b.

By substituting the elements of eigenvectors $\mathbf{v}$ and $\mathbf{w}$ as well as the respective mixed derivatives found in Step 3, after some algebraic manipulations, we obtain

$$\begin{aligned} a &= v_2 \sum_{j,k=1}^{6} w_j w_k \frac{\partial^2 f_2}{\partial x_j \partial x_k}(\mathbf{x}_0, \beta^*) + v_3 \sum_{j,k=1}^{6} w_j w_k \frac{\partial^2 f_3}{\partial x_j \partial x_k}(\mathbf{x}_0, \beta^*) \\ &= 2\beta(w_2 + \theta w_3)\left[(\gamma_v + \mu)w_1 + \sigma\theta(\gamma_u + \mu)w_6\right] \\ &= \frac{2\beta w_3^2\left[(\gamma_v + \mu)(\omega_V + \mu)(\gamma_1 + \mu) + \sigma\theta\bar{\pi}\gamma_1(\gamma_u + \mu)\right]}{\mu(\sigma\bar{\pi}\gamma_1)^2(\gamma_u + \mu)\left[\omega_V\gamma_1 + (\bar{\pi} + \mu)(\omega_V + \gamma_1 + \mu)\right]} \\ &\quad \times \left\{ \begin{array}{l} -\sigma\theta\bar{\pi}\gamma_1(\gamma_u + \mu)(\gamma_v + \mu)(\gamma_1 + \mu)\left[\omega_V + \mu + \sigma(\bar{\pi} + \mu)\right] \\ \quad + \left[(\omega_V + \mu)(\gamma_v + \mu)(\gamma_1 + \mu) + \sigma\theta\bar{\pi}\gamma_1(\gamma_u + \mu)\right] m_2 \\ \quad -(\gamma_v + \mu)^2(\gamma_1 + \mu)\left[(\omega_V + \mu)^2(\gamma_1 + \mu) + \omega_V\sigma\bar{\pi}\gamma_1\right] \end{array} \right\}, \end{aligned} \tag{4.14a}$$

$$
\begin{aligned}
b &= v_2 \sum_{j=1}^{6} w_j \frac{\partial^2 f_2}{\partial x_j \partial \beta}(\mathbf{x}_0, \beta^*) + v_3 \sum_{j=1}^{6} w_j \frac{\partial^2 f_3}{\partial x_j \partial \beta}(\mathbf{x}_0, \beta^*) \\
&= (w_2 + \theta w_3)\left[(\gamma_v + \mu)S_0 + \sigma\theta(\gamma_u + \mu)V_{20}\right] \\
&= \frac{w_3\left[(\gamma_v + \mu)(\omega_V + \mu)(\gamma_1 + \mu) + \sigma\theta\bar{\pi}\gamma_1(\gamma_u + \mu)\right]^2}{\sigma\bar{\pi}\gamma_1(\gamma_u + \mu)\left[\omega_V\gamma_1 + (\bar{\pi} + \mu)(\omega_V + \gamma_1 + \mu)\right]} > 0.
\end{aligned}
\tag{4.14b}
$$

According to [14], the local dynamics of the system (4.12) around the DFE are totally determined by the signs of a and b (see Theorem 2.1). Since all the parameter values as well as w_3 as given in (4.11) are non-negative, the quantity b in equation (4.14b) is always positive. On the other hand, the sign of a depends on the sign of expressions in the curly bracket in (4.14a). If $a > 0$, then there are unstable endemic equilibrium exhibiting backward bifurcation near the DFE, while if $a < 0$, there are locally asymptotically stable endemic equilibrium showing forward bifurcation near the DFE [84].

4.2.2 Analysis of the effective reproduction number

The interplay between the characteristics of imperfect vaccines in SIRVS epidemic model with two classes of vaccine-induced immunity and the disease outbreak threshold with vaccination as a control measure may be explained by carrying out some analysis of $\mathcal{R}_{\text{vac}}$ (eq. (4.3)) for the following three cases.

Case 1: A model with only one class of vaccinated individuals

The SIRVS epidemic model with two classes of vaccine-induced immunity as given in (4.1) could be reduced to one class by assume either that the vaccinated individuals lost their high vaccine-induced immunity immediately (i.e. $\gamma_1 \to \infty \Leftrightarrow \frac{1}{\gamma_1} \to 0$) or that the vaccine offers lifelong high vaccine-induced immunity (i.e. $\gamma_1 \to 0 \Leftrightarrow \frac{1}{\gamma_1} \to \infty$). The former (resp. the latter) corresponding to the period of high vaccine-induced immunity is so short (resp. long) that the V_1 (resp. V_2) class can be ignored.

By firstly applying the L'Hopital's rule to the expression $\mathcal{R}_{\text{vac}}$ in (4.3) and then assuming $\theta = 1$ and $\gamma_v = \gamma_u$, we have

$$\begin{aligned}\lim_{\gamma_1 \to \infty} \mathcal{R}_{\text{vac}} &= \lim_{\substack{\gamma_1 \to \infty \\ \theta \to 1 \\ \gamma_v \to \gamma_u}} \frac{\beta}{(\gamma_u + \mu)(\gamma_v + \mu)} \left[\frac{(\gamma_v + \mu)(\omega_V + \mu) + \sigma\theta\bar{\pi}(\gamma_u + \mu)}{\omega_V + (\bar{\pi} + \mu)} \right] \\ &= \frac{\beta}{(\gamma_u + \mu)} \left[\frac{\omega_V + \sigma\bar{\pi} + \mu}{\omega_V + \bar{\pi} + \mu} \right].\end{aligned} \tag{4.15}$$

The limit of $\mathcal{R}_{\text{vac}}$ above corresponds to the effective reproduction number of SIRVS with one class of vaccinated individuals with partially-protective vaccine-induced immunity. The expression (4.15) is always less than basic reproduction number $\mathcal{R}_0 = \frac{\beta}{\gamma_u + \mu}$ for $0 \leq \sigma < 1$. The smaller value of σ (i.e. the better vaccine efficacy, $1 - \sigma$), the greater reduction to the basic reproduction number.

On the other hand, when the period of high vaccine-induced immunity is long, we have

$$\lim_{\gamma_1 \to 0} \mathcal{R}_{\text{vac}} = \frac{\beta}{\gamma_u + \mu} \left[\frac{\mu}{\bar{\pi} + \mu} \right], \tag{4.16}$$

which corresponds to the product of the basic reproduction number $\mathcal{R}_0$ and $\frac{\mu}{\bar{\pi}+\mu}$. In this case, on average, a proportion $\frac{\mu}{\bar{\pi}+\mu}$ of the contact made by a single unvaccinated infective individual in the population would be with susceptible [52]. Its value will be always less than $\mathcal{R}_0$ if the population vaccination rate $\bar{\pi} > 0$. Notice that the expression (4.16) is independent of the parameters σ, θ, γ_v and ω_V.

Case 2: A model with two classes of vaccine-induced immunity. (a) Totally failure vaccine (TFV) versus fully protective vaccine (FPV)

When the vaccine is totally failure (i.e. $\sigma = 1$), the other two additional vaccine characteristics, namely the reduced infectivity and faster recovery for vaccinated infected individuals would become irrelevant. Therefore, we set $\theta = 1$ and $\gamma_v = \gamma_u$ in this scenario.

$$\begin{aligned}\mathcal{R}_{\text{vac}}^{\text{TFV}} &= \lim_{\sigma \to 1} \mathcal{R}_{\text{vac}} \\ &= \lim_{\substack{\sigma \to 1 \\ \theta \to 1 \\ \gamma_v \to \gamma_u}} \frac{\beta}{(\gamma_u + \mu)(\gamma_v + \mu)} \left[\frac{(\gamma_v + \mu)(\omega_V + \mu)(\gamma_1 + \mu) + \theta \gamma_1 \bar{\pi}(\gamma_u + \mu)}{\omega_V \gamma_1 + (\omega_V + \gamma_1 + \mu)(\bar{\pi} + \mu)} \right] \\ &= \frac{\beta}{(\gamma_u + \mu)} \left\{ \frac{(\omega_V + \mu)(\gamma_1 + \mu) + \gamma_1 \bar{\pi}}{[(\omega_V + \mu)(\gamma_1 + \mu) + \gamma_1 \bar{\pi}] + \bar{\pi}(\omega_V + \mu)} \right\}. \end{aligned} \tag{4.17}$$

Unlike the one-class vaccinated individuals model whereby no reduction on the reproduction number when $\sigma = 1$ (see expression in (4.15)), whenever the population vaccination rate $\bar{\pi} > 0$, the expression in the curly bracket in (4.17) will be always less than one due to appearance of $\bar{\pi}(\omega_V + \mu)$ in its denominator, where $\omega_V + \mu$ is the rate at which individuals leave the V_2 class.

When the vaccine confers full protection (i.e. $\sigma = 0$) to vaccinated individuals even though they only have low vaccine-induced immunity, the effective reproduction number for the two-class immunity SVIRS model becomes

$$\begin{aligned}\mathcal{R}_{\text{vac}}^{\text{FPV}} &= \lim_{\sigma \to 0} \mathcal{R}_{\text{vac}} \\ &= \frac{\beta}{(\gamma_u + \mu)} \left[\frac{(\omega_V + \mu)(\gamma_1 + \mu)}{(\omega_V + \mu)(\gamma_1 + \mu) + \bar{\pi}(\omega_V + \mu) + \gamma_1 \bar{\pi}} \right]. \end{aligned} \tag{4.18}$$

When $\sigma \to 0$, almost no vaccinated individuals in the V_2 class would be infected. Hence, the parameters θ and γ_v become irrelevant in determining the value of effective reproduction number. By comparing expressions (4.17) and (4.18), we found that $\mathcal{R}_{\text{vac}}^{\text{FPV}} < \mathcal{R}_{\text{vac}}^{\text{TFV}} < \mathcal{R}_0$, provided that γ_1 does not approach 0, which implies that the reduction to basic reproduction number is

larger whenever the vaccine offers full protection from infection risks to vaccinated individuals in the V_2 class. Both expressions (4.17) and (4.18) are more complicated than those (4.15) and (4.16) simply because they correspond to the coexistence of vaccinated individuals with high and low vaccine-induced immunity in the population.

(b) Lifelong and temporary low vaccine-induced immunity

If the duration of spending in the V_2 class is very long for vaccinated individuals, then with other parameters fixed, we have

$$\begin{aligned}\lim_{\omega_V \to 0} \mathcal{R}_{\text{vac}} &= \frac{\beta}{(\gamma_u+\mu)(\gamma_v+\mu)}\left[\frac{(\gamma_v+\mu)\mu(\gamma_1+\mu)+\sigma\theta\gamma_1\bar{\pi}(\gamma_u+\mu)}{(\gamma_1+\mu)(\bar{\pi}+\mu)}\right] \\ &= \frac{\beta}{\gamma_u+\mu}\left[\frac{\mu}{\bar{\pi}+\mu}\right] + \frac{\sigma\theta\beta}{\gamma_v+\mu} \times \left[\frac{\bar{\pi}}{\bar{\pi}+\mu} \times \frac{\gamma_1}{\gamma_1+\mu}\right].\end{aligned} \tag{4.19}$$

The first part of the expressions in (4.19) is exactly the one in (4.16) which is the case whereby the duration of high vaccine-induced immunity is sufficiently long. The second part could be interpreted as the expected number of newly infected individuals produced by a vaccinated infected individual when the reduced susceptibility for vaccinated individual is σ, multiply with two factors, namely the proportion of contact made would be with vaccinated individuals in the V_2 class (i.e. $\frac{\bar{\pi}}{\bar{\pi}+\mu}$) as well as the probability of losing high vaccine-induced immunity in their lifetime, instead of leaving V_1 class by dying (i.e. $\frac{\gamma_1}{\gamma_1+\mu}$) [52].

If vaccinated individuals only have temporary low vaccine-induced immunity, then applying L'Hopital' rule gives

$$\lim_{\omega_V \to \infty} \mathcal{R}_{\text{vac}} = \frac{\beta}{\gamma_u+\mu}\left[\frac{\gamma_1+\mu}{\bar{\pi}+\gamma_1+\mu}\right]. \tag{4.20}$$

Expression (4.20) differs from (4.16) by the appearance of parameter γ_1. As long as the population vaccination rate $\bar{\pi} > 0$, the vaccine would be able to

reduce the basic reproduction number in the two-class vaccine-induced immunity model even though vaccinated individuals would only stay in the V_2 class temporarily. Note that the parameters σ, θ and γ_v become irrelevant in this case.

Case 3: The effective reproduction number for immediate vaccination

Among the parameters in the effective reproduction number (4.3), we are most interested in the population vaccination rate, $\bar{\pi}$. We assume that if everyone in the population vaccinated (i.e. $\bar{\pi} \to \infty$), the vaccination is able to reduce $\mathcal{R}_{\text{vac}}$ below one, otherwise vaccination is useless in combating the disease [52]. It follows that we must assume

$$\lim_{\bar{\pi}\to\infty} \mathcal{R}_{\text{vac}} = \frac{\beta}{\gamma_v + \mu}\left[\frac{\sigma\theta\gamma_1}{\omega_V + \gamma_1 + \mu}\right] < 1. \tag{4.21}$$

Therefore, we have

$$\sigma\theta\beta\gamma_1 < (\gamma_v + \mu)(\omega_V + \gamma_1 + \mu). \tag{4.22}$$

The inequality (4.22) gives the condition of the combination parameter values $\{\beta, \theta, \sigma, \gamma_1, \gamma_v, \omega_V, \mu\}$ whereby the disease will be eradicated if everyone in the population vaccinated immediately. By rearranging $\mathcal{R}_{\text{vac}}(\bar{\pi}) < 1$, we arrive at

$$\bar{\pi} > \frac{(\gamma_v + \mu)(\omega_V + \mu)(\gamma_1 + \mu)\left[\frac{\beta}{\gamma_u+\mu} - 1\right]}{(\gamma_v + \mu)(\omega_V + \gamma_1 + \mu) - \sigma\theta\beta\gamma_1}. \tag{4.23}$$

As the condition given in (4.22), the denominator of the right-hand side of inequality (4.23) is always positive. Thus, the population vaccination rate $\bar{\pi}$ is positive if and only if $\frac{\beta}{\gamma_u+\mu} - 1 > 0$, i.e. $\mathcal{R}_0 > 1$.

In general, the SIRVS model with two-class of vaccine-induced immunity seems to behave consistent with the one-class imperfect vaccine model in

which the better vaccine efficacy, the greater reduction to the basic reproduction number will be. Also, the population vaccination rate is positive if and only if $\mathcal{R}_0 > 1$. However, with the two classes of vaccine-induced immunity, expressions (4.16) and (4.20) suggest that the vaccine efficacy does not appear to be significant in determining $\mathcal{R}_{\text{vac}}$ if a vaccine is able to provide long-term high immunity ($\gamma_1 \to \infty$) or vaccinated individuals only have temporary low immunity ($\omega_V \to \infty$).

4.3 The vaccination population games

4.3.1 Population-scale and individual-scale dynamics

Population-scale epidemic dynamics

In order to keep the population size constant, we exclude the recruitment rate, natural and disease-induced death rate in the extended model in [30], that is by setting $\Lambda = \mu = 0$ in model (4.1). Then, we have

$$\begin{aligned}
\frac{dS}{dt} &= -\lambda S - \bar{\pi} S + \omega_R R + \omega_V V_2, \\
\frac{dI}{dt} &= \lambda S - \gamma_u I, \\
\frac{dW}{dt} &= \sigma \lambda V_2 - \gamma_v W, \\
\frac{dR}{dt} &= \gamma_u I + \gamma_v W - \omega_R R, \\
\frac{dV_1}{dt} &= \bar{\pi} S - \gamma_1 V_1, \\
\frac{dV_2}{dt} &= \gamma_1 V_1 - \sigma \lambda V_2 - \omega_V V_2.
\end{aligned} \tag{4.24}$$

In model (4.24), the population-level continuous vaccination rate is given by $\bar{\pi}$, where the bar denotes the average rate in the population. The model (4.24) has three additional epidemiological aspects that have not previously been described in Model (3.31) in [79]. First, apart from the two waning rates of vaccine- and infection-acquired immunity, denoted by ω_V and ω_R, respectively, in model (4.24) the vaccinated individuals with high vaccine-

induced protection in the V_1 class move to the V_2 class with low vaccine-induced protection at the rate γ_1, which uses a gamma distribution for the vaccine-derived immunity. This implies that there is always a mixed state of vaccinators with full and partial protection from infection in model (4.24) provided that γ_1 does not approach ∞, whereas Model (3.31) in [79] could either have all fully- or partially-protected vaccinators, not both, depending on the pre-defined value of parameter σ. Second, the model (4.24) has two recovery rates γ_u and γ_v where the latter does not appear in Model (3.31) in [79]. Third, the model (4.24) has additional parameter θ which gives the reduced transmissibility in breakthrough infection for individuals in the W class. By incorporating the parameter θ in vaccination population games, the scenario that only vaccinated individuals bear the cost of vaccination while those who are not vaccinated benefit directly from the reduced transmissibility of vaccinated infected individuals can be explored. This shifts from the individual self-interest towards selflessness in vaccination decisions. Hence, the vaccination population game of model (4.24) provides an alternative to study the influence of altruism in vaccination decisions, as altruism does play an important role in vaccination decisions [91].

Similar to model (4.1), the model (4.24) has a disease-free equilibrium (DFE) given by $E_0 = (S_0, I_0, W_0, R_0, V_{10}, V_{20}) = (S_0, 0, 0, 0, V_{10}, V_{20})$ where

$$S_0 = \frac{\omega_V \gamma_1}{\omega_V \gamma_1 + (\omega_V + \gamma_1)\bar{\pi}}, V_{10} = \frac{\omega_V \bar{\pi}}{\omega_V \gamma_1 + (\omega_V + \gamma_1)\bar{\pi}}, V_{20} = \frac{\gamma_1 \bar{\pi}}{\omega_V \gamma_1 + (\omega_V + \gamma_1)\bar{\pi}} \tag{4.25}$$

and the effective reproduction number is given by

$$\mathcal{R}_{\text{vac}} = \frac{\beta}{\gamma_u \gamma_v} \left[\gamma_v S_0 + \sigma\theta\gamma_u V_{20}\right] = \frac{\beta}{\gamma_u \gamma_v} \left[\frac{\gamma_v \omega_V \gamma_1 + \sigma\theta\gamma_1 \bar{\pi}\gamma_u}{\omega_V \gamma_1 + (\omega_V + \gamma_1)\bar{\pi}}\right]. \tag{4.26}$$

Let $E^* = (S^*, I^*, R^*, W^*, V_1^*, V_2^*)$ represent any endemic equilibrium point (EEP) of the model (4.24). The non-zero equilibria of the model satisfy the following quadratic equation

$$a_2(\lambda^*)^2 + a_1\lambda^* + a_0 = 0, \tag{4.27}$$

where

$$a_2 = \sigma(\omega_R + \gamma_u)\gamma_1\gamma_v > 0, \tag{4.28a}$$

$$a_1 = \sigma\gamma_u\big[\gamma_1\bar{\pi}(\omega_R + \gamma_v) + \gamma_v\omega_R(\gamma_1 + \bar{\pi})\big] + \gamma_1\gamma_v\big[\omega_V(\omega_R + \gamma_u) - \beta\sigma\omega_R\big] \tag{4.28b}$$

$$a_0 = \omega_R\gamma_u\gamma_v\big[\gamma_1\omega_V + (\omega_V + \gamma_1)\bar{\pi}\big](1 - \mathcal{R}_{\text{vac}}). \tag{4.28c}$$

The model (4.24) has (i) a unique endemic equilibrium if $a_0 < 0$, (ii) a unique endemic equilibrium if $a_0 = 0$ ($\Leftrightarrow \mathcal{R}_{\text{vac}} = 1$) or $a_1^2 - 4a_2a_0 = 0$, and $a_1 < 0$, (iii) two endemic equilibria if $a_0 > 0$, $a_1 < 0$ and $a_1^2 - 4a_2a_0 > 0$, and (iv) no endemic equilibrium otherwise.

Since all the parameters value are non-negative, the coefficient a_2 is always positive. The coefficient a_0 is positive (resp. negative) if $\mathcal{R}_{\text{vac}}$ is less than (resp. greater than) 1. As in [108], the above cases can be deduced with the help of Descartes rule of signs which states that if the terms of a polynomial with real coefficients are arranged in descending order, then the number of positive roots of the polynomial is either equal to the number of sign changes between the non-zero coefficients or less than the sign changes by a multiple of 2 (as the polynomial may have complex roots which always come in pairs).

For case (i), whenever $a_2 > 0$ and $a_0 < 0$, no matter $a_1 > 0$ or $a_1 < 0$, there is always only one change of sign between the consecutive coefficients. Therefore, according to the Descartes rule of signs, there exists a unique endemic equilibrium if $a_0 < 0$. For case (ii), when $a_0 = 0$, the quadratic equation (4.27) reduces to $\lambda^*(a_2\lambda^* + a_1) = 0$ and hence $\lambda^* = 0$ or $\lambda^* = -\frac{a_1}{a_2}$. Alternatively, when $a_1^2 - 4a_2a_0 = 0$, solving equation (4.27) gives $\lambda^* = -\frac{a_1}{2a_2}$. For both subcases, it follows that equation (4.27) has a unique positive endemic equilibrium if $a_1 < 0$. For case (iii), if $a_0 > 0$ and $a_1 < 0$, we have exactly two

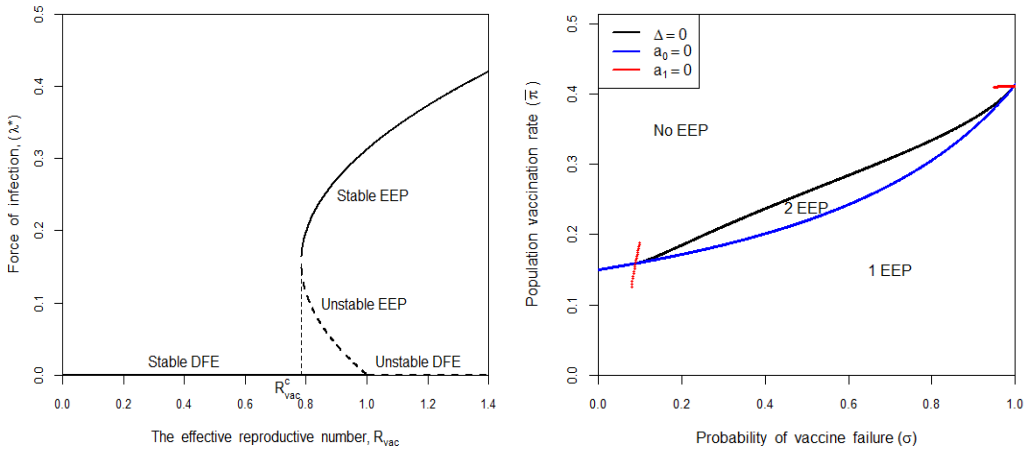

(a) (b)

Figure 4.1: Backward bifurcation diagram for model (4.24) in the $(\lambda^*, \mathcal{R}_{\text{vac}})$ and $(\bar{\pi}, \sigma)$ plane.

changes of signs and according to the Descartes rule of signs, there is possible two or no real positive root for the equation (4.27). Thus, the additional condition of the discriminant $a_1^2 - 4a_2a_0 > 0$ rules out the possibilities of having a pair of complex roots and we deduce that the model (4.24) has two endemic equilibria in this case.

The existence of two endemic equilibria in case (iii) suggests that the occurrence of backward bifurcation phenomenon in the SIRVS model with two classes of vaccine-induced immunity is also a direct consequence of modelling the imperfect vaccines [44]. Backward bifurcation phenomenon has important public health implications because it might not be sufficient to reduce $\mathcal{R}_{\text{vac}}$ below unity to eliminate the disease [10]. Depending on the initial sizes of the infective, the disease would persist if $\mathcal{R}_{\text{vac}}$ is close to unity [30]. Figure 4.1 gives the simulation of model (4.24) for the combination of parameter values $(\beta, \theta, \gamma_u, \gamma_v, \gamma_1, \omega_R, \omega_V, \bar{\pi}, \sigma) = (2, 0.85, 0.4, 2, 0.15, 0.5, 0.05, 0.25, 0.75)$ which illustrates the phenomenon of backward bifurcation in the SIRVS model with two classes of vaccine-induced immunity.

By setting the discriminant of equation (4.27) to zero (i.e. $\triangle = a_1^2 - 4a_2a_0 = 0$) and solving for the critical value of $\mathcal{R}_{\text{vac}}$, denoted by $\mathcal{R}_{\text{vac}}^c$, we have the sub-threshold

$$\mathcal{R}_{\text{vac}}^c = 1 - \frac{a_1^2}{4a_2\Theta}$$

where $\Theta = \omega_R\gamma_u\gamma_v\left[\omega_V\gamma_1 + (\omega_V + \gamma_1)\bar{\pi}\right]$. Figure 4.1(a) clearly shows that the backward bifurcation occurs at value $\mathcal{R}_{\text{vac}} = 1$ and a subsequent saddle-node (or fold) bifurcation (two endemic equilibria collide and disappear) at $\mathcal{R}_{\text{vac}}^c$. In the range of $\mathcal{R}_{\text{vac}}^c < \mathcal{R}_{\text{vac}} < 1$, both stable endemic and disease-free equilibrium coexist with an unstable endemic equilibrium. For the cases where the phenomenon of backward bifurcation occurs, the effective reproduction number must be reduced below $\mathcal{R}_{\text{vac}}^c$ in order to ensure that the disease dies out.

In the absence of vaccination, i.e. at $\bar{\pi} = 0$, $\mathcal{R}_{\text{vac}}$ reduces to basic reproduction number, $\mathcal{R}_0 = \frac{\beta}{\gamma_u}$, and the quadratic equation (4.27) together with (4.28) becomes

$$\sigma(\omega_R + \gamma_u)\gamma_1\gamma_v(\lambda^*)^2 + \left\{\gamma_1\gamma_v\left[\sigma\omega_R(\gamma_u - \beta) + \omega_V(\omega_R + \gamma_u)\right]\right\}\lambda^* + \omega_R\gamma_v\gamma_1\omega_V(\gamma_u - \beta) = 0. \quad (4.29)$$

Solving the quadratic equation (4.29) gives two solutions, $\lambda_{10}^* = (\beta - \gamma_u)\frac{\omega_R}{\omega_R + \gamma_u}$ and $\lambda_{20}^* = -\frac{\omega_V}{\sigma} < 0$. Since λ_{20}^* is biologically infeasible, we conclude that the force of infection corresponding to no vaccination in the population is given by

$$\lambda^*(\bar{\pi} = 0) = \lambda_{10}^* = (\beta - \gamma_u)\frac{\omega_R}{\omega_R + \gamma_u}. \quad (4.30)$$

Note that the vaccine-associated epidemiological (i.e. θ, γ_v) and immune (i.e. γ_1, ω_V) parameters do not appear in (4.30).

In the case where individuals in the population vaccinate instantly, $\bar{\pi} \to \infty$, by rearranging equation (4.27) and finding the limit of λ^* when $\bar{\pi} \to \infty$ using L'Hopital's rule, we obtain

$$\lim_{\bar{\pi}\to\infty} \lambda^* = \frac{\left[\sigma\theta\beta\gamma_1 - \gamma_v(\gamma_1 + \omega_V)\right]\omega_R}{\sigma\left[\gamma_1(\gamma_v + \omega_R) + \gamma_v\omega_R\right]}. \tag{4.31}$$

Hence, the equilibrium force of infection is

$$\lambda^* = \max\left\{0, \frac{\left[\sigma\theta\beta\gamma_1 - \gamma_v(\gamma_1 + \omega_V)\right]\omega_R}{\sigma\left[\gamma_1(\gamma_v + \omega_R) + \gamma_v\omega_R\right]}\right\}.$$

Note that this λ^* is independent of the unvaccinated infected individuals' recovery rate γ_u and the transmission rate becomes $\theta\beta$ in instant vaccination. Also, the expression (4.31) is non-negative if and only if the reverse of the inequality (4.22) is being satisfied. That is, if $\sigma\theta\beta\gamma_1 > \gamma_v(\gamma_1 + \omega_V)$, even the instant vaccination of everyone in the population will not eradicate the infectious diseases.

Individual-scale dynamics

An individual-scale model can be expressed as a Markov process with transition rates derived from the population-scale model. Specifically, the changes in a single representative individual's disease state when the population dynamics reach its steady state are described by the following continuous-time Markov process [79]:

$$\frac{d\mathbf{p}(t)}{dt} = \mathbf{Q}^*\mathbf{p}(t) \tag{4.32}$$

with $\mathbf{p}(0) = [1, 0, 0, 0, 0, 0]^T$. The initial condition $\mathbf{p}(0)$ means that every individual in the population starts in the susceptible state. $\mathbf{p}(t)$ is the probability density that an individual is susceptible, unvaccinated infected, vaccinated infected, recovered, vaccinated with high vaccine-induced immunity or vaccinated with low vaccine-induced immunity at time t, that is

$\mathbf{p}(t) = [S(t), I(t), W(t), R(t), V_1(t), V_2(t)]^T$. The full matrix form of equation (4.32) is given by

$$\begin{bmatrix} \frac{dS}{dt} \\ \frac{dI}{dt} \\ \frac{dW}{dt} \\ \frac{dR}{dt} \\ \frac{dV_1}{dt} \\ \frac{dV_2}{dt} \end{bmatrix} = \begin{bmatrix} -\lambda^* - \pi & 0 & 0 & \omega_R & 0 & \omega_V \\ \lambda^* & -\gamma_u & 0 & 0 & 0 & 0 \\ 0 & 0 & -\gamma_v & 0 & 0 & \sigma\lambda^* \\ 0 & \gamma_u & \gamma_v & -\omega_R & 0 & 0 \\ \pi & 0 & 0 & 0 & -\gamma_1 & 0 \\ 0 & 0 & 0 & 0 & \gamma_1 & -\sigma\lambda^* - \omega_V \end{bmatrix} \begin{bmatrix} S \\ I \\ W \\ R \\ V_1 \\ V_2 \end{bmatrix}. \quad (4.33)$$

Note that the individual vaccination rate, π is used in individual-scale dynamics. It could be the same or different from the population vaccination rate, $\bar{\pi}$.

4.3.2 Utility calculation

In this subsection, the expected utility function will be calculated according to the Markov decision process theory. In population games, the utility of any strategy depends on both the individual's strategy and population (resident) average strategy (i.e. choice, decision, behaviour, or investment). An individual's strategy may differ from the resident strategy. We assume that almost all individuals in the population use the population average strategy, and the population is so large that population epidemic dynamics are not significantly affected by the change of a single individual's strategy [92].

According to [79], the expected utility has the following closed form

$$U(a, \bar{a}) = \left[\mathbf{f}^T + \mathbf{1}^T(\mathbf{F} \bullet \mathbf{Q}^*)\right](h\mathbf{I} - \mathbf{Q}^*)^{-1}\mathbf{p}(0), \quad (4.34)$$

where a is an individual's strategy and $\bar{a}$ is its corresponding population average strategy, $U(a, \bar{a})$ indicates that the individual's utility depends on both the individual's decision and the population's average behaviour, h is the dis-

count rate, $\mathbf{I}$ is identity matrix, $\mathbf{f}$ is the vector of utility (or payoff) gains per unit time for individuals (or residents) of each state, $\mathbf{F}$ is the vector of instantaneous utility gains associated with each transition of state.

$$\mathbf{f} = \begin{bmatrix} 0 \\ -c_I \\ -c_W \\ 0 \\ 0 \\ 0 \end{bmatrix}, \qquad \mathbf{F} = \begin{bmatrix} 0 & 0 & 0 & 0 & 0 & 0 \\ 0 & 0 & 0 & 0 & 0 & 0 \\ 0 & 0 & 0 & 0 & 0 & 0 \\ 0 & 0 & 0 & 0 & 0 & 0 \\ -c_V & 0 & 0 & 0 & 0 & 0 \\ 0 & 0 & 0 & 0 & 0 & 0 \end{bmatrix}, \qquad \mathbf{1} = \begin{bmatrix} 1 \\ 1 \\ 1 \\ 1 \\ 1 \\ 1 \end{bmatrix}. \tag{4.35}$$

As individuals reside in the unvaccinated infected (resp. vaccinated infected) state, they accumulate the cost of infection, c_I (resp. c_W). The instantaneous vaccination cost c_V to the individual occurs in the transition from susceptible to vaccinated state in the V_1 class. The vaccination cost c_V is referred to not only the monetary cost, but also the psychological burden of possibility of developing vaccine side effects (VSE). $\mathbf{F} \bullet \mathbf{Q}^*$ is the Hadamard product, i.e. the product of the components of $\mathbf{F}$ and $\mathbf{Q}^*$. Thus, by using equations (4.35), the expected change in utility per unit time for individuals in each disease state is given by the vector $\mathbf{f}^T + \mathbf{1}^T(\mathbf{F} \bullet \mathbf{Q}^*) = [\,-\pi c_V \quad -c_I \quad -c_W \quad 0 \quad 0 \quad 0\,]$. Thus, by using equation (4.34) and taking $\lim_{h\to 0} hU(a, \bar{a})$, the utility of strategy π to an individual in a population at equilibrium with strategy $\bar{\pi}$ is given by

$$U(\pi, \bar{\pi}) = \frac{-\omega_R\gamma_1\left\{\lambda^*\left[(\lambda^*\sigma + \omega_V)\gamma_v c_I + \pi\sigma\gamma_u c_W\right] + \gamma_u\gamma_v\pi(\lambda^*\sigma + \omega_V)c_V\right\}}{u_{11}(\lambda^*)^2 + u_{12}\lambda^* + u_{13}}, \tag{4.36a}$$

where

$$u_{11} = \gamma_1\gamma_v(\gamma_u + \omega_R)\sigma, \tag{4.36b}$$

$$u_{12} = \gamma_1\gamma_v\left[\omega_V(\gamma_u + \omega_R) + \gamma_u\omega_R\sigma\right] + \sigma\pi\gamma_u\left[\omega_R(\gamma_1 + \gamma_v) + \gamma_1\gamma_v\right], \tag{4.36c}$$

$$u_{13} = \gamma_u\gamma_v\omega_R\left[\gamma_1\omega_V + (\gamma_1 + \omega_V)\pi\right]. \tag{4.36d}$$

Since the epidemiological parameters are all non-negative, the utility cal-

culated by equations (4.36) will be always less than 0 and hence termed as disutility. For a given population vaccination rate $\bar{\pi}$, individuals aim to minimize the loss of utility, i.e. maximize the disutility by choosing their own individual vaccination rate π. For simplicity, we define the relative cost of vaccination to cost of infection as $c = \frac{c_V}{c_I}$, where $0 \leq c \leq 1$ and set $\omega_R = \omega_V = \omega$, $c_W = c_I = 1$. The utility function $U(\pi, \bar{\pi})$ in (4.36) is an expression of various costs (c_I, c_W and c_V), epidemiological parameters (γ_1, γ_u, γ_v, ω_R, ω_V), the probability of vaccine failure (σ), individual vaccination rate (π), and the population force of infection at steady state (λ^*), with the population-level vaccination rate $\bar{\pi}$ implicitly embedded in λ^* through equations (4.27) and (4.28). Since equation (4.27) is not linear as well as the mathematical relation between $\bar{\pi}$ and λ^* is not always one-to-one, it is not possible to replace the terms λ^* in utility function (4.36) explicitly by the population-level vaccination rate $\bar{\pi}$ so as to investigate the individuals' best response (of their own vaccination rate π) on the population-level vaccination rate $\bar{\pi}$. Hence, for vaccination population games with imperfect vaccine, the individual best response correspondence, π_{best}, is defined differently for specific subsets of c in the following form:

$$\pi_{\text{best}}(c) = \begin{cases} 0 & \text{if } c > c_{\text{no}} \\ [0, \infty) & \text{if } c_{\text{instant}} \leq c \leq c_{\text{no}} \\ \infty & \text{if } c < c_{\text{instant}} \end{cases}, \tag{4.37}$$

where c_{no} and c_{instant} are the cost threshold for no vaccination and instant vaccination, respectively. We will derive these two thresholds in the next subsection.

In order to find the rate of change in utility when the individual vaccination rate π is varied, we differentiate the utility function (4.36) with respect to π, equate the resulting derivative to zero and change the subject of formula to c, we obtain the following critical value c.

$$c = \frac{\lambda^* \left[\sigma^2(\lambda^*)^2 c_{11} + \sigma\omega\lambda^* c_{12} + \omega^2 c_{13}\right]}{\sigma^2(\lambda^*)^3 c_{21} + \sigma\omega(\lambda^*)^2 c_{22} + \omega^2\lambda^* c_{23} + \omega^3 c_{24}}, \tag{4.38}$$

where $c_{11} = \gamma_v(\gamma_1 + \omega) - \gamma_1\gamma_u$, $c_{12} = 2\gamma_v(\omega + \gamma_1) - (\sigma + 1)\gamma_1\gamma_u$, $c_{13} = \gamma_v(\omega + \gamma_1) - \sigma\gamma_1\gamma_u$, $c_{21} = \gamma_1\gamma_v(\gamma_u + \omega)$, $c_{22} = \gamma_1\gamma_v\left[\gamma_u(\sigma + 2) + 2\omega\right]$, $c_{23} = \gamma_1\gamma_v(\omega + 2\sigma\gamma_u + \gamma_u)$ and $c_{24} = \gamma_1\gamma_u\gamma_v$. Rearranging equation (4.38), we obtain the following cubic equation in terms of λ^*:

$$A_3(\lambda^*)^3 + A_2(\lambda^*)^2 + A_1\lambda^* + A_0 = 0, \tag{4.39}$$

where

$$A_3 = \sigma^2\left[\gamma_1\gamma_v(\gamma_u + \omega)c + \gamma_1\gamma_u - \gamma_v(\gamma_1 + \omega)\right], \tag{4.40a}$$

$$A_2 = \sigma\omega\left\{\gamma_1\gamma_v\left[\gamma_u(\sigma + 2) + 2\omega\right]c + \gamma_1\gamma_u(\sigma + 1) - 2\gamma_v(\omega + \gamma_1)\right\}, \tag{4.40b}$$

$$A_1 = \omega^2\left\{\gamma_1\gamma_v(\omega + 2\sigma\gamma_u + \gamma_u)c + \sigma\gamma_1\gamma_u - \gamma_v(\omega + \gamma_1)\right\}, \tag{4.40c}$$

$$A_0 = \omega^3\gamma_1\gamma_u\gamma_v c > 0. \tag{4.40d}$$

Equations (4.27) and (4.39) not only differ in the order of its polynomial and the number of parameters involved, but also most importantly, the cubic equation (4.39) is the result of investigating the interplay among the relative cost of vaccination to infection c, the force of infection λ^* and the population vaccination rate, $\bar{\pi}$, whereas equation (4.27) is only focusing on the relation of the force of infection (λ^*) and the population vaccination rate ($\bar{\pi}$).

4.3.3 Population game analysis

We assume that individuals are fully rational in making their vaccination decision and have complete knowledge about the epidemiological parameters, including the three additional parameters in the two-class vaccine-acquired immunity model, namely the duration of staying in V_1 class after vaccination, the recovery rate and the reduced transmissibility of vaccinated infected individuals. As a direct consequence of splitting the vaccinated individuals with full protection (V_1) from those with partial protection (V_2), we further

assume that the first additional parameter (γ_1) is the factor being considered by rational individuals before they take into account the vaccine efficacy in their decision making, as vaccine efficacy is only relevant to vaccinated individuals after they have lost their high vaccine-induced immunity and move to the V_2 class in a rate γ_1. Meanwhile, the second (θ) and third (γ_v) additional parameters are factors being considered after the vaccine efficacy. These two factors play no role if the vaccine is very efficient (i.e. $\sigma \to 0$, see eq. (4.18)). These additional assumptions are not strong or not compulsory, either, but it will be useful in explaining our numerical simulation results later.

The Nash equilibrium vaccination rate is denoted as π^*. By taking $\omega_R = \omega_V = \omega$, we first find the threshold of the relative cost of vaccination to infection, c, for the zero population vaccination rate (i.e. $\pi^* = \bar{\pi} = 0$) by substituting equation (4.30) into equation (4.38). The resulting critical value c is the cost threshold for no vaccination, c_{no}. If

$$c > c_{\text{no}} = \frac{(\beta - \gamma_u)\left[(\gamma_1 + \omega)k_1 - \sigma\gamma_1\gamma_u(\beta + \omega)\right]}{\beta\gamma_1(\gamma_u + \omega)k_1}, \tag{4.41}$$

where $k_1 = \gamma_v\left[(1-\sigma)\gamma_u + \sigma\beta + \omega\right]$, then no one in the population will vaccinate. Similarly, by substituting equation (4.31) into equation (4.38), we conclude that if $\sigma\theta\beta\gamma_1 > \gamma_v(\gamma_1 + \omega_V)$ and

$$c < c_{\text{instant}} = \frac{(\gamma_1\theta\sigma\beta - k_4\gamma_v)\left\{\theta\sigma\beta(k_4\gamma_v - \gamma_1\gamma_u) - k_3\sigma\gamma_u + \gamma_v k_4 k_5\right\}}{\gamma_1\gamma_v\left\{k_5\gamma_1(\theta\sigma\beta)^2 + \theta\sigma\beta\left[k_3\sigma\gamma_u - k_5 k_2)\right] + \gamma_u\sigma\omega k_3 - \gamma_v\omega k_4 k_5\right\}}, \tag{4.42}$$

where $k_2 = \gamma_v(\gamma_1 + \omega) - \gamma_1\omega$, $k_3 = \omega(\gamma_1 + \gamma_v) + \gamma_v\gamma_1$, $k_4 = \gamma_1 + \omega$ and $k_5 = \gamma_u + \omega$, then susceptible individuals in the population will vaccinate instantly (i.e. $\pi^* = \bar{\pi} \to \infty$). Whenever

$$c_{\text{instant}} \leq c \leq c_{\text{no}}, \tag{4.43}$$

the vaccination rate in the population is finite (i.e. $\pi^* = \bar{\pi} \in (0, \infty)$).

Since every cubic equation with real coefficients has at least one solution among the real numbers, we find the closed-form of the discriminant of the cubic equation (4.39) with

$$\triangle = 18A_3A_2A_1A_0 - 4A_2^3A_0 + A_2^2A_1^2 - 4A_3A_1^3 - 27A_3^2A_0^2. \tag{4.44}$$

If $\triangle = 0$, then the cubic equation (4.39) has a multiple root and all its roots are real. This corresponds to the case where saddle-node (or fold) bifurcation occurs in the utility function (4.36), i.e. the multiple endemic equilibria λ^* (and its corresponding population vaccination rates $\bar{\pi}$, if exist) collide and merge into one. After some algebraic manipulations, we obtain the following quadratic equation for the location of saddle-node (or fold) bifurcation in terms of the variable c.

$$\begin{aligned} &k_7^2\Big(\left[\gamma_1\gamma_v\left[(\sigma-1)\gamma_u - \omega\right]\right]^2 c^2 \\ &+2\gamma_1\gamma_v\left[(\sigma-1)\gamma_u(\sigma\gamma_1\gamma_u + \gamma_1\omega + k_6) + \omega(\gamma_1\gamma_u - k_6)\right]c + (\sigma\gamma_1\gamma_u - k_6)^2\Big) = 0, \end{aligned} \tag{4.45}$$

where $k_6 = \gamma_v(\gamma_1+\omega)$ and $k_7 = \gamma_1\gamma_u\sigma(\sigma-1)\omega^3$. Therefore, with other parameters fixed, theoretically, bifurcation should occur at the roots of the quadratic equation (4.45), that is the number of endemic equilibrium and hence the Nash equilibria of vaccination rate should change from three to two, and then to only one.

However, by investigating various possibilities for the roots of cubic equation (4.39) using the Descartes rule of signs (as in [123]), we find that the necessary condition for the cubic equation (4.39) to have three positive real roots is that whenever Case 7 in Table 4.1 is satisfied. Let us assume that the equation (4.39) does have three positive real roots. It follows that the following three inequalities must be satisfied at the same time for the combination of parameter values selected in the numerical simulations.

Table 4.1: Number of possible positive real roots of equation (4.39)

Case	A_3	A_2	A_1	A_0	Number of sign changes	Number of possible positive real roots
1	+	+	+	+	0	0
2	+	+	−	+	2	2, 0
3	+	−	+	+	2	2, 0
4	−	+	+	+	1	1
5	+	−	−	+	2	2, 0
6	−	−	+	+	1	1
7	−	+	−	+	3	3, 1
8	−	−	−	+	1	1

$$\gamma_1\gamma_v(\gamma_u+\omega)c+\gamma_1\gamma_u<\gamma_v(\omega+\gamma_1), \tag{4.46a}$$

$$\frac{1}{2}\left\{\gamma_1\gamma_v\left[\gamma_u(\sigma+2)+2\omega\right]c+\gamma_1\gamma_u(1+\sigma)\right\}>\gamma_v(\omega+\gamma_1), \tag{4.46b}$$

$$\gamma_1\gamma_v(\omega+2\sigma\gamma_u+\gamma_u)c+\sigma\gamma_1\gamma_u<\gamma_v(\omega+\gamma_1). \tag{4.46c}$$

By using the transitivity of order in real number axioms (i.e. if $A < B$ and $B < C$, then $A < C$), the inequalities (4.46a) and (4.46b) give

$$2\gamma_1\gamma_v(\gamma_u+\omega)+2\gamma_1\gamma_u<2\gamma_1\gamma_v(\gamma_u+\omega)c+\gamma_1\gamma_v\gamma_u\sigma c+\gamma_1\gamma_u(1+\sigma).$$

After simplifying, we obtain $\sigma(\gamma_v c+1)>1$. Similarly, the inequalities (4.46b) and (4.46c) give $\sigma(3\gamma_v c+1)<1$. By applying the transitivity of order once more to these two resulting inequalities, we arrive at the inequality $\sigma(3\gamma_v c+1)<\sigma(\gamma_v c+1)$ which results in $3<1$. This contradicts with the basic properties of the real number. Hence, our earlier assumption that the cubic equation (4.39) has three positive real roots is not valid. Therefore, we rule out the possibility to have three positive real roots in the cubic equation (4.39). It follows that the phenomenon of pitchfork bifurcation and hysteresis loops are not possible for the cubic equation (4.39) meanwhile the saddle-node (or fold) bifurcation are still possible if Cases 2, 3, and 5 in Table 4.1 are satisfied.

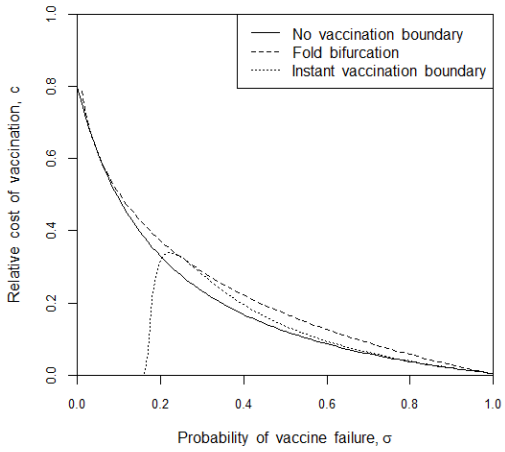

(a) $\gamma_u = \gamma_v = 1$, $\gamma_1 = 10$, $\omega = 0.05$, $\beta = 6$, $\theta = 1$

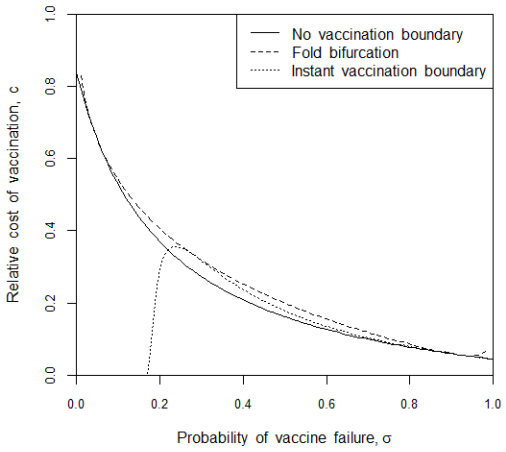

(b) Same as (a) except $\gamma_1 = 0.9$

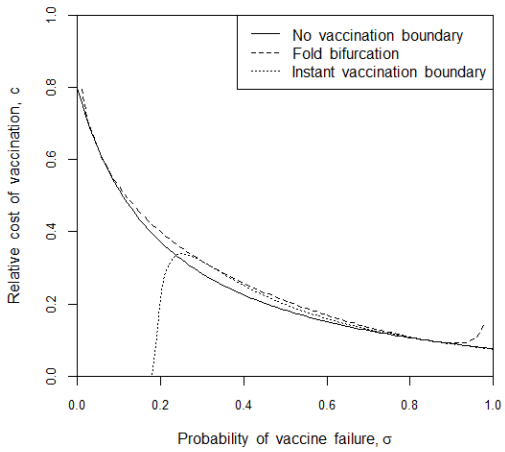

(c) Same as (a) except $\gamma_v = 1.1$

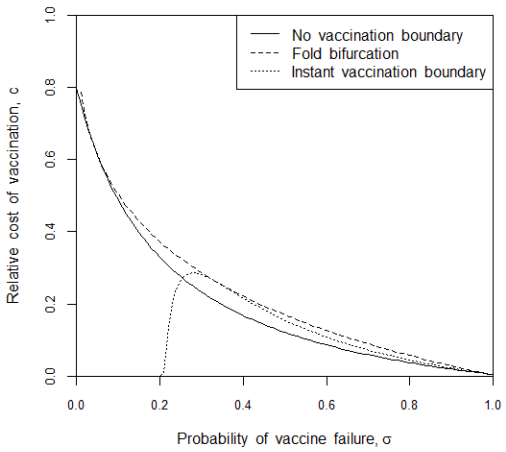

(d) Same as (a) except $\theta = 0.8$

Figure 4.2: Parameter-space (c-σ) diagram of the bifurcation structure in the Nash equalibria of equation (4.36).

4.4 Results and discussion

4.4.1 The cost thresholds for no, finite and instant vaccination for three additional characteristics of imperfect vaccine

In the previous section, we derived the cost threshold for no vaccination (eq. (4.41)) and instant vaccination (eq. (4.42)), as well as the condition for the location of fold bifurcation (eq. (4.45)) in the utility function (eq. (4.36)). In

the aspect of epidemiological parameters, the impact of the additional three characteristics of imperfect vaccine, namely γ_1, θ and γ_v in our proposed model, on the individual vaccination decision-making has not previously been described in the model (3.31) in [79]. However, if we assume that all vaccinated individuals in the V_1 class move to the V_2 class instantly (i.e. $\gamma_1 \to \infty$, say $\gamma_1 = 10$), and vaccinated infected individuals in the W class have the same infectiousness (i.e. $\theta = 1$) and recovery rate (i.e. $\gamma_v = \gamma_u$) as those unvaccinated infected individuals in the I class, our proposed model (and its corresponds cost thresholds and condition for the location of fold bifurcation) reduces to the model (3.31) in [79]. We recover the same pattern of parameter-space (c-σ) diagram of the bifurcation structure in the Nash equilibria, as depicted in Figure 4.2(a).

We then carried out some sensitivity analysis of the cost thresholds in order to have a rough idea on how each additional epidemiological parameter of imperfect vaccine influences the Nash equilibrium vaccination strategy in population game. If a small portion of vaccinated individuals stays in the V_1 class for some duration of time (i.e. $\gamma_1 < 1$), or vaccinated infected individuals recover slightly faster than the unvaccinated infected individuals (for instance, $\gamma_v = 1.1 > \gamma_u = 1$), then all three curves are shifted upward for $\sigma \to 1$ (Figures 4.2(b) and 4.2(c)). These two parameters tuning will also cause a marginally shift to the right for the instant vaccination boundary, as the lower bound of σ for instant vaccination boundary could be determined through solving inequality $\sigma\theta\beta\gamma_1 > \gamma_v(\gamma_1 + \omega_V)$. When vaccinated infected individuals have a slightly reduced transmissibility (e.g. $\theta = 0.8$), we observe that the curve for the instant vaccination boundary is shifted to the right on a larger scale (Figure 4.2(d)) compared to the cases of γ_1 and γ_v. These suggest that incorporating additional characteristics of imperfect vaccine may alter the individual best response for vaccination strategy.

To further investigate the impact of additional characteristics of imperfect

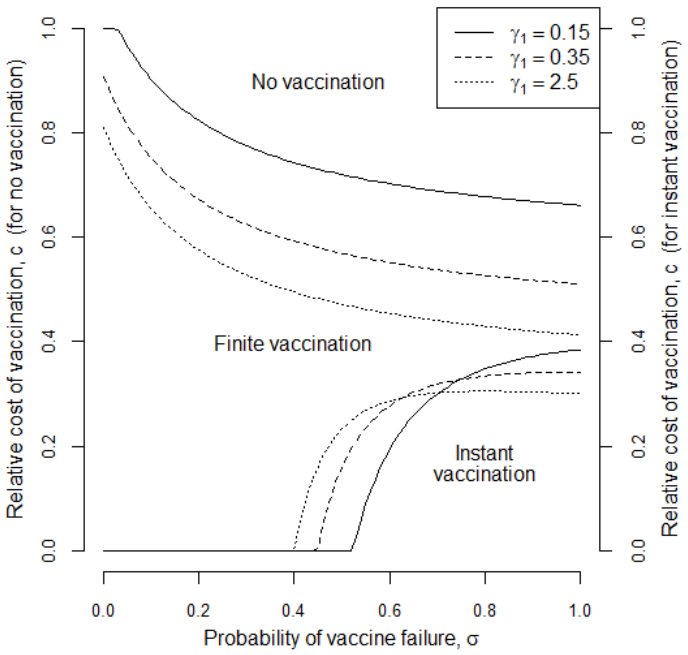

(a) $\theta = 0.85$

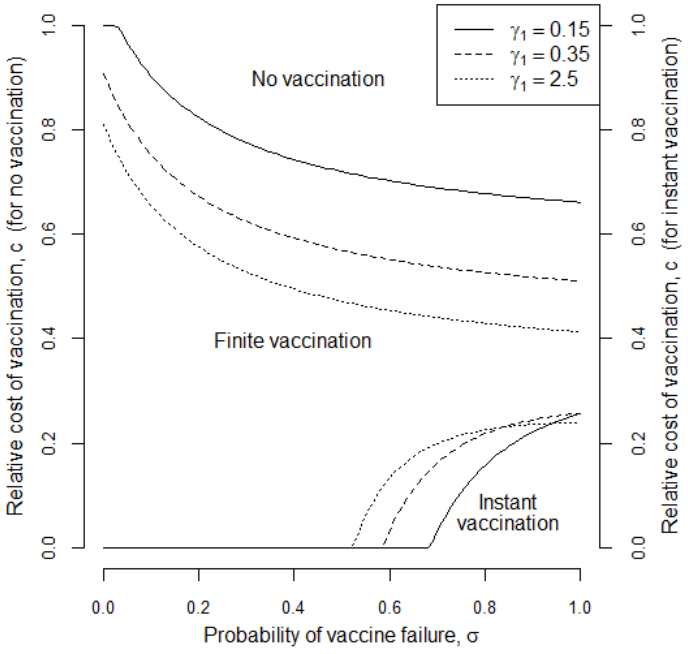

(b) $\theta = 0.65$

Figure 4.3: The cost thresholds for no and instant vaccination with various values of γ_1 and θ.

vaccine on vaccination behaviours, we plot the cost thresholds for no vaccination and instant vaccination for various values of $\gamma_1 = \{0.15, 0.35, 2.5\}$ and $\theta = \{0.85, 0.65\}$ in Figure 4.3. For both diagrams, the parameter values $(\beta, \gamma_u, \gamma_v, \omega) = (6, 1, 2, 0.05)$ are used.

As defined in equation (4.37), with the pairs of cost threshold for no and instant vaccination, the c-σ plane in Figure 4.3 could be divided into three regions, namely no vaccination, finite vaccination and instant vaccination. If both the c and σ values fall into the region of no (resp. instant) vaccination, no one (resp. everyone) in the population will opt for vaccination. However, as the equilibrium of force of infection λ^* at $\bar{\pi} \to \infty$ in equation (4.31) will be positive if and only if $\sigma\theta\beta\gamma_1 > \gamma_v(\gamma_1 + \omega)$ (where $\omega \equiv \omega_V$), the region of instant vaccination should be viewed as unfavourable from the perspective of infectious diseases control. This is because the region of instant vaccination is referred to as the scenario in which even though everyone in the population vaccinated immediately, the infectious diseases would still not be eradicated. Hence, the vaccine efficacy $(1 - \sigma)$ could be a major factor, if not the only one, causing the voluntary vaccination program not sufficient in reducing the basic reproduction number to below unity.

The relationship between relative cost of vaccination and vaccine efficacy for no vaccination is much more simple in which the cost threshold of no vaccination (eq. (4.41)) is a decreasing function of σ. For a specific vaccine efficacy, $1 - \sigma$, the longer duration the vaccinated individuals reside in the V_1 class (i.e. smaller γ_1), the higher the cost threshold for no vaccination (three upper curves in Figure 4.3(a)) will be. From the community perspective, the higher the cost threshold for no vaccination, the better it will be since individuals will not opt for vaccination if the relative cost of vaccination, c, is higher than the cost threshold of no vaccination. From an individual point of view, higher cost threshold for no vaccination implies that his/her utility is lower if he/she refuses to vaccinate, and hence rational individuals are highly

likely to vaccinate if γ_1 is small. As the higher values of σ correspond to the lower vaccine efficacy, and vice versa, when the transition rate from V_1 to V_2 class is low enough (for instance $\gamma_1 = 0.15$) and the vaccine efficacy is high enough (i.e. $\sigma \to 0$), the Nash equilibrium vaccination rate is always finite.

The effect of γ_1 on the instant vaccination boundary, albeit minimal, is not insignificant. As observed in Figure 4.2(b), any γ_1 value less than 1 will shift the three curves upward for $\sigma \to 1$. Therefore, in Figure 4.3(a) with $\theta = 0.85$, we found that the instant vaccination will only occur when $\sigma > 0.4$. For intermediate values of σ, the longer duration individuals stay in the V_1 class, the lower the relative cost will be for instant vaccination to occur. However, it is interesting to find that as $\sigma \to 1$, instant vaccination occurs for higher relative cost of vaccination when γ_1 is smaller. A possible explanation for this might be that the model (4.24) takes into account more realistic assumptions that the vaccine would offer, on one hand full protection to individuals in V_1 and on the other hand, partial protection to individuals in V_2. That is, a mixed vaccinated individuals with full and partial protection coexist in the population in the two-class vaccinated individuals model, while the one-class imperfect vaccine-induced immunity model in [79] assumes that vaccine offers either full protection or partial protection to all vaccinated individuals, depending on the pre-defined σ value. Thus, when the vaccine failure is almost certain, the model (3.31) in [79] predicts no one in the population will go for vaccination. It is therefore likely that the coexistence of vaccinated individuals with full and partial protection may have something to do with the dissimilarity between our vaccination population games in Figure 4.3(a) and the one in Figure 5(a) in [79].

The effect of the reduction of transmissibility (or infectivity), θ in breakthrough infection for individuals in the W class in relation to those in the I class on individuals vaccination strategy is illustrated in Figure 4.3(b). As θ only appears in the cost threshold for instant vaccination (4.42) but not in

the cost threshold for no vaccination (4.41), the three upper curves in Figure 4.3(b) are exactly those in Figure 4.3(a). When the reduction of transmissibility increases (i.e. smaller θ, for instance $\theta = 0.65$) and vaccinated individuals stay longer in the V_1 class (i.e. smaller γ_1), the unfavourable phenomenon of coexistence of instant vaccination and prevailing diseases occurs for lower relative cost of vaccination and narrower range of low vaccine efficacy (Figure 4.3(b)).

When vaccine may offer large reduction of infectivity to vaccinated infected individuals, vaccines can be of greater benefit to the society than to the recipient who bears the cost of vaccination. It follows that vaccination can be regarded as a somewhat altruistic behaviour [95]. If most people are altruistic, the spontaneous vaccination rate will not differ substantially from the social optimum [101]. Contrary to the selfishness assumption in the game theory, it can thus be suggested that altruism reduces the possibility of instant vaccination to occur but diseases may not be eradicated in our two-class vaccine-induced immunity epidemic model with additional reduction transmissibility parameter θ, despite the fact that vaccine is not fully perfect.

As Figure 4.2(c) reveals that for any γ_v value greater than γ_u, the cost thresholds for no vaccination and for instant vaccination will be shifted upward. We further examine the effect of γ_v on the vaccination rates in the two classes of vaccine-induced immunity model, in Figure 4.4. The most obvious finding to emerge from this figure is that when the γ_v value increases, the cost threshold for no vaccination are shifted upward, on a greater scale, especially for larger value of σ. When vaccine is very effective in protecting vaccinated individuals with low vaccine-induced immunity from getting infection, it is likely that individuals will only put slightest concern on the recovery rate for breakthrough infection in making their vaccination decisions. However, if vaccine is not effective in reducing vaccinated individuals' susceptibility, then the fact that vaccine is able to shorten the duration of infection will signifi-

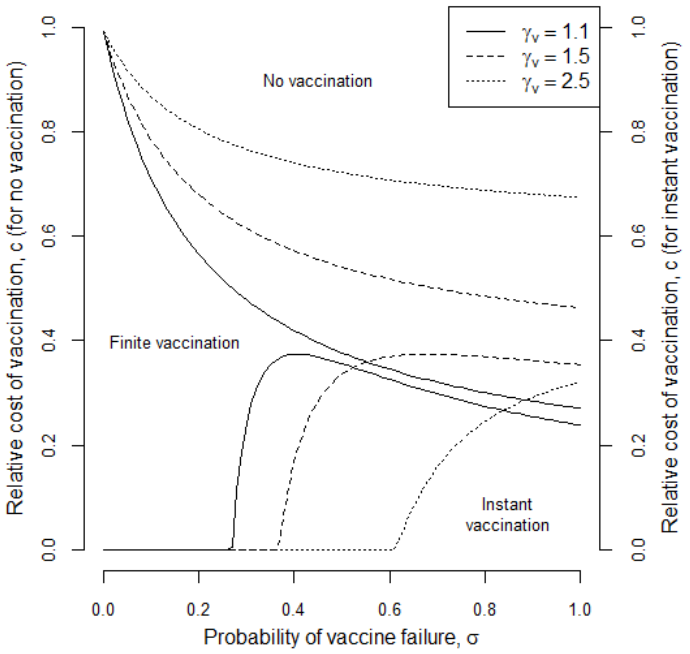

Figure 4.4: The cost thresholds for no and instant vaccination with various values of γ_v.

cantly raise the cost threshold for no vaccination. That is, individuals will not refuse to vaccinate for a higher relative cost of vaccination (i.e. lower utility) if vaccines offer faster recovery in breakthrough infection. On the other hand, the faster vaccineted infected individuals recovered, the unfavourable instant vaccination occurs for lower c and larger σ.

It is interesting to note that in all cases of Figures 4.3 and 4.4, when the probability of vaccine failure is low, i.e. $\sigma \to 0$, no one takes vaccination instantly. However, expression (4.15) implies that the better vaccine efficacy, the greater reduction to basic reproduction number will be and hence epidemic could be better controlled. Thus, with the population vaccination games framework, we are able to demonstrate that individuals would not refuse to vaccinate in all range of relative cost of vaccination to infection (i.e. finite vaccination rate always exists) when $\sigma \to 0$ provided that vaccinated individuals do not lose their high vaccine-induced immunity in a short time. These results further support the claim in [113] that although an increase in

vaccination effectiveness leads to vaccine uptake drops due to free-riding effects, the epidemic can be better mitigated. It could be argued that the drop of vaccine uptake in [113] might be attributed to no instant vaccination from self-interested individuals, meanwhile a possible explanation for better mitigation of epidemic despite of vaccine uptake drops might be that of the existence of finite vaccination rate in all range of relative vaccination costs when $\sigma \to 0$.

4.4.2 Nash equilibrium vaccination rate

We solve the cubic equation (4.39) together with (4.40) numerically for parameter values $(\beta, \theta, \gamma_1, \gamma_u, \gamma_v, \omega) = (6, 0.85, 0.15, 1, 2, 0.05)$ for $\sigma = 0.15$ and plot the graph of the equilibrium force of infection λ^* versus the relative cost of vaccination c in Figure 4.5(a). As agreed with the findings in inequalities (4.46), the graph gives at most two endemic equilibria. Furthermore, equation (4.45) and the numerical simulation in Figure 4.5(a) both give the location of fold bifurcation at $c = 0.874$. By substituting the force of infection λ^* obtained into the quadratic equation (4.27) with (4.28), and solving for population vaccination rate $\bar{\pi}$, the Nash equilibrium vaccination rate (i.e. $\pi^* = \bar{\pi} = \pi$) versus the relative cost of vaccination c is depicted in Figure 4.5(b). The existence of an equilibrium in the population games is referred to as a stable collection of individual strategies such that nobody has any incentive to change his own individual strategy [87]. We find that there is neither instant vaccination nor multiple Nash equilibria vaccination rates, for this specific combination of parameter values in vaccination population game with two-class vaccine-induced immunity. As the combination of parameter values used in Figures 4.5(a) and 4.5(b) are the same as the parameter values for the solid line curves in Figure 4.3(a), when $\sigma = 0.15$, the cost threshold for no vaccination is $c \approx 0.858$ (see Figure 4.3(a)). Thus, the curve of population equilibrium vaccination rate in Figure 4.5(b) is in good agreement with that of Figure 4.3(a). This implies that the two cost thresholds derived in Subsection 4.3.3 may be used to study the interplay among the relative cost

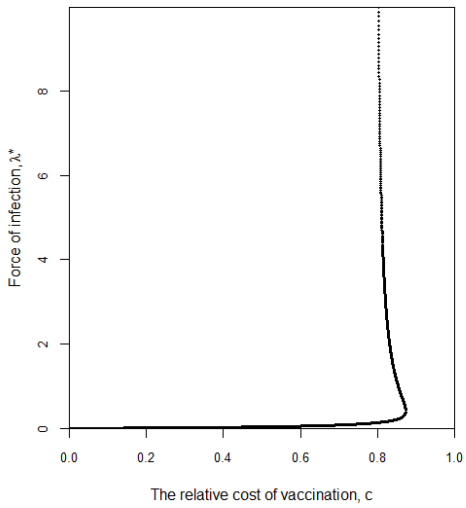

(a) $\sigma = 0.15$

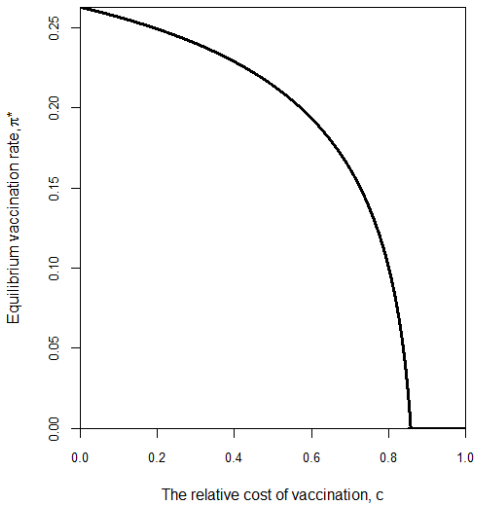

(b) $\sigma = 0.15$

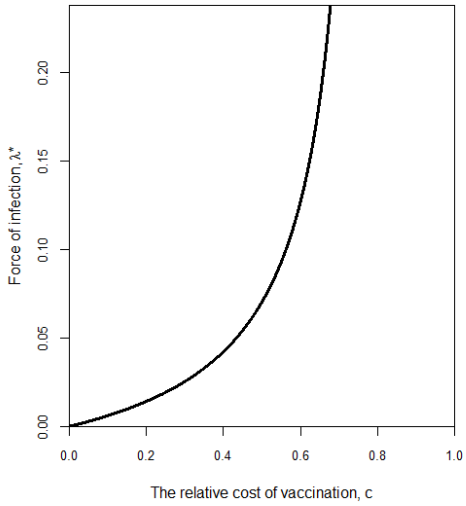

(c) $\sigma = 0.8$

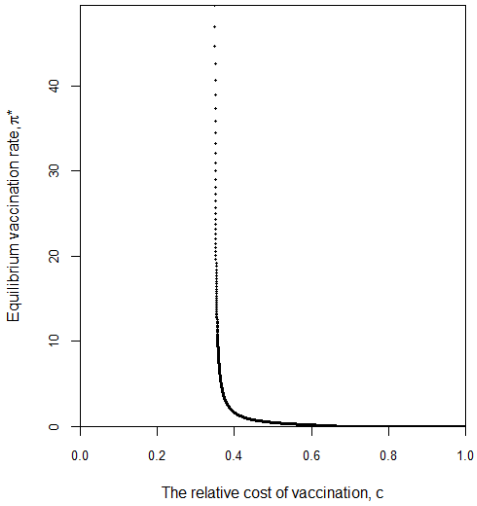

(d) $\sigma = 0.8$

Figure 4.5: Dependence of the force of infection λ^* and equilibrium vaccination rate π^* on the relative cost of vaccination c, for $\beta = 6$.

of vaccination to infection, c, the force of infection λ^* at steady state and the population vaccination rate $\bar{\pi}$, without having to solve the cubic equation (4.39) and the quadratic equation (4.27).

We then plot the graph of equilibrium force of infection λ^* (and its Nash equilibrium vaccination rate π^*) versus the relative cost of vaccination c for the same combination of parameter values except $\sigma = 0.8$. As can be seen on

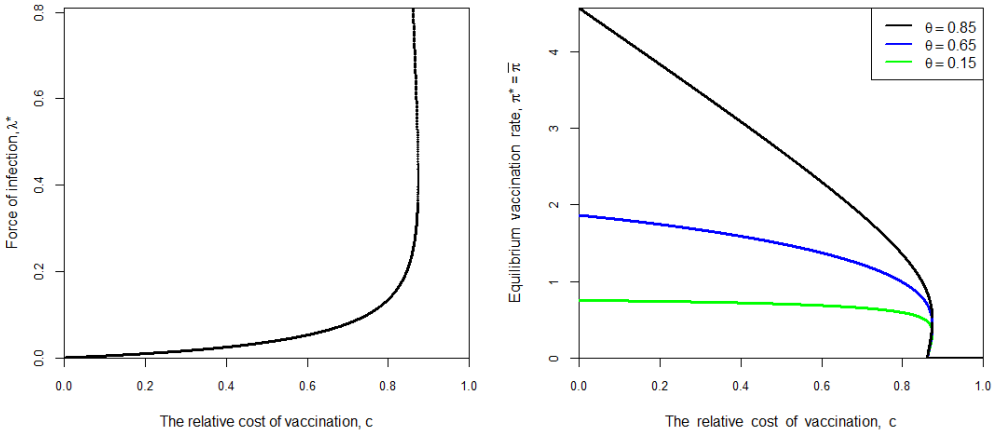

(a) (b)

Figure 4.6: Dependence of the force of infection λ^* and equilibrium vaccination rate $\pi^* = \bar{\pi}$ on the relative cost of vaccination c, for $\beta = 18$ and $\theta = \{0.85, 0.65, 0.15\}$.

the lower solid-line curve in Figure 4.3(a), instant vaccination occurs when $c < 0.429$. The same behaviour is observed in Figure 4.5(d) whereby the Nash equilibrium vaccination rates are greater than 1 for $c < 0.429$. If we calculate the corresponding force of infection λ^* (Figure 4.5(c)) (unlike Figure 4.5(a), we discard those $\lambda^* > \lambda^*(\pi^* = 0) = 0.238$ in this graph), we find that the force of infection is not zero even though individuals vaccinate instantly when $c < 0.429$. These results further support that the instant vaccination in the vaccination population game is not favourable from perspective of the infectious diseases control, simply because diseases will not be eradicated even though π^* is already high. Also, it seems possible that these unfavourable instant vaccinations are due to imperfect vaccines.

We then increase the disease transmission rate from $\beta = 6$ to $\beta = 18$ to investigate the individuals vaccination decision-making in the course of a highly contagious infectious disease, with $(\beta, \sigma, \gamma_1, \gamma_u, \gamma_v, \omega) = (18, 0.15, 0.15, 1, 2, 0.05)$ for $\theta = \{0.85, 0.65, 0.15\}$. As the force of infection $\lambda^*(\bar{\pi} = 0) = 0.810$, we discard the graph whenever the numerical simulation gives $\lambda^* > 0.810$ in Figure

4.6(a). Similar to Figure 4.5(a), the force of infection λ^* at steady state in Figure 4.6(a) shows the occurrence of the fold bifurcation at a specific value of $c_{\text{fold}} \approx 0.917$. When the c value is greater than c_{fold} there is no feasible endemic equilibrium but when the c value is smaller than and close to c_{fold}, there are two endemic equilibria. The phenomenon of fold bifurcation complicates the individual vaccination decision-making in the cases of highly contagious infectious disease in which the three Nash equilibria vaccination rates $\pi^* = \bar{\pi} = \pi$, corresponding to two finite vaccination rates and one no vaccination which coexist at $0.861 \leq c \leq 0.874$ (Figure 4.6(b)).

As θ is implicitly appear in $\lambda^* = \beta \frac{I^* + \theta W^*}{N^*}$, the curves in Figure 4.6(b) clearly shows that the greater reduction of infectivity to vaccinated infected individuals (i.e. smaller θ) would be able to reduce the possibility of the unfavourable phenomenon of instant vaccination coexistence with prevalent infectious diseases in the population. For instance, even though its corresponding λ^* are non-zero whenever $c < 0.861$ for all three θ values, finite vaccination (i.e. $\pi^* < 1$) is the Nash equilibrium strategy for $\theta = 0.15$ as compared to instant vaccination (i.e. $\pi^* > 1$) for $\theta = 0.65$ and 0.85.

4.5 Concluding remarks

We conclude this chapter with the following remarks.

(i) Rational individuals would not refuse to vaccinate if vaccines are able to provide longer duration of high vaccine-induced immunity to vaccinated individuals.

(ii) All individuals opt for vaccination instantly for an intermediate region of vaccine efficacy when vaccines neither offer much shorter duration of recovery nor greater reduction of transmissibility for vaccinated infected individuals in breakthrough infection.

(iii) Greater reduction of infectivity to vaccinated infected individuals would be able to reduce the possibility of the unfavourable phenomenon of instant vaccination coexistence with prevalent infectious diseases in the population whenever the vaccine is not effective in reducing vaccinated individuals' susceptibility.

(iv) When vaccine efficacy is low and vaccine does not offer faster recovery to vaccinated infected individuals, self-interested individuals are highly likely to refuse vaccination. However, the cost threshold for no vaccination is not affected by the scale of reduction of transmissibility offered by vaccines to vaccinated individuals.

Chapter 5

Asymmetric Smoothed Best Response in Voluntary Vaccination Decisions

5.1 Introduction

The effectiveness of health preventive strategy against infectious diseases is highly dependent on human self-initiated behaviour. The study of individual-level decision-making on adopting health protective actions becomes especially relevant considering that certain control measures are not mandatory. As vaccine-preventable diseases still pose a great threat to human population, it is of great important to have a better understanding on the individual voluntary vaccination decision-making. Individuals usually base their vaccination choices on a complex balance of perceived costs of vaccination and infection, which may be made through a simple cost-benefit analysis. The perceived cost of vaccination is highly influenced by the perceived probability of the vaccine complications, for instance, the vaccine adverse effects and the degree of protection conferred by vaccines. Also, the perceived cost of infection is closely related to the severity of the epidemic outbreak.

In the last decade, there is a growing number of literatures on incorporating the individual vaccination decision-making based on cost-benefit analysis into the epidemic models. In the language of game theory, the most simplest type of the vaccination behavioural rule is that all susceptibles (i.e. players

of the game) are assumed to have two strategies to choose, namely vaccination and non-vaccination strategies. By opting for vaccination strategy, it is assumed that individuals will go to vaccinate and the vaccine-induced immunity becomes effective immediately, whereas adopting non-vaccination strategy implies that individuals are subject to the risk of infection but they will have the chance to make a new vaccination decision in the future. This leads to an epidemic model with time-varying vaccination rate.

The classical game theory assumes that all players make their pure rational decisions based on the complete and accurate information to maximize their payoffs. Assuming other individuals' strategy is given, the strategy that produces the highest payoff for an individual is the best response for him/her. For two-strategy games, the step-wise function such as the Heaviside step function may be used to describe the best response correspondence. As for voluntary vaccination decision-making through cost-benefit considerations, when the benefit is perceived to be higher (resp. lower) than the perceived cost of vaccination, individuals will choose (resp. not choose) vaccination strategy. However, when the cost equals the benefit, the probability of vaccination lies in [0, 1], which is indeed random. Hence, the best response correspondence could be very sensitive to the epidemiology information used in cost-benefit analysis.

The use of the best response correspondence in investigating vaccination behavioural rule in epidemic models with well-mixed population could be found in a type of vaccination population game framework whereby the utility depends on both the individual's vaccination decision and the population's average vaccination rate [79, 92]. Also, it was used in structured population (i.e. network-based models) through agent-based simulation framework in [18, 72].

However, in epidemiology, precise knowledge of the cost and the benefit of

adopting a particular preventive strategy in the course of epidemic outbreak is not explicitly available. Hence, evolutionary game theory which assumes individuals are not fully rational is being considered in modelling voluntary vaccination decisions. In this bounded rationality paradigm, individuals are allowed to switch their strategy through imitating other's strategy which gives higher payoff (i.e. social learning). Through the use of a replicator dynamical equation and rescaling of the cost of infection to vaccination, the step-wise best response correspondence for cost-benefit analysis in [2, 25, 70] produces the logistic-like of vaccine coverage dynamics. It can thus be suggested that instead of non-smoothed best response correspondence, the smoothed version of best response behaviour may be expressed in the form of the sigmoid function. The mathematical functions with "S" shape including the logistic function, hyperbolic tangent function and Gompertz function, which are all differentiatable real functions.

Apart from using replicator equations to model the imitation process, in bounded rationality paradigm, individuals are also allowed to make mistakes by adopting a strategy which gives lower payoff. This smoothed best response version of imitation dynamics in vaccination behaviour was first studied by Fu and co-authors [35]. They used a type of logistic function known as Fermi updating learning rule to model the strategy switching of players through pairwise payoff comparisons. That is, an individual randomly chooses one other individual in the population as his/her role model to play the game. In their study, vaccine is assumed to be fully perfect and individuals use anecdotal evidence to estimate the cost and benefit of vaccination before making decision in the beginning of an epidemic season. If the strength of selection parameter in Fermi function (see parameter r in equation (5.6b)) is small, the individual with a higher payoff may adopt the strategy of a less successful role model. This characterization diverges from a fully rational decision in best response dynamics models to a bounded rationality decision.

Since then, this type of bounded rationality models has been extensively explored in various aspects of vaccination decision making for epidemic models in structured population, and is mainly implemented through agent-based simulation modelling framework. For instance, the vaccine with imperfect immunity [13, 113], the provision of subsidy to vaccination [120, 121], and the existence of committed vaccinators [58] were added to the framework in [35] to investigate the impact of these factors on vaccination decision making and hence the dynamics of vaccine coverage. The Fermi updating rule has been modified by including social preference [122], conformity [45], memory [118], average opinion from neighbours [11] or society [37] as the additional factors in determining how the cost and benefit of vaccination are being perceived. However, among these literatures, only few works [35, 58, 113, 120] give the analytical frameworks apart from the agent-based simulations.

The two trends for modelling vaccination behaviour in literature, namely the best response with Heaviside step function (mainly implemented through mean-field epidemic model) and the smoothed best response with Fermi function (mainly implemented through agent-based simulations), suggest that the smoothed best response could possibly be incorporated into mean-field epidemic models to study the similarity or the gap between full and bounded rationality vaccination decision assumptions through theoretical analysis. To this end, Xu and Cressman [116] studied the voluntary adult vaccination decision-making by constructing a mean-field epidemic model coupled with a cost-benefit analysis. The vaccination strategy adoption is governed by a logistic function. This is indeed the mean-field version of the Fermi updating function in the literature of vaccination behaviour.

Following the work in [116], in this chapter, we study the smoothed best response dynamics of vaccination behaviour with another type of sigmoid function known as Gompertz function. We formulate this Gompertz-type smoothed best response for individuals vaccination decision based on a sim-

ple cost-benefit analysis in the Susceptible-Infectious-Recovered-Vaccinated (SIRV) epidemic model with partial vaccine-induced immunity in Section 5.2. The dynamical behaviours of the system for both perfect vaccine and imperfect vaccine models are given in Section 5.3. Results and discussions are presented in Section 5.4 followed by some concluding remarks in Section 5.5.

5.2 Model formulations

We begin by considering a simple Susceptible-Infectious-Recovered-Vaccinated (SIRV) compartmental model with imperfect vaccine-induced immunity.

$$\frac{dS}{dt} = \Lambda - \beta\frac{I}{N}S - \phi\left[G(\triangle P)\right]S - \mu S, \tag{5.1a}$$

$$\frac{dI}{dt} = \beta\frac{I}{N}S + \sigma\beta\frac{I}{N}V - \gamma I - \mu I, \tag{5.1b}$$

$$\frac{dR}{dt} = \gamma I - \mu R, \tag{5.1c}$$

$$\frac{dV}{dt} = \phi\left[G(\triangle P)\right]S - \sigma\beta\frac{I}{N}V - \mu V, \tag{5.1d}$$

where $N = S + I + R + V$, Λ is the (constant) recruitment rate of susceptible corresponding to births and immigrations, μ is the constant natural death rate of the population, β is the disease transmission rate, γ is the recovery rate, $\sigma \in [0, 1)$ is the probability of vaccine failure while $1 - \sigma$ gives the vaccine efficacy and ϕ is the vaccination effort parameter [66]. $G(\triangle P)$ is the Gompertz-type smoothed best response function and $\phi\, G(\triangle P)$ gives the time-varying vaccination rate. $\triangle P$ is the difference between payoff for adopting vaccination (P_V) and non-vaccination (P_{NV}) strategies.

We assume that every susceptible merely uses a simple cost-benefit analysis in making decision whether or not to vaccinate in the course of an epidemic outbreak. That is, susceptible individuals do not involve in any social learning process in choosing their vaccination strategy. Since individuals are subjected to the risk of getting infection if they are not vaccinated, the perceived payoff

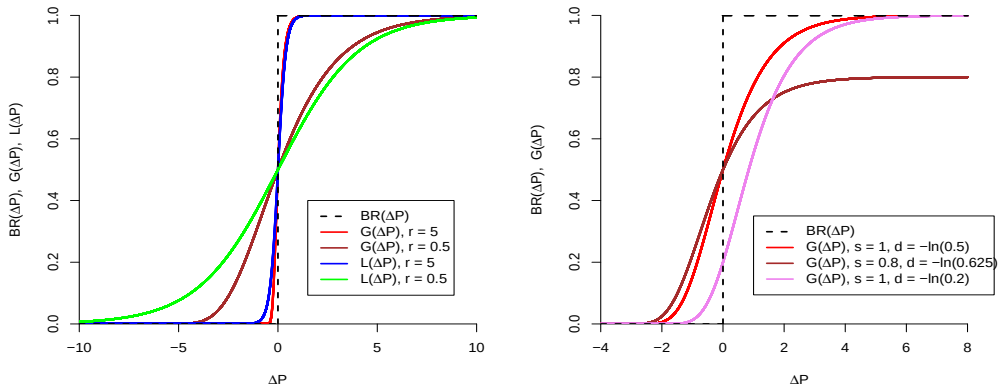

(a) $s = 1$, $d = -\ln(0.5)$ (b) $r = 1$

Figure 5.1: Graphs of best response correspondence, smoothed best response with Gompertz function and logistic function.

for adopting non-vaccination strategy could be described as $P_{NV} = -\beta\frac{I}{N}$, where we simply assume that the cost of non-vaccination is proportional to the disease transmission rate and depends on the state of the epidemic (i.e. the disease prevalence). When vaccination is voluntary, taking vaccination incurs not only monetary cost (e.g. time and money spent in getting vaccination) but also psychological cost (e.g. the risk of developing vaccine adverse effects (VAE)). We denote these costs of vaccination as c_v. When vaccine is not fully perfect, being vaccinated does not guarantee an individual free from infection risk. Individuals who opt for vaccination strategy would have to pay an extra cost if breakthrough infection occurred. Hence, the perceived payoff for vaccination strategy is defined as $P_V = -c_v - \sigma\beta\frac{I}{N}$. This implies that P_V is lower if the vaccine is less effective. Therefore, the payoff difference is given by

$$\begin{aligned} \triangle P &= P_V - P_{NV} \\ &= (1-\sigma)\beta\frac{I}{N} - c_v. \end{aligned} \tag{5.2}$$

If $P_V > P_{NV}$, then individuals are highly likely to vaccinate.

Unlike the full rationality models that use a Heaviside step function (5.3) to construct the best response correspondence

$$BR(\triangle P) = \begin{cases} 0 & \text{if} \quad \triangle P < 0 \\ [0,1] & \text{if} \quad \triangle P = 0 \\ 1 & \text{if} \quad \triangle P > 0, \end{cases} \tag{5.3}$$

a type of sigmoid function, known as Gompertz function, is implemented as our smoothed best response function, i.e.,

$$G(\triangle P) = s\, e^{-d\, e^{-r\, \triangle P}}, \tag{5.4}$$

where s is the upper horizontal asymptote of the Gompertz function, d is the displacement along typical x-axis (i.e. $\triangle P$-axis) and r gives the growth rate of the Gompertz curve. We only consider $s \in (0, 1]$, $d > 0$ and $r > 0$. Similar to the logistic function used in [116], $G(\triangle P)$ is defined as the probability of susceptible taking the vaccination based on the cost-benefit considerations. However, unlike the best response correspondence $BR(\triangle P)$ whereby individuals refuse to vaccinate once the cost is higher than the benefit, in smoothed best response, even if the cost of vaccination is higher than the benefit of getting vaccination, individuals will still opt for vaccination with probability in between $[0, \frac{1}{2})$. This leads to the bounded rationality assumptions in evolutionary game theory. On the other hand, individuals in best response will vaccinate with probability one once the benefit is higher than the cost. As for smoothed best response, this probability lies in $(\frac{1}{2}, 1]$.

Since we propose the use of the Gompertz function for quantifying the probability of individual receiving vaccination, we set $s = 1$ so as to have $G(\triangle P) \in [0, 1]$. However, we could simply assign the value of s less than unity if we were to model the existence of a proportion of population who refuse to take vaccination possibly for religious or psychological reasons. To

be consistent with the Fermi function and logistic function used in literature, we further assume $d = -\ln(d_0)$ so as to have $d = 0.693$ when we set $d_0 = 0.5$ (Figure 5.1(a)). By setting $d_0 = 0.5$, it means that an individual has 50-50 chance to adopt vaccination strategy when the payoff difference $\triangle P = 0$. Indeed, we may take other values of d_0, for instance, $d_0 = 0.2$, then $d = -\ln(0.2) = 1.609$ (i.e. a probability of 20% to vaccinate when $\triangle P = 0$ provided that $s = 1$, see Figure 5.1(b)) to reflect a scenario whereby individuals are more reluctant to vaccinate whenever they perceive that the cost equals the benefit of vaccination. For the individuals responsiveness, r, to the payoff difference, individuals are more sensitive to the payoff difference when r is large. Similar to the logistic function, the Gompertz function approaches the best response correspondence (5.3) as $r \to \infty$ (see Figure 5.1(a)). Substituting (5.2) into (5.4), we have

$$G(\triangle P) = s\, e^{-d\, e^{-r\left((1-\sigma)\beta \frac{I}{N} - c_v\right)}}. \tag{5.5}$$

The ϕG (i.e. $G(\triangle P)$ together with the vaccination effort parameter ϕ) gives the non-constant vaccination rate for the population. At individual level, this vaccination effort may also represent the proportion of susceptible individuals who make their vaccination decision per unit time, as defined in [116]. By assuming that disease prevalence is covered in media reports [66], in a way, system (5.1) provides a simple framework to study the prevalence-based vaccination behavioural change.

For comparison purposes, in the following, the simple logistic function $L(\triangle P)$ used in mean-field model [116], and its counterpart Fermi function $F(\triangle P)$ used in agent-based simulation framework (e.g. [35]) are given.

$$L(\triangle P) = \frac{e^{rP_V}}{e^{rP_V} + e^{rP_{NV}}}, \tag{5.6a}$$

$$F(\triangle P) = \frac{1}{1 + e^{-r(P_j - P_i)}}, \tag{5.6b}$$

where P_i and P_j are the payoffs for focal individual i and his/her role model (say, individual j), respectively, in a pairwise payoff comparison. In both equations (5.6), there are only one parameter value r for tuning. In contrast, there are three tunable parameters, namely s, d and r to be chosen to reflect the vaccination behaviour based on the Gompertz-type smoothed best response function. This allows us to model various types of scenarios, as stated in the aforementioned paragraph. Apart from that, the simple logistic curve (5.6) will approach both its upper and lower horizontal asymptotes symmetrically, whereas the Gompertz function will approach the upper horizontal asymptote much more gradually than the lower horizontal asymptote (Figure 5.1(a)). It can therefore be assumed that individuals require more motivation, in the form of greater payoff gain, to switch to vaccination strategy in the Gompertz smoothed best response. Meanwhile, they will refuse to vaccinate even with the slightest decline of payoff when the net payoff is negative (i.e. $P_{NV} > P_V$). This asymmetric nature of Gompertz function corroborates the ideas of asymmetric smoothed best response in [117], i.e. the risk-averse individuals are more sensitive to the payoff difference when the net payoff is negative.

5.3 Dynamical behaviour of the system

Since $N(t) = S(t) + I(t) + R(t) + V(t)$, the rate of change of the population in system (5.1) is given by $\frac{dN}{dt} = \Lambda - \mu N$. At $t \to \infty$, we have $N \to \frac{\Lambda}{\mu}$. Assuming that $\Lambda = \mu$, the population size is constant.

5.3.1 SIRV model with perfect vaccine

When vaccine is assumed to be perfect, $\sigma = 0$, the reduced form of the system (5.1) is

$$\frac{dS}{dt} = \mu - \beta\frac{I}{N}S - \phi\left[s\,e^{-d\,e^{-r\left(\beta\frac{I}{N}-c_v\right)}}\right]S - \mu S, \tag{5.7a}$$

$$\frac{dI}{dt} = \beta\frac{I}{N}S - \gamma I - \mu I, \tag{5.7b}$$

$$\frac{dR}{dt} = \gamma I - \mu R, \tag{5.7c}$$

$$\frac{dV}{dt} = \phi\left[s\,e^{-d\,e^{-r\left(\beta\frac{I}{N}-c_v\right)}}\right]S - \mu V. \tag{5.7d}$$

The disease free equilibrium (DFE) of system (5.7) is $E_0 = (S_0, I_0, R_0, V_0)$ where $I_0 = R_0 = 0$ and

$$S_0 = \frac{\mu}{\phi\left[s\,e^{-d\,e^{r\,c_v}}\right] + \mu}, \tag{5.8a}$$

$$V_0 = \frac{\phi\left[s\,e^{-d\,e^{r\,c_v}}\right]}{\phi\left[s\,e^{-d\,e^{r\,c_v}}\right] + \mu}. \tag{5.8b}$$

With the presence of voluntary vaccination as a control measure, the control reproduction number is given by

$$\mathcal{R}_{\mathrm{C}} = \mathcal{R}_0 S_0 = \frac{\beta}{\gamma+\mu}\left(\frac{\mu}{\phi\left[s\,e^{-d\,e^{r\,c_v}}\right] + \mu}\right), \tag{5.9}$$

where $\mathcal{R}_0 = \frac{\beta}{\gamma+\mu}$ is the basic reproduction number, which is a measure of disease outbreak severity in the absence of vaccination.

Theorem 5.1. *The disease free equilibrium of system (5.7) is locally asymptotically stable if* $\mathcal{R}_C < 1$ *and unstable if* $\mathcal{R}_C > 1$.

Proof. The Jacobian matrix of system (5.7) at DFE E_0 is

$$J(E_0) = \begin{bmatrix} -\phi\,g_0 - \mu & -\left(1 + rd\,e^{r\,c_v}\,\phi\,g_0\right)\beta\,S_0 & 0 & 0 \\ 0 & \beta\,S_0 - \gamma - \mu & 0 & 0 \\ 0 & \gamma & -\mu & 0 \\ \phi\,g_0 & rd\,e^{r\,c_v}\,\phi\,g_0\,\beta\,S_0 & 0 & -\mu \end{bmatrix}, \tag{5.10}$$

where $g_0 = s\,e^{-d\,e^{r\,c_v}} > 0$. The eigenvalues of the matrix $J(E_0)$ are given by $\lambda_1 = \lambda_2 = -\mu$, $\lambda_3 = -\phi\,g_0 - \mu$ and $\lambda_4 = \beta S_0 - \gamma - \mu$. If $\mathcal{R}_{\mathrm{C}} < 1$, then $\lambda_4 < 0$, and all the eigenvalues of $J(E_0)$ are negative and E_0 is locally asymptotically stable. □

The endemic equilibrium $E^* = (S^*, I^*, R^*, V^*)$ is obtained by first setting the right-hand side of last three equations in (5.7) to zero. Since $I^* \neq 0$, we get $S^* = \frac{(\gamma+\mu)N^*}{\beta}$, $R^* = \frac{\gamma}{\mu} I^*$ and

$$V^* = \frac{\phi \left[s\, e^{-d\, e^{-r\left(\beta \frac{I^*}{N^*} - c_v\right)}} \right] S^*}{\mu}.$$

Use $S^* + I^* + R^* + V^* = N^*$, and without loss of generality, let $N^* = 1$, then the nonzero equilibrium is governed by $h_1(I^*) = h_2(I^*)$ where

$$h_1(I^*) = \frac{\gamma + \mu}{\beta\mu} \phi \left[s\, e^{-d\, e^{-r(\beta I^* - c_v)}} \right], \tag{5.11a}$$

$$h_2(I^*) = 1 - \frac{\gamma + \mu}{\beta} - \frac{\gamma + \mu}{\mu} I^*. \tag{5.11b}$$

Setting $h_1(I^*) = h_2(I^*)$ leads to a transcendental-algebraic equation which cannot be solved analytically for I^*. Following the work in [56, 85], we show the existence of the endemic equilibrium through analytical study. Finding the derivatives of $h_1(I^*)$ and $h_2(I^*)$ with respect to I^*, respectively, we have

$$h_1'(I^*) = \frac{\gamma + \mu}{\mu} \phi \left[r\, d\, e^{-r(\beta I^* - c_v)} s\, e^{-d\, e^{-r(\beta I^* - c_v)}} \right] > 0, \tag{5.12a}$$

$$h_2'(I^*) = -\frac{\gamma + \mu}{\mu} < 0. \tag{5.12b}$$

Since all the parameter values are non-negative, then from (5.12), $h_1(I^*)$ is a monotonic increasing function and $h_2(I^*)$ is a linear decreasing function. When $I^* = 0$, we have $h_1(0) = \frac{\gamma+\mu}{\beta\mu} \phi \left[s\, e^{-d\, e^{r\, c_v}} \right] > 0$ provided that $\phi \neq 0$. Also, $h_2(0) = \frac{\beta - (\gamma+\mu)}{\beta} > 0$ provided that $\mathcal{R}_0 > 1$. It is easy to know that $h_1(0) < h_2(0)$ if and only if $\mathcal{R}_C > 1$. Also, as the second order derivative of $h_1(I^*)$ is given by

$$h_1''(I^*) = \frac{\phi\, r \beta g_2 \left(d\, e^{-r(\beta I^* - c_v)} - 1 \right)}{\mathcal{R}_0 \mu},$$

where $g_1 = s\, e^{-d\, e^{-r(\beta\, I^* - c_v)}} > 0$ and $g_2 = g_1 r d\, \beta\, e^{-r(\beta\, I^* - c_v)} > 0$. $h_1(I^*)$ is ei-

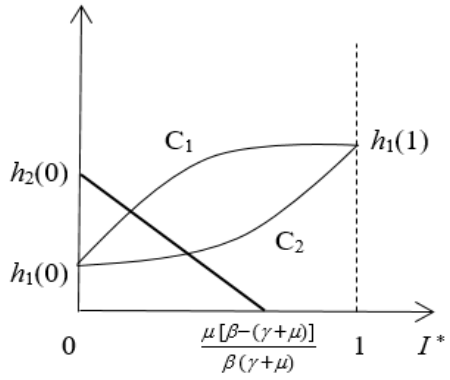

Figure 5.2: Illustrations of $h_1(I^*)$ (thin curves) and $h_2(I^*)$ (thick line) for showing the existence and uniqueness of I^*.

ther concave up (whenever $d > e^{r(\beta I^* - c_v)}$, see lower curve C_2) or concave down (whenever $d < e^{r(\beta I^* - c_v)}$, see upper curve C_1) (as sketched in Figure 5.2). In either way, we have one and only one point of intersection between the curve $h_1(I^*)$ and the line $h_2(I^*)$ for $0 < I^* < 1$. That is, I^* is unique if $\mathcal{R}_C > 1$ (and so as the endemic equilibrium E^* exists and is unique). And, there exists no point of intersection if $\mathcal{R}_C < 1$ which implies that $h_1(0) > h_2(0)$. Also, $h_2(I^*) = 0$ at $I^* = \frac{\mu[\beta-(\gamma+\mu)]}{\beta(\gamma+\mu)}$ implies that $0 < I^* < 1$ when $\mathcal{R}_0 > 1$.

Therefore, we conclude that system (5.7) has an unique endemic equilibrium E^*. We show that this endemic equilibrium is stable if $\mathcal{R}_C > 1$, in the following theorem.

Theorem 5.2: *The endemic equilibrium of system (5.7) is locally asymptotically stable if* $\mathcal{R}_C > 1$ *and unstable if* $\mathcal{R}_C < 1$.

Proof. The Jacobian matrix of system (5.7) at endemic equilibrium E^* is given by

$$J(E^*) = \begin{bmatrix} -\beta\, I^* - \phi\, g_1 - \mu & -\beta\, S^* - \phi\, g_2\, S^* & 0 & 0 \\ \beta\, I^* & \beta\, S^* - \gamma - \mu & 0 & 0 \\ 0 & \gamma & -\mu & 0 \\ \phi\, g_1 & \phi\, g_2\, S^* & 0 & -\mu \end{bmatrix}, \tag{5.13}$$

At $S^* = \frac{\gamma+\mu}{\beta}$,

$$\det(J(E^*)) = I^*(\gamma+\mu)\,(\phi\, g_2+\beta) > 0,$$
$$\mathrm{tr}(J(E^*)) = -\beta I^* - \phi\, g_1 - \mu < 0.$$

Hence, E^* is locally asymptotically stable. □

5.3.2 SIRV model with imperfect vaccine

When $0 < \sigma < 1$, the vaccine only provides partial immunity to vaccinated individuals and we shall analyse system (5.1). The DFE of system (5.1) is the same as E_0 but the effective reproduction number is given by

$$\mathcal{R}_{\text{eff}} = \mathcal{R}_0(S_0+\sigma V_0) = \frac{\beta}{\gamma+\mu}\left(\frac{\sigma\phi\left[s\, e^{-d\, e^{r\, c_v}}\right]+\mu}{\phi\left[s\, e^{-d\, e^{r\, c_v}}\right]+\mu}\right), \tag{5.14}$$

where (5.14) reduces to (5.9) whenever $\sigma = 0$.

Similar to Theorem 5.1, it is easy to show system (5.1) has stable DFE if $\mathcal{R}_{\text{eff}} < 1$.

Theorem 5.3. *The disease free equilibrium of system (5.1) is locally asymptotically stable if $\mathcal{R}_{\text{eff}} < 1$ and unstable if $\mathcal{R}_{\text{eff}} > 1$.*

Proof. The Jacobian matrix of system (5.1) at DFE E_0 is given by

$$\begin{bmatrix} -\phi\, g_0-\mu & -\{1+rd\, e^{r\, c_v}\,(1-\sigma)\,\phi\, g_0\}\,\beta\, S_0 & 0 & 0 \\ 0 & \beta(S_0+\sigma V_0)-\gamma-\mu & 0 & 0 \\ 0 & \gamma & -\mu & 0 \\ \phi\, g_0 & -\sigma\beta\, V_0 + rd\, e^{r\, c_v}\,(1-\sigma)\,\phi\, g_0\,\beta\, S_0 & 0 & -\mu \end{bmatrix}, \tag{5.15}$$

where $g_0 = s\, e^{-d\, e^{r\, c_v}} > 0$. The eigenvalues of the matrix (5.15) are given by $\eta_1 = \eta_2 = -\mu$, $\eta_3 = -\phi\, g_0 - \mu$ and $\eta_4 = \beta(S_0+\sigma V_0) - \gamma - \mu$. If $\mathcal{R}_{\text{eff}} < 1$, then $\lambda_4 < 0$ and all the eigenvalues of Jacobian matrix (5.15) are negative. Hence, E_0 is locally asymptotically stable. □

In epidemic models with perfect vaccine and constant vaccination rate, forward bifurcation takes place at reproduction number equal to unity. However, imperfect vaccine has been identified as one of the causes of backward

bifurcation [44], that is the existence of multiple endemic equilibria when $\mathcal{R}_{\text{eff}}$ is less than and close to unity. The infectious disease is much more difficult to be eliminated by vaccination if the phenomenon of backward bifurcation occurs [52]. Hence, we use the center manifold theorem in [14] to determine the type of transcritical bifurcation at $\mathcal{R}_{\text{eff}} = 1$.

For this purpose, we introduce the notations $x_1 \equiv S$, $x_2 \equiv I$, $x_3 \equiv R$, $x_4 \equiv V$ and $N = \sum_{j=1}^{4} x_j$. Thus, system (5.1) can be written as $\frac{d\mathbf{x}}{dt} = \mathbf{f}$ and $\mathbf{f} = [f_1, f_2, f_3, f_4]^T$ with

$$f_1 = \Lambda - \lambda x_1 - \phi \left[s\, e^{-d\, e^{-r[(1-\sigma)\lambda - c_v]}} \right] x_1 - \mu x_1, \tag{5.16a}$$

$$f_2 = \lambda(x_1 + \sigma x_4) - \gamma x_2 - \mu x_2, \tag{5.16b}$$

$$f_3 = \gamma x_2 - \mu x_3, \tag{5.16c}$$

$$f_4 = \phi \left[s\, e^{-d\, e^{-r[(1-\sigma)\lambda - c_v]}} \right] x_1 - \sigma\lambda x_4 - \mu x_4, \tag{5.16d}$$

where $\lambda = \beta \frac{\mu x_2}{\Lambda}$ at an equilibrium point.

The DFE corresponds to $\mathbf{x}_0 = (x_{10}, x_{20}, x_{30}, x_{40}) = (S_0, 0, 0, V_0)$. Taking β as bifurcation parameter, at $\mathcal{R}_{\text{eff}} = 1$, the critical value of β is $\beta^* = \frac{\gamma+\mu}{S_0 + \sigma V_0}$. The linearization matrix of (5.16) at $\mathbf{x}_0$ has the same eigenvalues as those given in Theorem 5.3. It is clear that the eigenvalue η_4 in Theorem 5.3 becomes zero when $\beta = \beta^*$. The left eigenvector associated with the zero eigenvalue is $\mathbf{v} = [v_1, v_2, v_3, v_4] = [0, 1, 0, 0]$ and the right eigenvector is $\mathbf{w} = [w_1, w_2, w_3, w_4]^T$ where

$$\begin{aligned}
w_1 &= -\frac{\mu(\gamma+\mu)\left[1 + (1-\sigma) r d \phi\, e^{r\, c_v} g_0\right]}{q}, \\
w_2 &= 1, \\
w_3 &= \frac{\gamma}{\mu}, \\
w_4 &= -\frac{(\gamma+\mu)\phi g_0 \left[\sigma\phi g_0 + \mu(\sigma+1) - \mu^2(1-\sigma) r d e^{r c_v}\right]}{\mu\, q},
\end{aligned} \tag{5.17}$$

in which $q = (\sigma\phi\, g_0 + \mu)(\phi\, g_0 + \mu)$ and $\mathbf{v} \cdot \mathbf{w} = 1$.

Since only the second component of $\mathbf{v}$ is non-zero, we calculate the second derivatives for f_2 evaluated at $\mathbf{x}_0$ as follows:

$$\frac{\partial^2 f_2}{\partial x_1 \partial x_2} = \beta^* \tfrac{\mu}{\Lambda}, \qquad \frac{\partial^2 f_2}{\partial x_2 \partial x_4} = \sigma\beta^* \tfrac{\mu}{\Lambda},$$
$$\frac{\partial^2 f_2}{\partial x_2 \partial \beta} = (S_0 + \sigma V_0)\tfrac{\mu}{\Lambda},$$

and all other derivatives are zero. We then determine the direction of transcritical bifurcation at $\mathcal{R}_{\text{eff}} = 1$ by computing the following values.

$$\begin{aligned} a &= v_2 \sum_{j,k=1}^{4} w_j w_k \frac{\partial^2 f_2}{\partial x_j \partial x_k}(\mathbf{x}_0, \beta^*) \\ &= 2\beta^* \tfrac{\mu}{\Lambda}(w_1 + \sigma\, w_4), \qquad (5.18a) \\ b &= v_2 \sum_{j=1}^{4} w_j \frac{\partial^2 f_2}{\partial x_j \partial \beta}(\mathbf{x}_0, \beta^*) \\ &= (S_0 + \sigma V_0)\tfrac{\mu}{\Lambda} > 0. \qquad (5.18b) \end{aligned}$$

Substituting expressions in (5.17) into (5.18a), after some algebraic manipulations, we have

$$a = -\frac{2\beta^*}{\Lambda q}(\gamma + \mu)\left[\mu^2(1-\sigma)^2 r d\, e^{r\, c_v}\phi\, g_0 + q_1\right] < 0, \qquad (5.19)$$

where $q_1 = \sigma^2\phi\, g_0(\phi\, g_0 + \mu) + \mu(\sigma\phi\, g_0 + \mu)$. Since $a < 0$ and together with $b > 0$, we conclude that forward bifurcation occurs at $\mathcal{R}_{\text{eff}} = 1$. We rule out the possibility of backward bifurcation in system (5.1) with partial vaccine-induced immunity in the scenario whereby individuals use a simple cost-benefit analysis in voluntary decision-making.

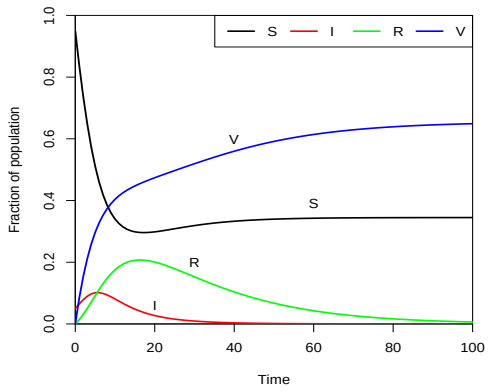

(a) Logistic: $\beta = 0.625$, $\gamma = 0.25$, $c_v = 0.2$

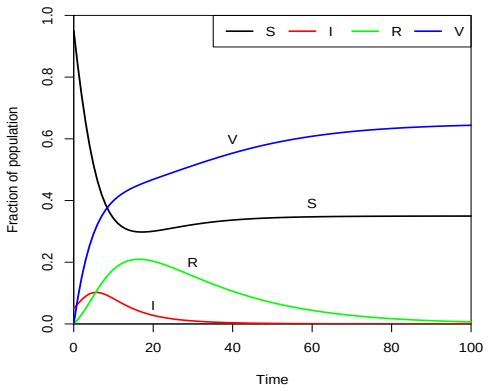

(b) Gompertz: Same as (a)

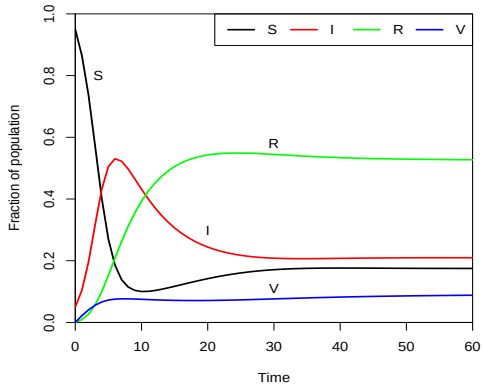

(c) Logistic: $\beta = 1$, $\gamma = 0.125$, $c_v = 4$

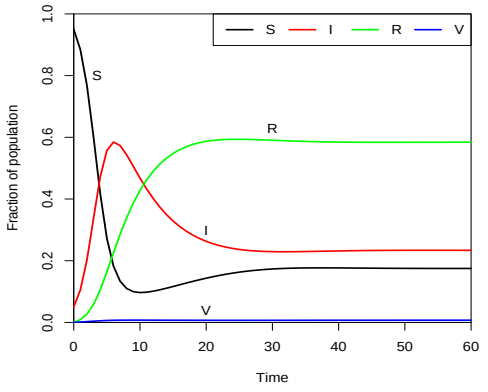

(d) Gompertz: Same as (c)

Figure 5.3: Time evolution of SIRV dynamics with perfect vaccine model whereby the vaccination rate is governed by logistic and Gompertz smoothed best response functions.

5.4 Results and discussion

5.4.1 SIRV dynamics with perfect vaccine

Unless other specified, the set of parameter values $(\beta, \gamma, \Lambda, \mu, c_v, \phi, s, d, r) = (0.625, 0.25, 0.05, 0.05, 0.2, 0.2, 1, -\ln(0.5), 1)$ is used for all simulations in this chapter, together with initial conditions $S(0) = 0.95$, $I(0) = 0.05$. We first simulate the SIRV dynamics with perfect vaccine ($\sigma = 0$) with two types of smoothed best response functions, namely logistic and Gompertz functions, by using $r = 0.5$ in Figure 5.3. As for the logistic smoothed best response dynamics, we simply replace $G(\triangle P)$ in system (5.7) with $L(\triangle P)$ in

(5.6a) and its corresponding control reproduction number is calculated using $\mathcal{R}_C = \mathcal{R}_0 \frac{\mu}{\phi(1+e^{r\,c_v})^{-1}+\mu}$. We find that both logistic and Gompertz functions give very similar epidemic dynamics and vaccination coverage throughout the simulation time (Figure 5.3(a) and 5.3(b)) when the risk of disease spreading is intermediate ($\mathcal{R}_0 = 2.0833$) and the low cost of vaccination ($c_v = 0.2$) is considered. The epidemics die out as the control reproduction numbers ($\mathcal{R}_C = 0.7184$ for logistic and $\mathcal{R}_C = 0.7286$ for Gompertz) are less than unity.

However, when the basic reproduction number ($\mathcal{R}_0 = 5.7143$) and the cost of vaccination ($c_v = 4$) are both relatively high, it is found that the vaccination uptake level resulting from both functions are significantly different (Figure 5.3(c) and 5.3(d)). The logistic smoothed best response still yields significant vaccine uptake levels whereas the Gompertz function does not. It seems possible that this discrepancy is due to the asymmetry property of Gompertz function. When the cost of vaccination is higher than the benefit of getting vaccination (i.e. the net payoff is negative, $\triangle P < 0$), the probability of taking vaccination drops more steeply in the Gompertz function model compared to that using the logistic function. This distinction between the Gompertz and logistic function models is more pronounced when individuals are not very responsive to payoff difference, for instance when $r = 0.5$, as can be seen in Figure 5.1(a). This result is in agreement with the finding in [117]. We thus claim that whenever individuals are more sensitive to negative net payoff in asymmetric vaccination strategy, individuals are said to be risk-averse. The disease may be more difficult to be controlled by voluntary vaccination with asymmetric smoothed best response when the cost of vaccination is very high.

We next examine the impact of parameters s, d, r in the Gompertz function (5.4) and the vaccination effort parameter ϕ on the disease equilibrium point of the SIRV model with perfect vaccine (5.7) in Figure 5.4. The simulations end at $t = 100$ unit time with $\triangle t = 1$. As we assume that s is less than unity to reflect the scenarios whereby a certain proportion (i.e. $(1-s)100\%$) of

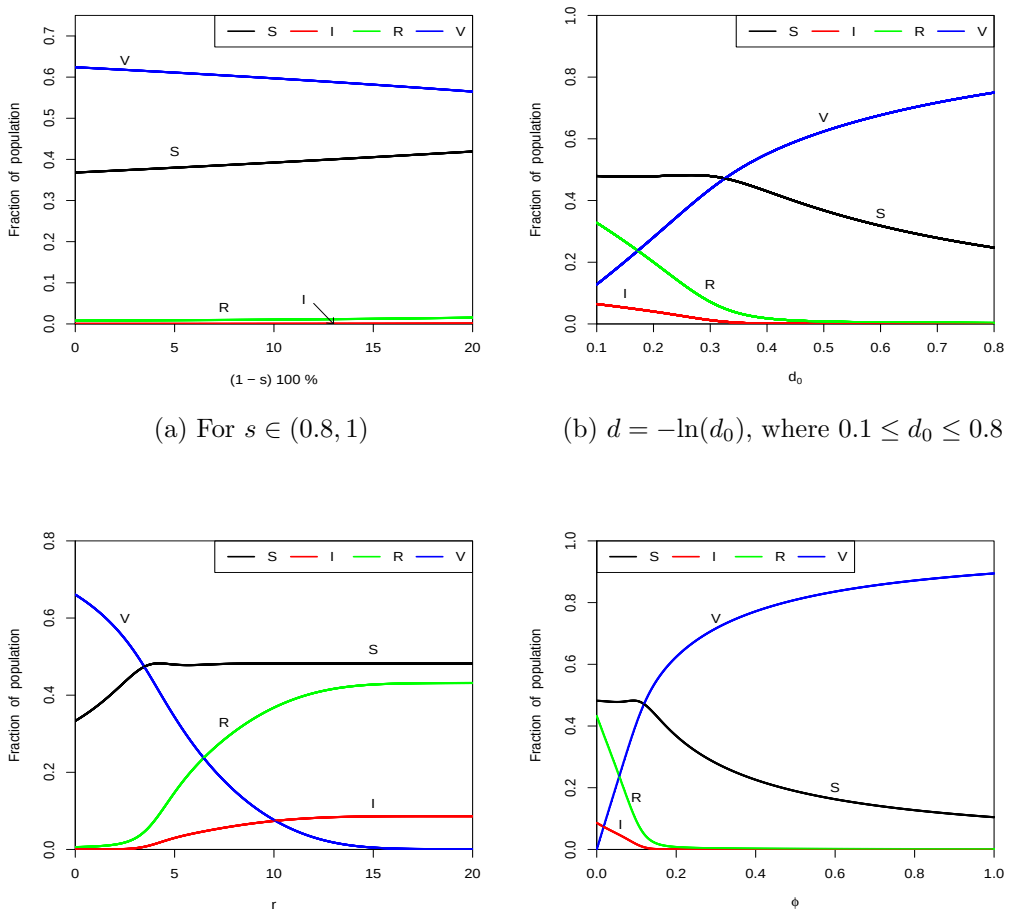

(a) For $s \in (0.8, 1)$

(b) $d = -\ln(d_0)$, where $0.1 \leq d_0 \leq 0.8$

(c) $0 < r \leq 20$

(d) $0 \leq \phi \leq 1$

Figure 5.4: The impact of parameter s, d, r and ϕ on the equilibrium of SIRV perfect vaccine model with Gompertz smoothed best response function.

the individuals in population are vaccine refusers, we find that an increase of proportion of vaccine refusers does not substantially influence the vaccine uptake level (Figure 5.4(a)), as compared to other parameters being investigated in Figure 5.4. A possible explanation for this might be that our modelling framework assumes not all susceptibles taking the effort to rely on the cost-benefit analysis in deciding whether or not to vaccinate at each time step, as the vaccination effort parameter used here is relatively small ($\phi = 0.2$).

The impacts of parameters d and ϕ on disease equilibrium structure and vaccine uptake level, albeit not exactly in the same way, do have some sim-

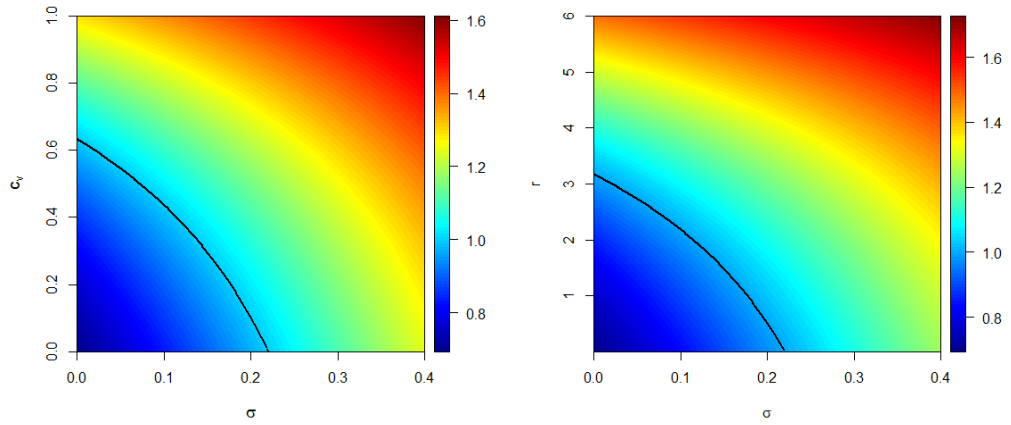

(a) $0 \leq c_v \leq 1$ and $0 \leq \sigma \leq 0.4$

(b) $0.001 \leq r \leq 6$ and $0 \leq \sigma \leq 0.4$

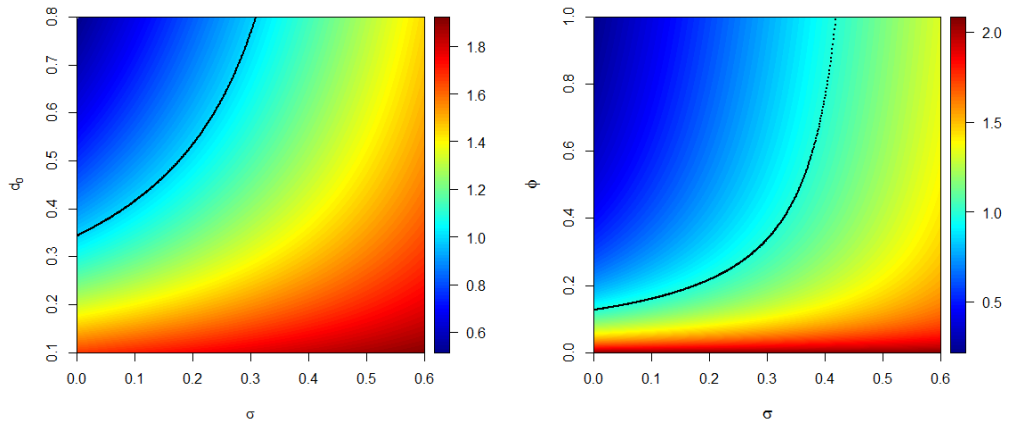

(c) $0.1 \leq d_0 \leq 0.8$, where $d = -\ln(d_0)$ and $0 \leq \sigma \leq 0.6$

(d) $0 \leq \phi \leq 1$ and $0 \leq \sigma \leq 0.6$

Figure 5.5: The parameter-space $\{c_v, r, d, \phi\} - \sigma$ diagrams for the effective reproduction number $\mathcal{R}_{\text{eff}}$ of the SIRV imperfect vaccine model with the Gompertz smoothed best response function.

ilarities. As we have $d = -\ln(d_0)$, it is indeed d_0, not d, that represents the probability of individuals choosing vaccination strategy when the payoff difference $\triangle P = 0$, and we also observe that the disease with $\mathcal{R}_0 = 2.0833$ is under controlled only when d_0 is not too small (Figure 5.4(b)). Similar observation is obtained in Figure 5.4(d) in which disease is being eradicated only when the vaccination effort parameter ϕ is greater than 0.15. Indeed, no one takes vaccination if $\phi = 0$. The results in Figure 5.4(d) are consistent

with the one obtained by using the logistic smoothed best response function in [116]. With the combination parameter values used in Figure 5.4, it can thus be suggested that a small increment in ϕ, when its value is still low, may lead to a sharply increase in vaccine uptake level. On the other hand, the increases produced by increments in d_0, despite significant, however, are not as encouraging as those produced by ϕ. Similar to the finding in [116] for logistic smoothed best response function, the increases of individuals' responsiveness to payoff difference, r, would cause the vaccine uptake level to decrease when the Gompertz function is used (Figure 5.4(c)).

5.4.2 SIRV dynamics with imperfect vaccine

For the SIRV model with imperfect vaccine, equation (5.2) implies that the higher the probability of vaccine failure σ, the lower payoff benefit in choosing vaccination strategy. We expect the vaccine uptake level would be lower and the disease spreading would be more severe than the case of perfect vaccine. Hence, we study how the probability of vaccine failure σ influences the dynamical behaviour of the system numerically by presenting the changes of the effective reproduction number $\mathcal{R}_{\text{eff}}$ for various parameter-space in Figure 5.5. The solid curves in all panels denote the points where both parameter values give $\mathcal{R}_{\text{eff}} = 1$. For the combination parameter values used, we find that an increase of the cost of vaccination, c_v, or the individual responsiveness to payoff difference, r, would cause the epidemic outbreak even worse with reduced vaccine efficacy (Figure 5.5(a) and 5.5(b)). However, it is interesting to find that increasing the probability of choosing vaccination strategy when $\triangle P = 0$ or increasing the vaccination effort parameter ϕ may offset the negative effect of increasing σ in our SIRV model with Gompertz smoothed best response in the vaccination decision making.

5.5 Concluding remarks

We propose the Gompertz-type asymmetric smoothed best response function in modelling the voluntary vaccination strategy of each individual based on a cost-benefit analysis in an epidemic model with perfect and partial vaccine-induced immunity. For the case of perfect vaccine, we prove that the disease free equilibrium is locally asymptotically stable when the control reproduction number is less than unity. We show that the endemic equilibrium exists and is unique if the control reproduction number is greater than unity through qualitative analysis. The endemic equilibrium, if it exists, is locally asymptotically stable. For the case of imperfect vaccine, the forward bifurcation occurs when the effective reproduction number is unity.

We conclude this chapter with the following remarks.

(i) The Gompertz smoothed best response gives the similar epidemic dynamics and vaccine uptake level as the logistic function when the risk of disease spreading is intermediate and the cost of vaccination is low, but it diverges from logistic function when the cost of vaccination is relatively high. The asymmetry property of the Gompert function is a major factor that gives rise to this discrepancy. This suggests that the Gompertz function may be suitable in modelling the nature of risk-averse individuals who are usually more careful in accepting vaccination but refuse to vaccinate when the cost is only marginally higher than its benefit.

(ii) An increase of vaccination effort and the probability of taking vaccination when the cost and benefit are perceived to be the same would be beneficial to disease control through voluntary vaccination, whereas the greater responsiveness of individuals to the payoff difference would reduce the vaccine uptake level.

(iii) When vaccine efficacy decreases, increasing the probability of choosing vaccination strategy when the cost equals the benefit and/or increasing the vaccination effort offset the reduction in the degree of protection provided by vaccines.

Chapter 6

Conclusions and Future Work

6.1 Summary of the research

This thesis focuses on modelling the self-initiated health protective behavioural change and the vaccination behaviour in the course of epidemic outbreaks. Within the game theoretical modelling framework, we model the former behavioural change by using two-subpopulation replicator dynamical equations whereas the latter through the following two ways. First, an utility function in terms of both individual- and population-scale vaccination rate are used to express the preference of individuals opting for vaccination, in the vaccination population game framework. Second, the asymmetric smoothed best response dynamics is described in Gompertz function for individuals' vaccination decision-making in an epidemic model with the prevalence-dependent vaccination rate.

All the approaches share a few common features. First, individuals are modelled as making use of the cost-benefit considerations in their behavioural changes. That is, upon receiving the disease prevalence information, they weigh the perceived benefits and costs of adopting certain strategy. This is indeed the most essence part of disease-behaviour models with game theory components where the strategy adoption is payoff-driven. Second, all the models assume that the disease information is available to the individuals in the population which is unavoidably unrealistic but to keep the models as

simple as possible. On the other hand, the ratio of the cost of behavioural change (i.e. adopting vaccination strategy) to the cost of disease is used in the framework of vaccination population game in Chapter Four. This implies that the perceived cost of the behavioural change would never be greater than the perceived cost of disease itself. Meanwhile, this normalization does not appear in the frameworks used in Chapter Three and Five, which means that the perceived cost of behavioural changes could be higher than its perceived benefit.

For modelling the self-initiated health protective behavioural changes in Chapter Three, we find that without imitations, the natural selection drives only a small number of susceptibles to switch their strategy. With imitation process, the strategies distribution will depend on the initial proportion of susceptible with normal and altered strategies in both subpopulations, the magnitude of the social group pressure and the amount of extra profit given to susceptible adopting the preferred behaviour in respective subpopulation. This in a way reflects the influence of the existing preference, the conformity of the coordinated behaviour and the rewards (or punishments) in shaping the imitation dynamics and hence the epidemic dynamics. It is interesting to find that the social group pressure could be a "double-edged sword" in promoting the adoption of the pre-cautionary health protective behaviour. Although the mean-field model is used, the heterogeneity of groups is being investigated in terms of different relative strengths and different preferences of subpopulations. It is found that all these factors give rise to rich dynamics of imitations and epidemics.

In Chapter Four, we look into the impact of three additional characteristics of imperfect vaccine in a two-class vaccine-induced immunity model on the vaccination behaviour with the vaccination population game framework. Intuitively, rational individuals would opt for vaccination if vaccines are able to provide longer duration of high immunity to vaccinated people.

When vaccine is not effective in reducing the susceptibility of the vaccinated individuals, the greater reduction of infectivity to vaccinated infected individuals would be beneficial in circumventing the persistence of disease even instant vaccination is achieved. However, it is somewhat surprising that the scale of this reduction of transmissibility does not affect the cost threshold for no vaccination. In addition, without faster recovery in breakthrough infection, the self-interested individuals are highly likely to refuse vaccination when the vaccine efficacy is low. As the imperfect vaccine gives rise to the phenomenon of backward bifurcation, the vaccination population game with three additional characteristics of imperfect vaccine also results in multiple Nash equilibria vaccination rates which complicates the disease control efforts.

The Gompertz-type of the asymmetrically smoothed best response function is proposed in modelling the individuals' voluntary vaccination strategy based on a simple cost-benefit consideration in epidemic model with perfect and partial vaccine-induced immunity in Chapter Five. We find that an increase of vaccination effort and the probability of taking vaccination when the cost and benefit are perceived to be the same would be beneficial to disease control through voluntary vaccination, whereas the greater responsiveness of individuals to the payoff difference would reduce the vaccination rate. Another important finding is that the asymmetric property of the smoothed best response produces a different vaccine uptake level from the symmetric one in an otherwise similar pattern when the cost of vaccination is perceived to be very high. This reflects that the risk-averse individuals have a more downward inclination to vaccination than the rational people in general. Contrary to expectations, the study in this chapter did not find any significant difference between the vaccination strategy adoptions for vaccine that offers full and partial protection to vaccinated individuals. However, a note of caution is due here since it is simply that the probability of vaccine failure is being modelled as a factor in reducing the perceived benefit of getting vaccination.

6.2 Future works

The average reduction of force of infection for behavioural changes involving the self-initiated pre-cautionary health protective actions in Chapter Three takes a pre-defined reduction factor multiplied with the prevalence-based strategy frequencies of susceptibles in the population. This leads to a smoothed game dynamics which implies that people start to have strategy interactions (and hence possibly alter their behaviours) as long as there are some disease incidences in the population. This smoothed and continuous modelling framework, despite giving promising results on the coupled imitation and epidemic dynamics, does not reflect the more realistic scenarios. For instance, the pre-cautionary measures which are usually triggered once the number of infected individuals exceeds a threshold level [115] and/or the information on the disease outbreak would only be covered in media when the number of infected cases reaches some critical number [107]. In reality, not only control measures imposed by public health authorities or pscyhological effects induced by media coverage on disease outbreaks would result in non-smoothed (i.e. piecewise continuous) transmission rate [106], game-theoretical approaches of individuals' self-initiated pre-cautionary health protective behaviours might also be developed in a modelling framework of non-smoothed dynamical systems in further investigations, so as to reflect the nature of people who only consider strategy switching once the disease prevalence reaches a certain threshold.

Despite the promising results obtained in investigating the impact of imperfect vaccine in the framework of vaccination population game in Chapter Four, there are still many unanswered questions about the optimal vaccination policy even when the vaccine is assumed to be perfect. The recent works in this respect including the formulation of a policy problem as an optimal control problem [53]. On the other domain, the relationships between the individual investments in pre-cautionary health protective actions and the public

health policies are investigated in [55]. These indicate that further studies, which take into account of the policy aspects, will need to be undertaken in modelling human behaviour in disease spreading so as to provide more meaningful insights and guides, especially to public health policy makers, in the effort of combating the infectious diseases.

As the disease prevalence-based of continuous vaccination with the asymmetrically smoothed best response function is developed in Chapter Five with the aims to provide a corresponding mean-field version of model to the agent-based simulation framework with Fermi strategy updating rule, in which the simulation framework models a repeated vaccination decision-making before each of the epidemic season. While the framework in Chapter Five does not take into account of seasonality, further studies, which take into account of seasonal force [28], will need to be undertaken in order to better explain the nature of risk-averse individuals in vaccination decision-making for influenza.

Bibliography

[1] C. Bauch, A. d'Onofrio, and P. Manfredi. Behavioral epidemiology of infectious diseases: an overview. In *Modeling the Interplay Between Human Behavior and the Spread of Infectious Diseases*, pages 1–19. Springer, 2013.

[2] C. T. Bauch. Imitation dynamics predict vaccinating behaviour. *Proceedings of the Royal Society of London B: Biological Sciences*, 272(1573):1669–1675, 2005.

[3] C. T. Bauch and D. J. Earn. Vaccination and the theory of games. *Proceedings of the National Academy of Sciences of the United States of America*, 101(36):13391–13394, 2004.

[4] C. T. Bauch and A. P. Galvani. Social factors in epidemiology. *Science*, 342(6154):47–49, 2013.

[5] C. T. Bauch, A. P. Galvani, and D. J. Earn. Group interest versus self-interest in smallpox vaccination policy. *Proceedings of the National Academy of Sciences*, 100(18):10564–10567, 2003.

[6] S. Bhattacharyya and C. Bauch. A game dynamic model for delayer strategies in vaccinating behaviour for pediatric infectious diseases. *Journal of Theoretical Biology*, 267(3):276–282, 2010.

[7] F. Brauer. Backward bifurcations in simple vaccination/treatment models. *Journal of Biological Dynamics*, 5(5):410–418, 2011.

[8] R. Breban. Health newscasts for increasing influenza vaccination coverage: an inductive reasoning game approach. *PLoS ONE*, 6(12):e28300, 2011.

[9] B. Buonomo, A. d'Onofrio, and D. Lacitignola. Global stability of an SIR epidemic model with information dependent vaccination. *Mathematical Biosciences*, 216(1):9–16, 2008.

[10] B. Buonomo and D. Lacitignola. Forces of infection allowing for backward bifurcation in an epidemic model with vaccination and treatment. *Acta Applicandae Mathematicae*, 122(1):283–293, 2012.

[11] C.-R. Cai, Z.-X. Wu, and J.-Y. Guan. Effect of vaccination strategies on the dynamic behavior of epidemic spreading and vaccine coverage. *Chaos, Solitons and Fractals*, 62:36–43, 2014.

[12] E. Campbell and M. Salathé. Complex social contagion makes networks more vulnerable to disease outbreaks. *Scientific Reports*, 3, 2013.

[13] A. Cardillo, C. Reyes-Suárez, F. Naranjo, and J. Gómez-Gardeñes. Evolutionary vaccination dilemma in complex networks. *Physical Review E*, 88(3):032803, 2013.

[14] C. Castillo-Chavez and B. Song. Dynamical models of tuberculosis and their applications. *Mathematical Biosciences and Engineering*, 1(2):361–404, 2004.

[15] (CDC)a. Vaccine information statement: Chickenpox vaccine - what you need to know. http://www.cdc.gov/vaccines/hcp/vis/vis-statements/varicella.html, 2013. Accessed: 2016-08-28.

[16] (CDC)b. Pregnancy and whooping cough: Effectiveness of whooping cough vaccines. http://www.cdc.gov/pertussis/pregnant/mom/vacc-effectiveness.html, 2016. Accessed: 2016-08-28.

[17] A. Cherif, K. Barley, and M. Hurtado. Homo-psychologicus: Reactionary behavioural aspects of epidemics. *Epidemics*, 14:45–53, 2016.

[18] D. M. Cornforth, T. C. Reluga, E. Shim, C. T. Bauch, A. P. Galvani, and L. A. Meyers. Erratic flu vaccination emerges from short-sighted behavior in contact networks. *PLoS Comput. Biol.*, 7(1):e1001062, 2011.

[19] R. Cressman. Evolutionary game theory with two groups of individuals. *Games and Economic Behavior*, 11(2):237–253, 1995.

[20] R. Cressman. Frequency-dependent stability for two-species interactions. *Theoretical Population Biology*, 49(2):189–210, 1996.

[21] J. Cui, Y. Sun, and H. Zhu. The impact of media on the control of infectious diseases. *Journal of Dynamics and Differential Equations*, 20(1):31–53, 2008.

[22] S. Del Valle, H. Hethcote, J. M. Hyman, and C. Castillo-Chavez. Effects of behavioral changes in a smallpox attack model. *Mathematical Biosciences*, 195(2):228–251, 2005.

[23] O. Diekmann, J. A. P. Heesterbeek, and J. A. Metz. On the definition and the computation of the basic reproduction ratio R0 in models for infectious diseases in heterogeneous populations. *Journal of Mathematical Biology*, 28(4):365–382, 1990.

[24] F. Ding, Y. Liu, B. Shen, and X.-M. Si. An evolutionary game theory model of binary opinion formation. *Physica A: Statistical Mechanics and its Applications*, 389(8):1745–1752, 2010.

[25] A. d'Onofrio, P. Manfredi, and P. Poletti. The interplay of public intervention and private choices in determining the outcome of vaccination programmes. *PLoS ONE*, 7(10):e45653, 2012.

[26] A. d'Onofrio, P. Manfredi, and E. Salinelli. Vaccinating behaviour, information, and the dynamics of SIR vaccine preventable diseases. *Theoretical Population Biology*, 71(3):301–317, 2007.

[27] A. d'Onofrio, P. Manfredi, and E. Salinelli. Fatal SIR diseases and rational exemption to vaccination. *Mathematical Medicine and Biology*, 25(4):337–357, 2008.

[28] P. Doutor, P. Rodrigues, M. do Céu Soares, and F. A. Chalub. Optimal vaccination strategies and rational behaviour in seasonal epidemics. *Journal of Mathematical Biology*, pages 1–29, 2016.

[29] (ECDC). ECDC daily update: 2009 influenza A (H1N1) pandemic - 18 Jan 2010. http://ecdc.europa.eu/en/healthtopics/Documents/100118-Influenza-AH1N1-Situation-Report-0900hrs.pdf, 2010. Accessed: 2016-11-12.

[30] E. Elbasha, C. Podder, and A. Gumel. Analyzing the dynamics of an SIRS vaccination model with waning natural and vaccine-induced immunity. *Nonlinear Analysis: Real World Applications*, 12(5):2692–2705, 2011.

[31] C. Farrington. On vaccine efficacy and reproduction numbers. *Mathematical Biosciences*, 185(1):89–109, 2003.

[32] N. Ferguson. Capturing human behaviour. *Nature*, 446(7137):733–733, 2007.

[33] A. Fierro and A. Liccardo. Lattice model for influenza spreading with spontaneous behavioral changes. *PLoS ONE*, 8(12):e83641, 2013.

[34] D. Friedman. On economic applications of evolutionary game theory. *Journal of Evolutionary Economics*, 8(1):15–43, 1998.

[35] F. Fu, D. I. Rosenbloom, L. Wang, and M. A. Nowak. Imitation dynamics of vaccination behaviour on social networks. *Proceedings of the Royal Society of London B: Biological Sciences*, 278(1702):42–49, 2011.

[36] D. Fudenberg and D. K. Levine. *The Theory of Learning in Games*, volume 2. MIT press, 1998.

[37] E. Fukuda, S. Kokubo, J. Tanimoto, Z. Wang, A. Hagishima, and N. Ikegaya. Risk assessment for infectious disease and its impact on voluntary vaccination behavior in social networks. *Chaos, Solitons and Fractals*, 68:1–9, 2014.

[38] S. Funk, S. Bansal, C. T. Bauch, K. T. Eames, W. J. Edmunds, A. P. Galvani, and P. Klepac. Nine challenges in incorporating the dynamics of behaviour in infectious diseases models. *Epidemics*, 10:21–25, 2015.

[39] S. Funk, M. Salathé, and V. A. Jansen. Modelling the influence of human behaviour on the spread of infectious diseases: a review. *Journal of the Royal Society Interface*, 7(50):1247–1256, 2010.

[40] S. Gandon, M. Mackinnon, S. Nee, and A. Read. Imperfect vaccination: some epidemiological and evolutionary consequences. *Proceedings of the Royal Society of London B: Biological Sciences*, 270(1520):1129–1136, 2003.

[41] M. G. M. Gomes, L. J. White, and G. F. Medley. Infection, reinfection, and vaccination under suboptimal immune protection: epidemiological perspectives. *Journal of Theoretical Biology*, 228(4):539–549, 2004.

[42] C. Granell, S. Gómez, and A. Arenas. Dynamical interplay between awareness and epidemic spreading in multiplex networks. *Physical Review Letters*, 111(12):128701, 2013.

[43] S. Gregson, G. P. Garnett, C. A. Nyamukapa, T. B. Hallett, J. J. Lewis, P. R. Mason, S. K. Chandiwana, and R. M. Anderson. HIV decline associated with behavior change in eastern Zimbabwe. *Science*, 311(5761):664–666, 2006.

[44] A. Gumel. Causes of backward bifurcations in some epidemiological models. *Journal of Mathematical Analysis and Applications*, 395(1):355–365, 2012.

[45] D. Han and M. Sun. Can memory and conformism resolve the vaccination dilemma? *Physica A: Statistical Mechanics and its Applications*, 415:95–104, 2014.

[46] J. Heffernan and M. J. Keeling. Implications of vaccination and waning immunity. *Proceedings of the Royal Society of London B: Biological Sciences*, pages rspb–2009, 2009.

[47] D. Helbing and A. Johansson. Cooperation, norms, and revolutions: a unified game-theoretical approach. *PLoS ONE*, 5(10):e12530, 2010.

[48] D. Helbing and A. Johansson. Evolutionary dynamics of populations with conflicting interactions: Classification and analytical treatment considering asymmetry and power. *Physical Review E*, 81(1):016112, 2010.

[49] T. Kar and P. K. Mondal. Global dynamics of a tuberculosis epidemic model and the influence of backward bifurcation. *Journal of Mathematical Modelling and Algorithms*, 11(4):433–459, 2012.

[50] M. Keeling, M. Tildesley, T. House, and L. Danon. The mathematics of vaccination. *Math. Today*, 49:40–43, 2013.

[51] E. Klein, R. Laxminarayan, D. L. Smith, and C. A. Gilligan. Economic incentives and mathematical models of disease. *Environment and Development Economics*, 12(05):707–732, 2007.

[52] C. M. Kribs-Zaleta and M. Martcheva. Vaccination strategies and backward bifurcation in an age-since-infection structured model. *Mathematical Biosciences*, 177:317–332, 2002.

[53] L. Laguzet and G. Turinici. Global optimal vaccination in the SIR model: properties of the value function and application to cost-effectiveness analysis. *Mathematical Biosciences*, 263:180–197, 2015.

[54] J. T. Lau, X. Yang, H. Tsui, E. Pang, and J. H. Kim. SARS preventive and risk behaviours of Hong Kong air travellers. *Epidemiology and Infection*, 132(04):727–736, 2004.

[55] J. Li, D. V. Lindberg, R. A. Smith, and T. C. Reluga. Provisioning of public health can be designed to anticipate public policy responses. 2013.

[56] Y. Li and J. Cui. The effect of constant and pulse vaccination on SIS epidemic models incorporating media coverage. *Communications in Nonlinear Science and Numerical Simulation*, 14(5):2353–2365, 2009.

[57] C.-M. Liao and S.-H. You. Assessing risk perception and behavioral responses to influenza epidemics: linking information theory to probabilistic risk modeling. *Stochastic Environmental Research and Risk Assessment*, 28(2):189–200, 2014.

[58] X.-T. Liu, Z.-X. Wu, and L. Zhang. Impact of committed individuals on vaccination behavior. *Physical Review E*, 86(5):051132, 2012.

[59] F. Magpantay, M. Riolo, M. D. de Cellès, A. A. King, and P. Rohani. Epidemiological consequences of imperfect vaccines for immunizing infections. *SIAM Journal on Applied Mathematics*, 74(6):1810–1830, 2014.

[60] P. Manfredi, P. Della Posta, A. d'Onofrio, E. Salinelli, F. Centrone, C. Meo, and P. Poletti. Optimal vaccination choice, vaccination games, and rational exemption: an appraisal. *Vaccine*, 28(1):98–109, 2009.

[61] M. Marathe and A. K. S. Vullikanti. Computational epidemiology. *Communications of the ACM*, 56(7):88–96, 2013.

[62] M. L. N. Mbah, J. Liu, C. T. Bauch, Y. I. Tekel, J. Medlock, L. A. Meyers, and A. P. Galvani. The impact of imitation on vaccination behavior in social contact networks. *PLoS Comput. Biol.*, 8(4):e1002469, 2012.

[63] A. R. Mclean and S. M. Blower. Imperfect vaccines and herd immunity to HIV. *Proceedings of the Royal Society of London B: Biological Sciences*, 253(1336):9–13, 1993.

[64] C. E. Mills, J. M. Robins, and M. Lipsitch. Transmissibility of 1918 pandemic influenza. *Nature*, 432(7019):904–906, 2004.

[65] S. Moghadas. Modelling the effect of imperfect vaccines on disease epidemiology. *Discrete And Continuous Dynamical Systems Series B*, 4:999–1012, 2004.

[66] C. Molina and D. J. Earn. Game theory of pre-emptive vaccination before bioterrorism or accidental release of smallpox. *Journal of The Royal Society Interface*, 12(107):20141387, 2015.

[67] L. Montopoli, S. Bhattacharyya, and C. T. Bauch. The free rider problem in vaccination policy and implications for global eradication of infectious diseases: a two-country game dynamic model. *Canadian Applied Mathematics Quarterly*, 17(2):317–338, 2009.

[68] F. Nazari, A. Gumel, and E. Elbasha. Differential characteristics of primary infection and re-infection can cause backward bifurcation in HCV transmission dynamics. *Mathematical Biosciences*, 263:51–69, 2015.

[69] E. K. Nisbet and M. L. Gick. Can health psychology help the planet? applying theory and models of health behaviour to environmental actions. *Canadian Psychology/Psychologie Canadienne*, 49(4):296, 2008.

[70] T. Oraby, V. Thampi, and C. T. Bauch. The influence of social norms on the dynamics of vaccinating behaviour for paediatric infectious diseases. *Proceedings of the Royal Society of London B: Biological Sciences*, 281(1780):20133172, 2014.

[71] J.-H. Park, H.-K. Cheong, D.-Y. Son, S.-U. Kim, and C.-M. Ha. Perceptions and behaviors related to hand hygiene for the prevention of

H1N1 influenza transmission among Korean university students during the peak pandemic period. *BMC Infectious Diseases*, 10(1):1, 2010.

[72] A. Perisic and C. T. Bauch. Social contact networks and disease eradicability under voluntary vaccination. *PLoS Comput. Biol.*, 5(2):e1000280, 2009.

[73] N. Perra, D. Balcan, B. Gonçalves, and A. Vespignani. Towards a characterization of behavior-disease models. *PLoS ONE*, 6(8):e23084, 2011.

[74] P. Poletti, M. Ajelli, and S. Merler. The effect of risk perception on the 2009 H1N1 pandemic influenza dynamics. *PLoS ONE*, 6(2):e16460, 2011.

[75] P. Poletti, M. Ajelli, and S. Merler. Risk perception and effectiveness of uncoordinated behavioral responses in an emerging epidemic. *Mathematical Biosciences*, 238(2):80–89, 2012.

[76] T. C. Reluga. An SIS epidemiology game with two subpopulations. *Journal of Biological Dynamics*, 3(5):515–531, 2009.

[77] T. C. Reluga. Game theory of social distancing in response to an epidemic. *PLoS Comput. Biol.*, 6(5):e1000793, 2010.

[78] T. C. Reluga, C. T. Bauch, and A. P. Galvani. Evolving public perceptions and stability in vaccine uptake. *Mathematical Biosciences*, 204(2):185–198, 2006.

[79] T. C. Reluga and A. P. Galvani. A general approach for population games with application to vaccination. *Mathematical Biosciences*, 230(2):67–78, 2011.

[80] T. C. Reluga and J. Medlock. Resistance mechanisms matter in SIR models. *Mathematical Biosciences and Engineering*, 4(3):553, 2007.

[81] T. C. Reluga, J. Medlock, and A. S. Perelson. Backward bifurcations and multiple equilibria in epidemic models with structured immunity. *Journal of Theoretical Biology*, 252(1):155–165, 2008.

[82] M. Roberts and J. Heesterbeek. A new method for estimating the effort required to control an infectious disease. *Proceedings of the Royal Society of London B: Biological Sciences*, 270(1522):1359–1364, 2003.

[83] Z. Ruan, M. Tang, and Z. Liu. Epidemic spreading with information-driven vaccination. *Physical Review E*, 86(3):036117, 2012.

[84] M. Safan, M. Kretzschmar, and K. P. Hadeler. Vaccination based control of infections in SIRS models with reinfection: special reference to pertussis. *Journal of Mathematical Biology*, 67(5):1083–1110, 2013.

[85] G. P. Sahu and J. Dhar. Dynamics of an SEQIHRS epidemic model with media coverage, quarantine and isolation in a community with pre-existing immunity. *Journal of Mathematical Analysis and Applications*, 421(2):1651–1672, 2015.

[86] M. Salathé and S. Bonhoeffer. The effect of opinion clustering on disease outbreaks. *Journal of The Royal Society Interface*, 5(29):1505–1508, 2008.

[87] F. Salvarani and G. Turinici. Individual vaccination equilibrium for imperfect vaccine efficacy and limited persistence. *https://hal.archives-ouvertes.fr/hal-01302557v2*, 2016.

[88] P. Schuster, K. Sigmund, J. Hofbauer, R. Gottlieb, and P. Merz. Selfregulation of behaviour in animal societies. *Biological Cybernetics*, 40(1):17–25, 1981.

[89] O. Sharomi, C. Podder, A. Gumel, and B. Song. Mathematical analysis of the transmission dynamics of HIV/TB coinfection in the presence of treatment. *Mathematical Biosciences and Engineering*, 5(1):145, 2008.

[90] L. B. Shaw and I. B. Schwartz. Enhanced vaccine control of epidemics in adaptive networks. *Physical Review E*, 81(4):046120, 2010.

[91] E. Shim, G. B. Chapman, J. P. Townsend, and A. P. Galvani. The influence of altruism on influenza vaccination decisions. *Journal of The Royal Society Interface*, page rsif20120115, 2012.

[92] E. Shim, J. J. Grefenstette, S. M. Albert, B. E. Cakouros, and D. S. Burke. A game dynamic model for vaccine skeptics and vaccine believers: measles as an example. *Journal of Theoretical Biology*, 295:194–203, 2012.

[93] E. Shim, L. Meyers, and A. P. Galvani. Optimal H1N1 vaccination strategies based on self-interest versus group interest. *BMC Public Health*, 11(1):1, 2011.

[94] R. D. Smith. Responding to global infectious disease outbreaks: lessons from SARS on the role of risk perception, communication and management. *Social Science and Medicine*, 63(12):3113–3123, 2006.

[95] P. Stephanie. Vaccination and other altruistic medical treatments: should autonomy or communitarianism prevail? *Medical Law International*, 4(3-4):223–243, 2000.

[96] J. Sun and J. Tang. A survey of models and algorithms for social influence analysis. In *Social Network Data Analytics*, pages 177–214. Springer, 2011.

[97] G. Szabó and G. Fath. Evolutionary games on graphs. *Physics Reports*, 446(4):97–216, 2007.

[98] J. K. Taubenberger and D. M. Morens. 1918 influenza: the mother of all pandemics. *Rev. Biomed.*, 17:69–79, 2006.

[99] P. D. Taylor. Evolutionarily stable strategies with two types of player. *Journal of Applied Probability*, pages 76–83, 1979.

[100] P. D. Taylor and L. B. Jonker. Evolutionary stable strategies and game dynamics. *Mathematical Biosciences*, 40(1-2):145–156, 1978.

[101] Y. Tsutsui, U. Benzion, and S. Shahrabani. Economic and behavioral factors in an individual's decision to take the influenza vaccination in Japan. *The Journal of Socio-Economics*, 41(5):594–602, 2012.

[102] S. Tully, M. Cojocaru, and C. T. Bauch. Coevolution of risk perception, sexual behaviour, and HIV transmission in an agent-based model. *Journal of Theoretical Biology*, 337:125–132, 2013.

[103] P. Van den Driessche and J. Watmough. Further notes on the basic reproduction number. In *Mathematical Epidemiology*, pages 159–178. Springer, 2008.

[104] R. Vardavas, R. Breban, and S. Blower. Can influenza epidemics be prevented by voluntary vaccination? *PLoS Comput. Biol.*, 3(5):e85, 2007.

[105] R. Vardavas, R. Breban, and S. Blower. A universal long-term flu vaccine may not prevent severe epidemics. *BMC Research Notes*, 3(1):92, 2010.

[106] A. Wang and Y. Xiao. A Filippov system describing media effects on the spread of infectious diseases. *Nonlinear Analysis: Hybrid Systems*, 11:84–97, 2014.

[107] L. Wang, D. Zhou, Z. Liu, D. Xu, and X. Zhang. Media alert in an SIS epidemic model with logistic growth. *Journal of Biological Dynamics*, pages 1–18, 2016.

[108] I. M. Wangari, S. Davis, and L. Stone. Backward bifurcation in epidemic models: Problems arising with aggregated bifurcation parameters. *Applied Mathematical Modelling*, 40(2):1669–1675, 2016.

[109] G. A. Weinberg and P. G. Szilagyi. Vaccine epidemiology: efficacy, effectiveness, and the translational research roadmap. *Journal of Infectious Diseases*, 201(11):1607–1610, 2010.

[110] C. Wells and C. Bauch. The impact of personal experiences with infection and vaccination on behaviour–incidence dynamics of seasonal influenza. *Epidemics*, 4(3):139–151, 2012.

[111] A. Wheelock, M. Miraldo, A. Parand, C. Vincent, and N. Sevdalis. Journey to vaccination: a protocol for a multinational qualitative study. *BMJ Open*, 4(1):e004279, 2014.

[112] (WHO). Summary of probable SARS cases with onset of illness from 1 November 2002 to 31 July 2003 (based on data as of the 31 December 2003). http://www.who.int/csr/sars/country/table2004-04-21/en.html. Accessed: 2016-11-03.

[113] B. Wu, F. Fu, and L. Wang. Imperfect vaccine aggravates the long-standing dilemma of voluntary vaccination. *PLoS ONE*, 6(6):e20577, 2011.

[114] S. Xia and J. Liu. A computational approach to characterizing the impact of social influence on individuals vaccination decision making. *PLoS ONE*, 8(4):e60373, 2013.

[115] Y. Xiao, X. Xu, and S. Tang. Sliding mode control of outbreaks of emerging infectious diseases. *Bulletin of Mathematical Biology*, 74(10):2403–2422, 2012.

[116] F. Xu and R. Cressman. Disease control through voluntary vaccination decisions based on the smoothed best response. *Computational and Mathematical Methods in Medicine*, 2014:ID 825734, 2014.

[117] F. Xu and R. Cressman. Voluntary vaccination strategy and the spread of sexually transmitted diseases. *Mathematical Biosciences*, 274:94–107, 2016.

[118] H. Zhang, F. Fu, W. Zhang, and B. Wang. Rational behavior is a "double-edged sword" when considering voluntary vaccination. *Physica A: Statistical Mechanics and its Applications*, 391(20):4807–4815, 2012.

[119] H. Zhang, J. Zhang, P. Li, M. Small, and B. Wang. Risk estimation of infectious diseases determines the effectiveness of the control strategy. *Physica D: Nonlinear Phenomena*, 240(11):943–948, 2011.

[120] H.-F. Zhang, Z.-X. Wu, M. Tang, and Y.-C. Lai. Effects of behavioral response and vaccination policy on epidemic spreading-an approach based on evolutionary-game dynamics. *Scientific Reports*, 4, 2014.

[121] H.-F. Zhang, Z.-X. Wu, X.-K. Xu, M. Small, L. Wang, and B.-H. Wang. Impacts of subsidy policies on vaccination decisions in contact networks. *Physical Review E*, 88(1):012813, 2013.

[122] Y. Zhang. The impact of other-regarding tendencies on the spatial vaccination game. *Chaos, Solitons and Fractals*, 56:209–215, 2013.

[123] X. Zhou, X. Shi, and H. Cheng. Modelling and stability analysis for a tuberculosis model with healthy education and treatment. *Computational and Applied Mathematics*, 32(2):245–260, 2013.

"Every reasonable effort has been made to acknowledge the owners of copyright material. I would be pleased to hear from any copyright owner who has been omitted or incorrectly acknowledged."

Appendix A: Multi-population game-dynamical replicator equations

Following [47, 48], for two subpopulations, the set of mutual-coupled game-dynamical replicator equations is given by

$$\frac{dp_i^a(t)}{dt} = p_i^a(t)\kappa\left[E_i^a(t) - A_a(t)\right]. \tag{1}$$

The superscripts $a, b \in \{1, 2\}$ denote different subpopulations, subscripts $i, j \in \{1, 2\}$ denote different behaviours (or strategies), the "expected success", $E_i^a(t) = \sum_{b=1}^{2}\sum_{j=1}^{2} A_{ij}^{ab} f_b\, p_j^b(t)$ for the fraction of individuals belonging to subpopulation a, $f_a \geq 0$, with $\sum_a f_a = 1$, and the proportion of individuals belonging to subpopulation a characterized by strategy i at time t, $p_i^a(t) \geq 0$, with $\sum_i p_i^a(t) = 1$. Also, the average success in subpopulation a is given by $A_a(t) = \sum_{k=1}^{2} p_k^a(t) E_k^a(t)$.

Equation (1) differs from the one stated in [48] in which the parameter κ is added to model the imitation dynamics under the influence of epidemic dynamics. In this situation, the strategies or behaviours spread proportionally to their success, but not inherited. In the language of evolutionary game theory, κ is a proportionality constant denoting how willing the players are to switch to new strategy based on the payoff difference.

Following notations in equation (1), the game-dynamical equation for strategy $i = 1$ in subpopulation $a = 1$ is derived as follows:

Table 1: The payoff matrices for two-subpopulation asymmetric game

The payoff matrix for individuals belonging to subpopulation 1

(i) A_{ij}^{11}, within-subpopulation interactions

Focal agent's behaviour	Interaction partner's behaviour $j=1^*$	$j=2$
$i=1^*$	r_1	s_1
$i=2$	t_1	p_1

(ii) A_{ij}^{12}, between-subpopulation interactions

Focal agent's behaviour	Interaction partner's behaviour $j=1$	$j=2^*$
$i=1^*$	R_1	S_1
$i=2$	T_1	P_1

The payoff matrix for individuals belonging to subpopulation 2

(i) A_{ij}^{22}, within-subpopulation interactions

Focal agent's behaviour	Interaction partner's behaviour $j=1$	$j=2^*$
$i=1$	p_2	t_2
$i=2^*$	s_2	r_2

(ii) A_{ij}^{21}, between-subpopulation interactions

Focal agent's behaviour	Interaction partner's behaviour $j=1^*$	$j=2$
$i=1$	P_2	T_2
$i=2^*$	S_2	R_2

* The preferred behaviour for susceptibles in their respective subpopulations. Ref: [47, 48]

$$\begin{aligned}\frac{dp_1^1(t)}{dt} &= p_1^1(t)\,\kappa\left[E_1^1(t) - A_1(t)\right] \\ &= p_1^1(t)\,\kappa\left[E_1^1(t) - \left\{p_1^1(t)\,E_1^1(t) + p_2^1(t)\,E_2^1(t)\right\}\right] \\ &= p_1^1(t)\,\kappa\left[E_1^1(t) - \left\{p_1^1(t)\,E_1^1(t) + (1-p_1^1(t))\,E_2^1(t)\right\}\right] \\ &= \kappa\, p_1^1(t)(1-p_1^1(t))\left[E_1^1(t) - E_2^1(t)\right].\end{aligned}$$

Let $p_1^1(t) = p(t)$ be the proportion of individuals with the (preferred) strategy 1 in subpopulation 1 and $p_2^1(t) = 1 - p_1^1(t) = 1 - p(t)$. The above equation becomes

$$\frac{dp(t)}{dt} = \kappa\, p(t)\,(1-p(t))\left[E_1^1(t) - E_2^1(t)\right]. \tag{2a}$$

Similarly, the game-dynamical equation for strategy $j = 2$ in subpopulation $b = 2$ is given by

$$\frac{dq(t)}{dt} = \kappa\, q(t)\,(1-q(t))\left[E_1^2(t) - E_2^2(t)\right]. \tag{2b}$$

In their multi-population game-dynamical replicator equations, Helbing and Johannson [47, 48] derived the expected success of strategy interactions from the 2×2 payoff matrices for two-subpopulation asymmetric game, as

given in Table 1. In classical game theory, the notations in the elements of matrices in Table 1 are associated to r (reward), s (sucker's payoff), t (temptation), and p (punishment). Notice that the payoffs for within-subpopulation interactions are denoted by lowercase letters r, s, p, and t, whereas uppercase letters R, S, P and T are used for payoffs for between-subpopulation interactions. To reflect incompatible preferences of two subpopulations, the payoff matrix of individuals belonging to subpopulation 2 is assumed to be "inverted" or "mirrored" of the payoff matrix of individuals in subpopulation 1 [47], and vice versa. However, in the context of adopting normal or altered strategies in the course of epidemic outbreak in Chapter Three, the issue is always whether one will be beneficial or not from adopting certain strategy. Hence, the r, s, p, and t (resp. R, S, P, and T) in the formulations in Chapter Three are simply variables used to denote the payoff value received by individuals (or agents) in the pairwise strategy interactions.

By using the payoff matrices of A_{ij}^{11} and A_{ij}^{12} in Table 1 and substituting $E_1^1(t) = \sum_{b=1}^{2}\sum_{j=1}^{2} A_{1j}^{1b} f_b\, p_j^b(t)$ and $E_2^1(t) = \sum_{b=1}^{2}\sum_{j=1}^{2} A_{2j}^{1b} f_b\, p_j^b(t)$ into equation (2a), after some algebra, we obtain the game-dynamical equation for subpopulation 1, as follows:

$$\frac{dp(t)}{dt} = \kappa\, p(t)\,(1-p(t))\Big[(r_1 - t_1) f p(t) + (s_1 - p_1) f (1-p(t)) + (R_1 - T_1)(1-f)(1-q(t)) + (S_1 - P_1)(1-f) q(t)\Big]. \quad (3a)$$

Similarly, the game-dynamical equation for subpopulation 2 is

$$\frac{dq(t)}{dt} = \kappa\, q(t)\,(1-q(t))\Big[(S_2 - P_2) f p(t) + (R_2 - T_2) f (1-p(t)) + (s_2 - p_2)(1-f)(1-q(t)) + (r_2 - t_2)(1-f) q(t)\Big]. \quad (3b)$$

The system of equations (3) consists of 16 payoff-dependent model parameters. They could be reduced for simplicity through several ways. Following [47, 48], let $b_a = s_a - p_a$, $B_a = S_a - P_a$, $c_a = r_a - t_a$, and $C_a = R_a - T_a$, the

system (3) becomes

$$\frac{dp(t)}{dt} = \kappa\, p(t)\,(1-p(t))\big[b_1 f + (c_1 - b_1)\, f\, p(t) + C_1(1-f) + (B_1 - C_1)(1-f)q(t)\big], \tag{4a}$$

$$\frac{dq(t)}{dt} = \kappa\, q(t)\,(1-q(t))\big[b_2(1-f) + (c_2 - b_2)(1-f)q(t) + C_2 f + (B_2 - C_2) f\, p(t)\big]. \tag{4b}$$

The system (4) has 8 payoff-dependent model parameters.

Appendix B: The derivation of the effective reproduction number by using the next generation matrix

We first find the effective reproduction number (4.3) for system (4.1) by using the procedure in Section 2.3, as follows.

Step 1: Let I and W be the disease compartments, we have

$$\mathcal{F} = \begin{bmatrix} \beta\frac{I+\theta W}{N}S \\ \sigma\beta\frac{I+\theta W}{N}V_2 \end{bmatrix}, \qquad \mathcal{V} = \begin{bmatrix} (\gamma_u+\mu)I \\ (\gamma_v+\mu)W \end{bmatrix}.$$

Step 2: Find the linearization of the relevant rate equations in Step 1 at DFE,

$$\mathsf{F} = \begin{bmatrix} \beta\frac{S_0}{N} & \beta\theta\frac{S_0}{N} \\ \sigma\beta\frac{V_{20}}{N} & \sigma\beta\theta\frac{V_{20}}{N} \end{bmatrix}, \qquad \mathsf{V} = \begin{bmatrix} \gamma_u+\mu & 0 \\ 0 & \gamma_v+\mu \end{bmatrix},$$

and the next generation matrix is given by

$$K = \mathsf{F}\mathsf{V}^{-1} = \begin{bmatrix} \frac{\beta}{\gamma_u+\mu}\frac{S_0}{N} & \frac{\beta\theta}{\gamma_v+\mu}\frac{S_0}{N} \\ \frac{\sigma\beta}{\gamma_u+\mu}\frac{V_{20}}{N} & \frac{\sigma\beta\theta}{\gamma_v+\mu}\frac{V_{20}}{N} \end{bmatrix}.$$

Step 3: The dominant eigenvalue of matrix K is the effective reproduction number

$$\mathcal{R}_{\text{vac}} = \frac{\beta S_0}{\gamma_u+\mu} + \frac{\sigma\beta\theta V_{20}}{\gamma_v+\mu}. \tag{5}$$

The expression (5) could be interpreted as the sum of the number of secondary infection of unvaccinated susceptible individuals produced by a primary infected person in the I class and the number of secondary infections of vaccinated susceptible individuals produced by a primary infected person in the W class. As the primary infected person (also known as the "index case", or "patient zero", in epidemiology) could be simply referred to as the first individual in the population showing the symptoms of the infectious disease, the existing of two primary infection cases in the above interpretation may be misleading. Also, this interpretation rules out the possibility of disease transmission from individuals in the I (resp. W) class to individuals in the V_2 (resp. S) class, which the number of infections is not insignificant. Therefore, it is necessary to adopt different notations (and hence different interpretations) to deal with the reproduction number involving more than one class of infected and/or susceptible individuals.

Following [103], we denote $\beta \equiv \beta_{uu}$, $\beta\theta \equiv \beta_{uv}$, $\sigma\beta \equiv \beta_{vu}$ and $\sigma\beta\theta \equiv \beta_{vv}$, then the next generation matrix in Step 2 above becomes

$$K = \begin{bmatrix} \frac{\beta_{uu}}{\gamma_u+\mu}\frac{S_0}{N} & \frac{\beta_{uv}}{\gamma_v+\mu}\frac{S_0}{N} \\ \frac{\beta_{vu}}{\gamma_u+\mu}\frac{V_{20}}{N} & \frac{\beta_{vv}}{\gamma_v+\mu}\frac{V_{20}}{N} \end{bmatrix} \equiv \begin{bmatrix} \mathcal{R}_{uu} & \mathcal{R}_{uv} \\ \mathcal{R}_{vu} & \mathcal{R}_{vv} \end{bmatrix}. \tag{6}$$

The dominant eigenvalue of the matrix K in (6) is given by

$$\mathcal{R}_{\text{vac}} = \frac{\mathcal{R}_{uu}+\mathcal{R}_{vv}}{2} + \frac{1}{2}\sqrt{(\mathcal{R}_{uu}+\mathcal{R}_{vv})^2 - 4\mathcal{R}_{uu}\mathcal{R}_{vv} + 4\mathcal{R}_{uv}\mathcal{R}_{vu}}. \tag{7}$$

It follows that the disease eradication threshold condition $\mathcal{R}_{\text{vac}} < 1$ is now equivalent to the following pair of conditions.

$$\begin{aligned} \frac{1}{2}(\mathcal{R}_{uu}+\mathcal{R}_{vv}) &< 1, \\ \mathcal{R}_{uu}+\mathcal{R}_{vv}-\mathcal{R}_{uu}\mathcal{R}_{vv}+\mathcal{R}_{uv}\mathcal{R}_{vu} &< 1. \end{aligned}$$

Hence, following [103], we shall interpret the reproduction number $\mathcal{R}_{\text{vac}}$ as the

number of secondary infections, both vaccinated and unvaccinated, produced by an index case distributed in both disease compartments, with one part in the I class and $\sigma\frac{V_{20}}{S_0}$ parts in the W class.